# FUNCTIONAL IMPACTS OF TRANSGENIC OVEREXPRESSION OF UDP-galactose: CERAMIDE GALACTOSYLTRANSFERASE and POLYSIALYLTRANSFERASE ON THE DEVELOPMENT OF OLIGODENDROCYTES AND MYELIN MAINTENANCE

DISSERTATION

Zur Elangung des Doktorgrades
Der
Mathematisch-Naturwissenschaftlichen Fakultät
Der
Rheinischen Friedrich-Wilhelms-Universität Bonn

Vorgelegt von

*Simon Ngamli Fewou*

Aus

Nkongsamba/Kamerun

Bonn, 2005

Angefertigt mit Genehmigung der Mathematisch-Naturwissenschaftlichen Fakultät der Rheinischen Friedrich-Wilhelms-Universität Bonn

1. Referent: Prof. Dr. Volkmar Gieselmann
2. Referent: Prof. Dr. Konrad Sandhoff

Tag der Promotion: 12-05-2005

*To my mother*

# TABLE OF CONTENTS

6            **PART I**

**Reversal of non-hydroxy:alpha-hydroxy galactosylceramide ratio and demyelination in transgenic mice overexpressing UDP-galactose:ceramide galactosyltransferase**

# **ABBREVIATIONS**

| | |
|---|---|
| µCi | Micro curie |
| µg | Microgram |
| µl | Micro litter |
| β-actin | Beta-actin |
| A2B5 | Antibody recognizing an epitope common to sialogangliosides and sulfatide from the plasma membranes of neurons and glial cells |
| AIDA | Advanced Image Data Analyzer |
| BCIP | 5-bromo-4-chloro-3-indoyl phosphate |
| bFGF | Basic fibroblast growth factor |
| bp | base pair |
| BrdU | 5-Bromo-2´-deoxyuridine |
| BSA | Bovine serum albumin |
| cDNA | Complementary deoxy ribonucleic acid |
| CGT | UDP-galactose: ceramide galactosyltransferase |
| CHO | Chinese hamster ovarian |
| CNPase | 2´, 3´-cyclic nucleotide 3´-phosphodiesterase |
| CNS | Central nervous system |
| CPM | Count per minute |
| cRNA | Complementary ribonucleic acid |
| CsCl | Cesium chloride |
| CST | 3-$O$-sulfogalactosylceramide |
| DAPI | 2, 6-diamidino-2-phenylindole |
| dCTP | Deoxy cytidine 5´-triphosphate |
| ddH$_2$O | Double distilled water |
| DE MALDI-TOF | Delayed extraction matrix-assisted laser desorption ionization-time-of-flight |
| DEPC | Diethylpropyl pyrocarbonate |
| DIG | Digoxigenin |

| | |
|---|---|
| DMEM | Dulbecco´s modified eagle medium |
| DNA | Deoxy ribonucleic acid |
| dNTP | Deoxy nucleotide triphosphate |
| DIV | Division |
| EDTA | Ethylenediaminetetraacetic acid |
| ER | Endoplasmic reticulum |
| FA2H | Fatty acid 2-hydroxylase |
| FCS | Fetal calf serum |
| FGF | Fibroblast growth factor |
| GalC | Galactosylceramide |
| GD3 | Ganglioside GD3 |
| GFAP | Glial fibrilary acidic protein |
| GlcCer | Glucosylceramide |
| HBSS | Hank´s balanced salt solution |
| Hepes | $N_2$-2-hydroxyethylpiperazine-N´-2-ethane sulfonic acid |
| HFA | Hydroxy fatty |
| HFA-Cer | Hydroxy fatty ceramide |
| HFA-GalC | Hydroxy fatty galactosylceramide |
| HFA-Sulf | Hydroxy fatty sulfatide |
| HPTLC | High performance thin layer chromatography |
| HRP | Horseradish Peroxidase |
| Ig | Immunoglobulin |
| kb | Kilo base |
| KBq | Kilo becquerel |
| kDa | Kilo dalton |
| Kdn | 5-deamino-3, 5-dideoxyneuraminic acid (2-keto-3-deoxynonulosonic acid) |
| LBP | Large basic protein |
| LTD | Long term depression |
| LTP | Long term potentiation |
| MAG | Myelin-associated glycoprotein |

| | |
|---|---|
| MAL | Myelin and lymphocyte |
| MBP | Myelin basic protein |
| MDL | Major dense line |
| MGDG | 1,2-di-0-(β-D-galactopyranosyl)-*sn*-glycerol |
| MLD | Metachromatic leukodystrophy |
| mm$^2$ | Millimeter square |
| MOG | Myelin and oligodendrocyte glycoprotein |
| mRNA | Messenger ribonucleic acid |
| NBT | Nitro blue tetrazolium |
| NCAM | Neural cell adhesion molecule |
| Neu5Ac | 5-N-acetylneuraminic acid |
| Neu5Gc | 5-N-glycolylneuraminic acid |
| NFA | Non-hydroxy fatty acid |
| NFA-Cer | Non-hydroxy fatty acid ceramide |
| NFA-GalC | Non-hydroxy fatty acid galactosylceramide |
| NFA-Sulf | Non-hydroxy fatty acid sulfatide |
| ng | Nanogram |
| O4 | Antibody against sulfatide and also recognizing an uncharacterized sulfated antigen |
| OL | Oligodendrocyte |
| Olf | Olfactory factor |
| OPCs | Oligodendrocyte precursor cells |
| ORF | Open reading frame |
| PAPS | 3'-phosphoadenosyl-5'-phosphosulfate |
| PCR | Polymerase chain reaction |
| PDGF | Platelet derived growth factor |
| PDGFRα-R | Platelet derived growth factor alpha-receptor |
| PFA | Paraformaldehyde |
| PLP | Proteolipid protein |
| PMSF | Phenylmethylsulfonylfluorid |
| PND | Post natal day |
| PNS | Peripheral nervous system |

| | |
|---|---|
| PSA | Polysialic acid |
| PST | Polysialyltransferase |
| RIP | Receptor interacting Protein |
| RNA | Ribonucleic acid |
| RT | Room temperature |
| SBP | Small basic protein |
| SCIP | Suppressed cyclic AMP-inducible-protein |
| SDS | Sodium dodecyl sulfate |
| SDS-PAGE | SDS-polyacrylamide gel electrophoresis |
| SEM | Standard error of the mean |
| SSC | Salt sodium citrate |
| Sulf | Sulfatide |
| SVZ | Subventricular zone |
| TAE | Tris acetic acid EDTA |
| TBS | Tris-buffered saline |
| tRNA | 2´-Deoxycytidine 5´-triphosphate |
| TIT | 3,3,5-triiodo-L-thyronine |
| U | Unit |
| UDP | Uridine 5´-diphosphate |
| UTP | Uridine 5´-triphosphate |
| UTR | untranslated region |
| UV | Ultra violet |
| VLCFA | Very long chain fatty acid |
| VZ | Ventricular zone |

# 2     ABSTRACTS

## 2.1    PLP-CGT TRANSGENIC MICE

Galactosylceramide (GalC) and its sulfated derivative (sulfatide) are major lipid components of the myelin membrane constituting about 30% of its lipid content. They fulfill essential functions in oligodendrocyte differentiation, formation and maintenance of myelin. Transgenic mice overexpressing UDP-galactose: ceramide galactosyltransferase (CGT) in oligodendrocytes under the control of the proteolipid protein (PLP) promoter were generated. Elevated CGT activity led to a significant increase in non-hydroxy fatty acid galactosylceramide. In contrast, however, a substantial decrease in the normally predominant -hydroxy fatty acid form of GalC was observed. As a consequence, total GalC levels were only marginally elevated in the transgenic mice. These mice exhibit deficits in motor behavior and develop a progressive hind limbs paralysis. *In vitro* study of oligodendrocyte development indicates an increase in oligodendrocyte number. This result was confirmed *in vivo*, where a significant increase of PLP positive cells was observed in the corpus callosum of PLP-CGT mice. Surprisingly, more cells expressing the MBP protein *in vitro* did not have the morphology of a myelin-forming oligodendrocyte, indicating a possible inhibition of the synthesis of the myelin membrane *in vitro*. Ultrastructural analysis revealed severe impairment in the formation of compact myelin and a progressive demyelination in the central nervous system, accompanied by axonal degeneration, vacuolation and massive astrogliosis. The composition of myelin proteins was unchanged with the exception of a significant progressive up regulation of the raft-associated MAL protein. MAL up regulation was not due to an increase in mRNA expression, suggesting reduced degradation of MAL. Taken together these results strongly suggest that the HFA- to NFA-GalC ratio is an important factor in the formation and maintenance of compact myelin.

## 2.2  <u>PLP-PST TRANSGENIC MICE</u>

Oligodendrocyte differentiation and myelin formation are two subsequent cellular mechanisms timely separated. During development, oligodendrocyte progenitor cells migrate from their place of origin to their destination, expressing a high level of the polysialic acid (PSA). PSA is a long linear homopolymer of sialic acid. In the vertebrate embryo, PSA appears exclusively attached covalently to a cell surface protein called neural cell adhesion molecule (NCAM). In this context, PSA has been shown to be an important modulator of cell interactions during development, for example, in axonal pathfinding and branching, response of axons to loss of synaptic activity and in the migration of muscle cells. The function of PSA has been proposed to influence not only interactions mediated by NCAM itself, but cell-cell interactions in general. PSA is also known to be involved in the migration, proliferation and differentiation of oligodendrocyte precursors (OPCs).

In order to investigate potential physiological consequences of increased level of polysialic acid (PSA) in oligodendrocytes, we generated transgenic mice that overexpress polysialyltransferase (PST/ST8Sia IV) under the control of the proteolipid protein (PLP) promoter. In the central nervous system of PLP-PST mice (PLP-PST), PST was overexpressed by oligodendrocytes. Furthermore, increase of PSA concentration in the CNS induces no behavioral deficit of PLP-PST mice. Most importantly, elevation of PSA concentration induces increase of differentiated oligodendrocytes of the spinal cord and brainstem, but a reduction of oligodendrocyte numbers in the corpus callosum. The number of oligodendrocyte progenitor cells was unchanged in all the brain regions investigated. Moreover, biochemical analysis indicates reduction of MBP level during myelination but normal expression of other oligodendrocyte/myelin specific proteins. Structural analysis of the myelin sheath indicates a normal myelination in the CNS and PNS of PLP-PST transgenic mice. Importantly, PLP-PST mice demyelinate at adult age. Demyelination was accompanied by redundant myelinated axons and axonal degeneration leading to vacuolation.

# 3   <u>INTRODUCTION</u>

The mammalian brain develops as a tube containing a fluid-filled ventricular compartment. As the development of the brain proceeds, new zones, among which the subventricular zone (SVZ), appears and gives rise to many glial cells (Lois and Alvarez-Buylla, 1993; Doetsch and Alvarez-Buylla, 1996; Barres, 1999). Oligodendrocyte precursor cells (OPCs) develop from the neuroepithelial precursors that line the lumen of the spinal cord and the ventricles of the brain. OPCs from the spinal cord and brainstem are generated in the sub-domain of the VZ near the floor plate and those from the optic nerve are generated in a specialized part of the ventricular zone (VZ) (Yu et al., 1994; Ono et al., 1995, 1997). In all cases, OPCs migrate from their place of birth to their destination, where they differentiate. Migrating OPCs express markers such as platelet derived growth factor (PDGF), basic fibroblast growth factor (bFGF), hepatocyte growth factor (HGF) that stimulates their motility and polysialic acid (PSA) (Milner et al., 1997). PSA is constituted of long chains of α-2,8 sialic acid which is negatively charged and posttranslationally modifies the neural cell adhesion molecule (NCAM). Furthermore, PSA is involved in axon guidance, interferes with the adhesive forces, thus promoting changes in cell interactions, and thereby facilitates plasticity in the structure and function of the nervous system (Rutishauser et al., 1988; Rutishauser and Landmesser, 1996; Eckhardt et al., 2000). At the destination, OPCs settle along fiber tracts of the future white matter of the CNS and acquire the capacity to differentiate. Differentiated oligodendrocytes are characterized by the change of their morphology, the expression of different markers such as proteins and lipids and the synthesis of the myelin membrane, which comprises 30% of galactosylceramide and sulfatide (Taylor et al., 2002). The high level of GalC and sulfatide in the myelin sheath leads to the prediction that they play an important role in OL and myelin biology. GalC and sulfatide regulate oligodendrocyte differentiation (Bansal and Pfeiffer, 1989; Bansal et al., 1999; Hirahara et al., 2004) and participate in the

synthesis of a compact myelin sheath. Mice lacking GalC and sulfatide are able to form apparently normal myelin, which, however, exhibits subtle structural abnormalities (Bosio et al., 1996; Coetzee et al., 1996). Myelin of these mice is thinner and unstable (Bosio et al., 1998a; Dupree et al., 1998; Honke et al., 2002). Disorganized paranodal regions and multiple myelinated axons in CGT knock-out mice suggest altered axo-glial interactions (Marcus and Popko, 2002). A functional consequence of these alterations is a significantly reduced nerve conduction velocity (Coetzee et al., 1996). Compensatory upregulation of HFA-glucosylceramide in CGT deficient mice, which is normally undetectable, seems to prevent more severe symptoms (Coetzee et al., 1996).

To investigate the effects due to an increase of GalC and PSA concentration on the oligodendrocyte behavior and myelin formation, transgenic mice overexpressing PST or CGT in the CNS have been generated under the control of the proteolipid protein (PLP) promoter. Transgenic mice over expressing PST in the CNS show a significant increase of the level of oligodendrocytes in the spinal cord and brain stem during myelination. Biochemically, PST mice show no changes in the myelin protein concentration, except MBP, for which a mild decrease in the protein and mRNA level was observed. Structurally, mice overexpressing PST in the CNS develop normal myelin content and structure during myelination and show demyelination and aberrant myelin structure at the adult age.

Concerning PLP-CGT transgenic mice, inversion of the HFA:NFA-GalC ratio were observed. This inversion of lipids ratio was accompanied by formation of apparently unstable and uncompacted myelin, and a progressive demyelination. This results strongly suggest that the HFA:NFA-GalC ratio is a critical factor in the formation and maintenance of compact myelin. In addition to the change of the HFA:NFA-GalC ratio, a significant upregulation of the MAL protein was observed in these mice. *In vitro*, transgenic CGT cells show an increase of oligodendocyte number, but a low amount of the myelin forming cells according to morphological analysis, indicating that cells overexpressing CGT were not able to differentiate fully. This result was confirmed in vivo by in

situ hybridization where a significant increase in PLP positive cells was observed in the corpus callosum.

# 4    <u>LITERATURE REVIEW</u>

During development, directed migration of oligodendrocyte and neuron precursor cells is essential for myelin formation in the central nervous system (CNS). Progenitors expressing high amount of PSA are generated in the ventricular zone and migrate to their destinations (Lee et al., 2000). Cell adhesion molecules such as integrins, cadherins and NCAM, in particular its embryonic polysialylated isoform (PSA-NCAM), have also been shown to be implicated in the control of the migration (Wang et al., 1994; Blaschuk et al., 2000).

At their destination, migrated cells start to differentiate by synthesizing different antigens (proteins and lipids) at each stage and finally the myelin membrane.

## 4.1. Genomic organization and molecular characteristics of mouse polysialyltransferase (PST-1/ST8SiaIV) and rat UDP-galactose: ceramide galactosyltransferase (CGT).

### 4.1.1 Description of the polysialyltransferases

The addition of polysialic acid residues to the terminus of glycoprotein oligosaccharides is a developmentally and posttranslationally regulated process (Kiss and Rougon, 1997; Mühlenhoff et al., 1998). In the CNS, two enzymes are responsible for the polysialylation of NCAM: α-2,8-polysialyltransferases ST8Sia IV/PST-1 and ST8Sia II/STX (Brett et al., 2001; Franceschini et al., 2001; Mühlenhoff et al., 1996). ST8Sia II (STX) and ST8Sia IV (PST-1) are polysialic acid synthases that catalyze polysialic acid formation on NCAM *in vivo* and *in vitro* (Kitazume-Kawaguchi, 2001) (Fig. 1).

Genotypically, ST8Sia IV is composed of 5 exons separated from each other by 4 introns that contribute to the expression of a 5.2 kb mRNA after splicing. Two non-coding regions are situated in exon 1 and 5. The expression of PST mRNA is regulated by a promoter that lacks TATA- and CCAAT-like sequences. Analysis of this promoter indicates that the region between

nucleotide –443 and –162 is sufficient for expression (Eckhardt and Gerady-Schahn, 1998). cDNA synthesized by reverse transcription, indicated a size of 2026 base pairs (bp) with an open reading frame (ORF) of 1080 bp encoding a protein of 359 amino acids with a predicted molecular weight of about 41.2 kD (Eckhardt et al., 1995). Primary structure shows characteristic features of the sialyltransferase family, containing two motifs as described by Drickamer (1993). The presence of 13 hydrophobic amino acids at its N-terminal domain suggests that PST is retained in the Golgi (Eckhardt et al., 1995). Amino acid analysis demonstrates that PST shares 59% homology with STX/ST8Sia II (Livingston and Paulson, 1993), the sialyltransferase of unknown specificity, and 28% with GD3 synthase (Blackman et al., 1991).
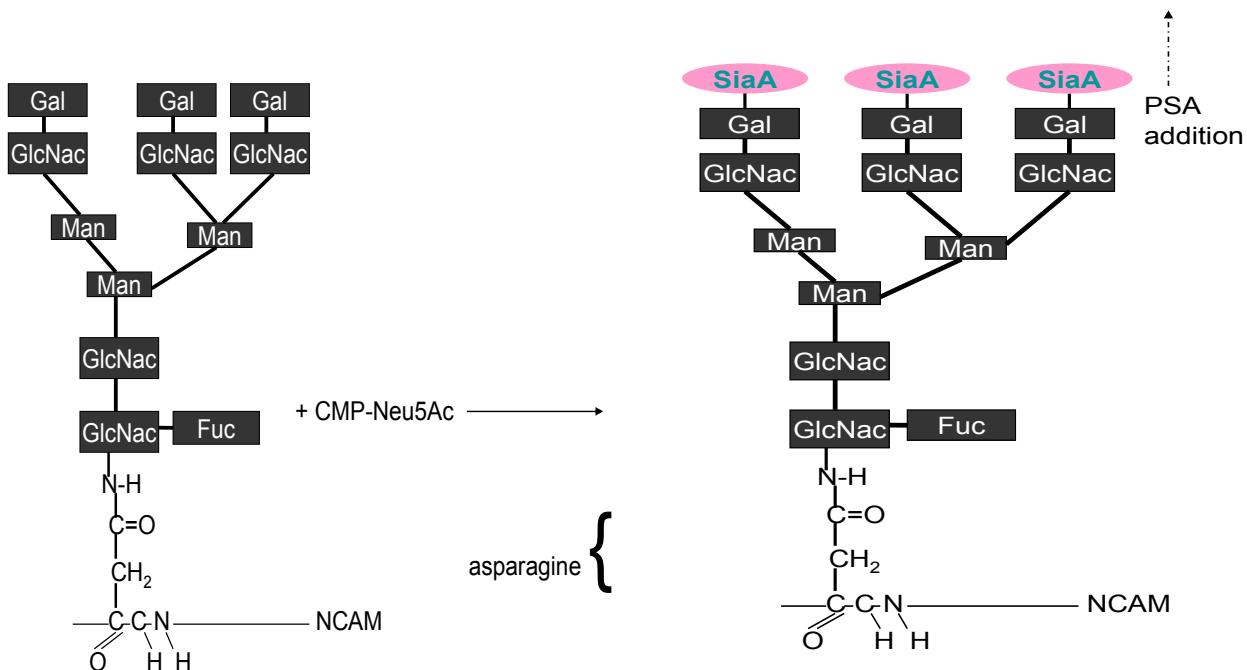


**Fig.1 Reaction of the polymerization of the polysialic acid on NCAM**. The scheme represents the animal structure of oligosaccharides of the NCAM molecule recognized by PST-1, and the composition of the polysialylated cores as described by Mühlenhoff et al., 1996

### 4.1.2 Description of UDP-galactose: ceramide galactosyltransferase and the fatty acid 2-hydroxylade

The myelin sheaths of both CNS and peripheral nervous system (PNS) are a multilayer membrane system consisting of 70 to 85% lipids and 15 to 30% proteins (Morell et al., 1994). Myelin synthesis requires the co-ordinated expression of genes encoding the myelin structural proteins, lipids and biosynthetic enzymes such as UPD-galactose: ceremide galactosyltransferase

(CGT). CGT transfers galactose to ceramide to form the galactolipids galactosylceramide (GalC) (fig. 2), which is composed of two isoforms, differing from each other by the presence or absence of a hydroxy group on the fatty acid. The 2-hydroxylation of the fatty acid occurs during *de novo* ceramide synthesis and is catalyzed by the fatty acid 2-hydroxylase (FA2H). The mammalian FA2H is a 42.8 kDa protein containing 372 amino acids sharing 36 % identity and 46 % similarity with the yeast Fah1 protein (Anderson et al. 2004). FA2H is co-localized with CGT to the endoplasmic reticulum (Eckhardt et al., 2005), indicating that these two enzymes work in concert in the synthesis of the two isoforms of GalC, since ceramide is the substrate of CGT. Until recently, it was not clear whether the FA2H adds the hydroxyl group on a free fatty acid or on the ceramide. In his article, Anderson et al. (2004) have demonstrated that the hydroxyl group is added on the free fatty acid during *de novo* synthesis of ceramide.
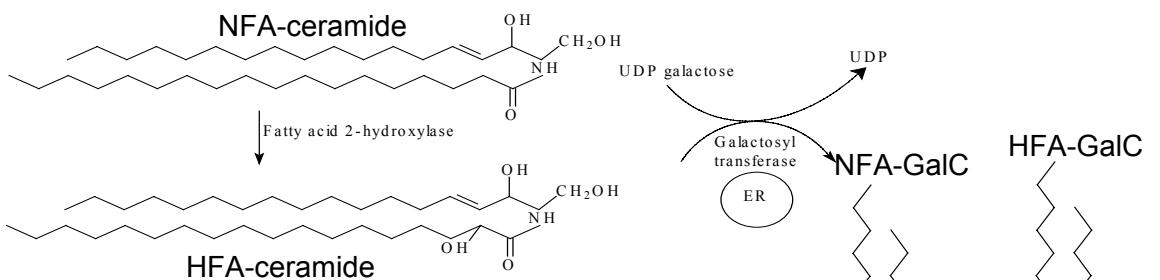


**Fig. 2 The pathway of sulfatide synthesis.** The two last steps of the synthesis of sulfatide are spatially separated. Note the synthesis of GalC in the endoplamic reticulum and sulfatide in the Golgi apparatus.
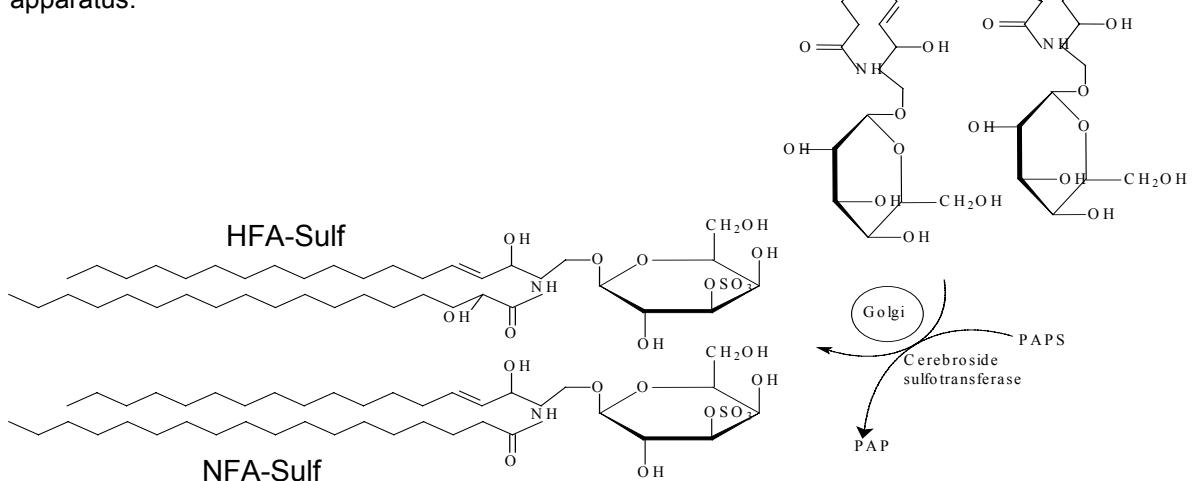
Analysis of mouse genome has shown that CGT occupies the band E3-F1 of chromosome 3. Structurally, the mouse CGT gene is composed of 6 exons that span a minimum of 70 kb of DNA. The 5′-untranslated region is encoded by an exon located 25 kb upstream of the first protein-encoding exon. Protein analysis coupled to DNA analysis shows that the first exon is non-coding and the remaining five exons contain the coding region and the 3′-UTR. Exon 2 (822 nt) is the one which codes for about half of the protein (Coetzee et al. 1996).

Promoter analysis of myelin-specific genes has shown many ubiquitous and specific cis- and trans-acting factors that regulate tissue specificity. Analysis of CGT promoter indicates that only a few hundred base pairs spanning from –527 to –98 were able to direct the specificity of the CGT expression in oligodendrocytes (Yonemasu et al., 1998). Luciferase reporter data (Yonemasu et al., 1998) show that this region (–527 to –98) contains putative positive regulatory sequences such as an Olf-1 binding site (at –492) [(Kudrycki et al., 1993); the olfactory-specific factor contributes to the specific expression of an olfactory-specific gene. The Olf-1-binding consensus sequence was defined as TCCCC (A/T) NGGAG], Krox20/24 binding site (at –119 GAGGGGGCG –111, –113 GCGGGCG –106) [Chavier et al., 1990; Taira and Baraban, 1997. Krox20 is a mouse zinc finger gene expressed in a segment-specific manner and restricted to the early PNS and Krox24 is expressed both in the CNS and PNS]. The CGT promoter also contains a purine-rich region (–127 to –116), which is important for the regulation of CGT gene expression because of its extraordinary high conservation among many myelin-specific gene promoters. For example: In PLP gene promoter, two sites were found to be conserved at the same position (–75 to –63) in the mouse, rat and human. Homologous sequences have been found in other myelin genes such as 2′,3′-cyclic nucleotide 3′-phosphodiesterase (CNPase) at –173 and –160 in human, MBP at –51, for both human and mouse, myelin-associated glycoprotein (MAG) at –25 and +103 in mouse and rat, myelin oligodendrocyte glycoprotein (MOG) at –293 (Hudson et al. 1996). As in the other myelin-specific gene promoters [mouse MAG promoter (69% in –169 to

–5) and PLP promoter (60% in –87 to –41)], a GC rich domain is also found in the CGT promoter (Yonemasu et al. 1998).

The CGT promoter is also characterized by the presence of sequences containing negative regulatory elements. These sequences are characterized by the binding site for the suppressed-cyclic AMP-inducible-protein (SCIP) (He and Rosenfeld, 1991) (–709 to –527). The rat CGT promoter controls the expression of a 4.6 kb mRNA, which gives rise to a cDNA with an ORF of 1623 bp which codes for a protein of 541 amino acids with a molecular mass of 61.126 kDa (Stahl et al., 1994). CGT is a class I integral membrane protein containing three putative glycosylation sites, a hydrophobic carboxy-terminus, and localized in the endoplasmic reticulum (Schulte and Stoffel, 1993; Schulte and Stoffel, 1995; Sprong et al., 1998).

## 4.2 Functions and structures of both polysialic acid and CGT products.

### 4.2.1 Functions and structure of PSA.

In mammalian cells, the expression of PSA is developmentally regulated and is found at highest levels in the embryonic and neonatal brain attached to NCAM (Finne et al. 1987). PSA is also expressed in other embryonic and neonatal tissues such as heart and kidney (Finne et al., 1987; Roth et al., 1987). In the adult animal brain, the level of PSA is decreased and maintained in selected areas such as hippocampus and olfactory system (Seki and Arai 1993; Cremer et al., 2000). PSA is also expressed on the surface of cancer cells such as lung carcinoma (Kibbelaar et al. 1989; Komminoth et al., 1991), Wilm´s tumor (Roth et al., 1988) and neuroblastomas (Livingstone et al., 1988; Hildebrandt et al., 1998; Figarella-Branger et al., 1990), where it may play an anti-adhesive role and promote cell growth and metastasis (Fukuda, 1996; Scheidegger et al., 1994). In general, PSA has an anti-adhesive role in the CNS, promotes plasticity in cell interactions, is critical for axon guidance and pathfinding, neurite outgrowth, and cell migration (Bruses and Rutishauser, 2001; Rutishauser and Landmesser, 1996; Rutishauser, 1996; Durbec and

Cremer, 2001; Kiss and Rougon, 1997). Data from either NCAM or PST/ST8Sia IV knockout mice indicates that, PSA promotes long term potentiation (Cremer et al., 1994; Eckhardt et al. 2000) and others have shown that polysialylated NCAM modulates cellular signal transduction by organizing cell surface receptors and sequestering ligands (Durbec and Cremer, 2001). Structurally, PSA is composed of monomers of derivatives of nine carbon sugar neuraminic acid. The three major building units of PSA are 5-N-acetylneuraminic acid (Neu5Ac), 5-N-glycolylneuraminic acid (Neu5Gc) and 5-deamino-3, 5-dideoxyneuraminic acid (2-keto-3-deoxynonulosonic acid, Kdn) (fig. 3).

In mammals, PSA has exclusive homopolymeric structures of sialic acids joined by α-2,8-glycosidic bonds and the predominant unit is shown to be the Neu5Ac and Kdn. Readily synthesized PSA chain form a large, negatively and highly hydrated structure (Mühlenhoff et al., 1998).
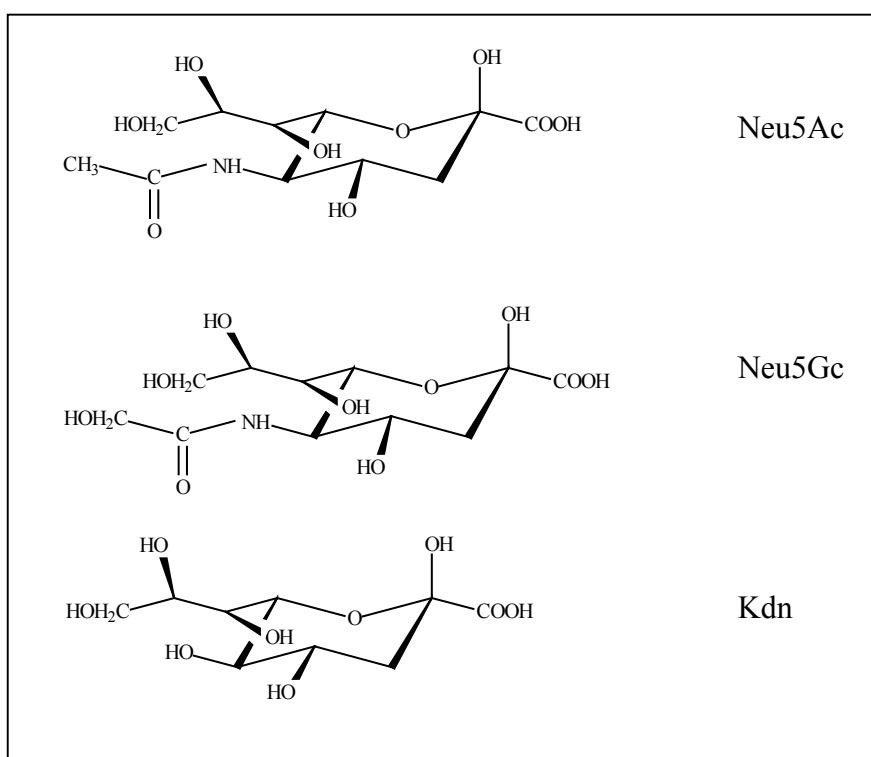


**Fig.3: Structure of the three major building units of polysialic acid:** 5-N-acetylneuraminic acid (Neu5Ac), 5-N-glycolylneuraminic acid (Neu5Gc) and 5-deamino-3, 5-dideoxyneuraminic acid (2-keto-3-deoxynonulosonic) acid, (Kdn) (Mühlenhoff et al., 1998).

## 4.2.2 Functions and structures of GalC and MGDG.

Galactosylation of ceramide and 1,2-diacylglyceride occurs in the endoplasmic reticulum lumen by a galactosyltransferase that uses UDP-galactose to form both GalC and monogalactosyldiacylglycerol (MGDG). GalC and its sulfated derivative (sulfatide) are galactolipids synthesized by oligodendrocytes in the CNS and Schwann cells in the PNS and comprise 20 and 7% of total myelin lipids, respectively, in the CNS (Taylor et al., 2003). In the last 20 years, GalC function was intensively investigated, both *in vitro* and *in vivo*. *In vitro* data indicate that GalC and sulfatide play a role in the mediation of calcium responses in oligodendrocytes (Dyer and Benjamins, 1991), in the cellular events like cell-axon interaction (Ranscht et al., 1987), in oligodendrocyte differentiation (Bansal and Pfeiffer, 1989) and the membrane sheath outgrowth (Dyer and Benjamins, 1990). The isolation of the gene encoding CGT has enabled the genetic analysis of its function. Particularly, Coetzee et al. (1996) and Bosio et al. (1996) used a gene targeting approach in embryonic stem cells to generate mutant mice with an inactive CGT gene. Analysis of CGT-null mice suggests that GalC plays an important role in the myelin structure and function, notably in the paranodal formation, in positioning of the myelinated internodal segment, the interaction of myelinated cells with axons and the stability of myelin structure.

Structurally, GalC is constituted of the sphingosine backbone, which is synthesized by the condensation of the serine with palmitate. The addition of a fatty acid to the sphingosine gives rise to ceramide, which is the substrate used to generate GalC. GalC occurs in two isoforms with a ratio of about ½, respectively, for NFA-GalC and HFA-GalC (Koul et al., 1988; Nonaka and Kishimoto, 1979; Shimomura et al., 1984). The structural analysis shows that differences between the two isoforms reside in the hydroxylation of the fatty acids. Cell fractionation data show a relative higher activity of CGT for the synthesis of HFA-GalC in the fraction enriched in Golgi markers than the one enriched in the endoplasmic reticulum markers. In contrast, the activity of CGT for the synthesis of NFA-GalC was higher in the ER-fraction (Vos et al., 1994).

In addition, the activity of CGT for the synthesis of the HFA-GalC is found in the myelin membrane (Costantino-Ceccarini and Suzuki, 1975; Koul et al., 1980), which contains in contrast a negligible activity for the synthesis of NFA-GalC (Koul et al., 1980).

MGDG [1,2-diacyl-0-(β-D-galactopyranosyl)-*sn*-glycerol] is formed by the transfer of galactose from UDP-galactose to 1,2-diacylglycerol (for structure, see Fig. 4). in the presence of the microsomal fraction of rat brain (Wenger et al., 1968; Inoue et al., 1971). Knocking out the CGT gene completely depletes the myelin membrane not only from GalC and sulfatide, but also from MGDG (Stoffel and Bosio, 1997), indicating that CGT is the enzyme responsible for the synthesis of GalC and MGDG. Wenger et al. (1968) and Inoue et al. (1971), also demonstrated that MGDG biosynthesis by the microsomal fraction of brain was non existent before 10 days of age, reaches a higher level at 17 days of age, and decreased to lower levels with age. Deshmukh et al (1971) also demonstrated that the accumulation of MGDG correlated with the myelination period. Further data (Schmidt and Althaus, 1994) indicate that MGDG is a marker of myelination and activates the protein kinase C during the formation of myelin.
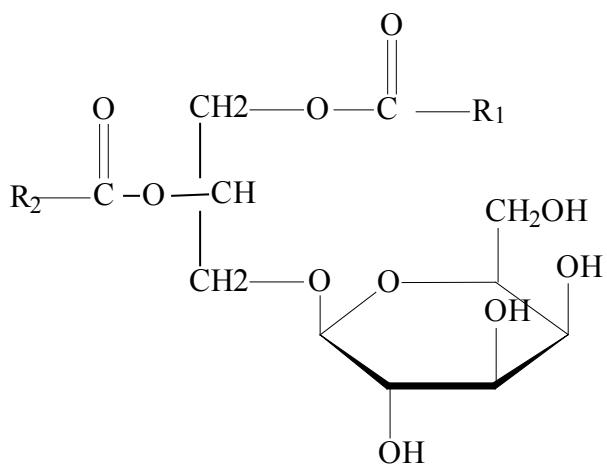


**Fig. 4: Structure of the monogalactosyldiacylglycerol**.

## 4.3 Cells of the nervous system: their generation and functions

The nervous system of vertebrates ensures rapid communication between widely separated parts of the body. The CNS starts to develop from a

homogenous cell mass by a process named gastrulation in which the ectoderm is generated (Odell et al. 1981; Wilt 1987). By a process called neurulation, which occurs during the early embryogenesis, the dorsal midline of the ectoderm rolls itself into a tube and its edges stick together and form the neural tube, a dorsal hollow nerve cord that constitutes the rudiment of the entire adult CNS (Colas and Schoenwolf, 2001). During the next stage of development, called "histogenesis" (formation of tissues), cells of the nervous system proliferate, migrate from the center of the neural tube to the peripheral location, mature by growth of the processes, myelinate and develop synapses with the other cells.

### 4.3.1 Neurons

The development of the brain after birth is due to an increase of the number of neurons, and supporting cells (glia), the development of neural processes and synapses, and the generation of myelin. Morphologically, mature neurons are constituted of the cell body, dendrites and axons. Each part plays a specific role in the neuronal function. For example, dendrites carry impulses to the main part of the neuron (cell body), while axons send impulses away from the neuron. Axons can be distinguished from dendrites by their smooth surface, and branches that appear farther from the cell body than those of dendrites. In addition, there is usually only one axon per cell body, whereas there are multiple dendrites. Different types of neurons have different morphologies. Also in the communicating role, neurons transmit signals to neighboring neurons via specialized connections called synapses. During transmission of a specific signal, impulses are sent from one neuron to the next throughout axons by migration of neurotransmitter-filled vesicles to the pre-synaptic membrane, followed by membrane fusion and release of neurotransmitters. In general, the fundamental task of the neuron is to receive, conduct, and transmit signals (Ramón y Cajal, 1937).

### 4.3.2 Glial cells

As the development of the brain proceeds, a new zone appears right beneath the ventricular zone, the sub ventricular zone (SVZ), which gives rise to many glial cells. Some of these cells migrate into the olfactory bulb where they give rise to neurons (Lois and Alvarez-Buylla, 1993; Doetsch and Alvarez-Buylla, 1996). In addition to neurons, the nervous system contains five major different types of non-neuronal cells, or "glia" cells. Glial cells actually form a bulk of cells of the nervous system, comprising over 90% of the total cells. Glial cell types include astrocytes, microglia, Schwann cells, oligodendroglia and satellite cells.

### 4.3.2.1 Astrocytes

Astrocytes can easily be distinguished morphologically by their star shape and are found in primary cultures of brain cells. Astrocytes have been classified as glial cell according to various criteria such as structures, locations, origins, antigenic profile and functions. On the basis of structure and function, two types of astrocytes can be identified: (1) fibrous astrocytes – these are predominantly present in the white matter and have small cell bodies with numerous extensions. A large number of microfilaments are characteristically present in the cytoplasm of these cells. (2) Protoplasmic astrocytes – these are predominantly present in the gray matter and have few microfilaments in their cytoplasm. These two types of astrocytes express different antigens and originate from two distinct precursor cells. A unique type of astrocyte, called the radial cells, appears transiently during embryogenesis of the cerebral cortex. A functionally distinct class of astrocytes called reactive astrocytes can be identified at the site of injury in the CNS (Ridet et al., 1997).

Functionally, astrocytes provide support during neural development, embryogenesis of the cerebral cortex, aid in maintaining the ionic homeostasis, clear the extracellular $K^+$, prevent $K^+$ accumulation during neuronal stimulation, provide nutritional support to neurons and help in

maintaining the blood brain barrier by extending "foot process" that may almost completely surround the brain capillaries. Furthermore, astrocytes are known to preserve host tissue following injury by secreting neurotrophic factors that protect neurons from damaging and also several proteases and protease inhibitors that modulate growth of neurites (Powell and Geller, 1999).

### *4.3.2.2 Microglia*

Among glial cell types of the CNS, microglia are macrophage-like cells of the brain that are capable of serving typical phagocytic functions. Although it is generally accepted that they are derived from mesoderm (del Rio-Hortega, 1932; for a contrary view, see Schelper and Adrian, 1986; Fedoroff, 1995), their developmental origin remains debatable (Theele and Streit, 1993; Altman, 1994). The two major views being that they derive either from neuroepithelial cells (Lewis, 1968; Neuhaus and Federoff, 1994) or from hematopoietic cells (ex. monocytes) (Perry and Gordon, 1988; Ling and Wong, 1993; Ling, 1979; Streit et al., 1988). Considering the last point of view, it is not clear whether they entered the fetal brain directly from a distinct pool of myelomonocyte stem cells or first entered the blood stream as circulatory monocytes (reviewed in Ling and Wong, 1993). However, the essential function of the ameboid microglia is considered to phagocytise dead cells, including neurons which undergo apoptosis in late embryonic to early postnatal stages (Nakajima and Kohsaka, 2001). As the brain develops ameboid microglia, decrease in number and appear to be replaced by increasing numbers of ramified microglia, which have small cell bodies with long branched processes. Although amoeboid microglia is generally believed to transform into ramified microglia during brain development, the exact relationship between these two types of microglia is still unclear. Ramified microglia is thought to be functionally inactive or in a resting state and are called "resting microglia". As long as the brain is maintained in healthy condition, the microglia cell density and ramified morphology is sustained (see Nakajima and Kohsaka, 2001).

### 4.3.2.3 Oligodendrocytes

During development of the vertebrate CNS, oligodendrocytes, the myelin-forming cells in the CNS, originate from the neuroepithelial cells of the neural tube. As mentioned above, during the development of the neural tube, two new zones appear: the ventricular zone and the sub ventricular zone (SVZ), which is the germinal matrix of the forebrain (Doetsch et al., 1997). Lineage tracing studies of perinatal SVZ cells using stereotactically injected retrovirus support the view that the majority of progenitors within this germinal matrix are glial precursors, that generate astrocytes and oligodendrocytes (Luskin et al., 1988; Levison and Goldman, 1993; McKerracher et al., 1994). Although the majority of cells give rise to homogeneous progeny, some SVZ cells give rise to both oligodendrocytes and astrocytes, and rare cells will develop into both neurons and glia (Levison and Goldman, 1993). Nevertheless, according to other data, it doesn't seem that all oligodendrocytes originate from the same area of the SVZ. In the neonatal rat cerebrum, oligodendrocytes arise postnatally from the lateral ventricles of the SVZ (Levison and Goldman, 1993; Zerlin et al., 1995). Similarly, several studies using transgenic mice (plp-LacZ) (Spassky et al., 1998), the 5-bromo-2´-deoxyuridine (BrdU) incorporation assay (McMahon and MacDermott, 2001) and a special dye (Dil) associated with specific markers of the oligodendrocytes lineage (Warf et al. 1991), demonstrate that oligodendrocytes of the spinal cord arise from the ventral and dorsal VZ after birth and migrate to the peripheral regions of the cord. However, glial precursors use radial glia to migrate from their onset sites to the sites of the differentiation and maturation (O´Rourke et al., 1992). The most important function of oligodendrocytes in the CNS and Schwann cells in the PNS is to synthesize the myelin sheath which wraps axons at certain positions in order to increase the nerve conduction velocity in a saltatory manner.

### *4.3.2.3.1 Differentiation and maturation of oligodendrocyte progenitors*

Oligodendrocyte appear subsequently along the spinal cord in a rostrocaudal wave of differentiation, first in the ventral funiculus and later in the dorsal and lateral funiculi, the large axonal bundles that become the white matter tracts of the spinal cord (Yu et al., 1994). Post mitotic oligodendrocytes appear in the forebrain only after birth. Apart from their origin, differentiation and maturation of oligodendrocytes proceeds through distinct stages, which can be identified by dramatic changes in cell morphology and by various markers, some of which are characteristic myelin components. Numerous stages have been reported (Fig. 5), but they can be simplified and placed into two main groups: an immature stage (also called premyelinating stage), where oligodendrocytes are post mitotic but do not myelinate yet, and a mature myelinating stage. Note that differentiation of mouse oligodendrocytes is similar to that of rat after the stage at which O4 is acquired, whereas mouse progenitors show greater variety at the level of progenitor and pre-oligodendrocytes stages, both in their morphology and in the expression of markers, such as A2B5 and GD3 (Fanarraga et al., 1995).
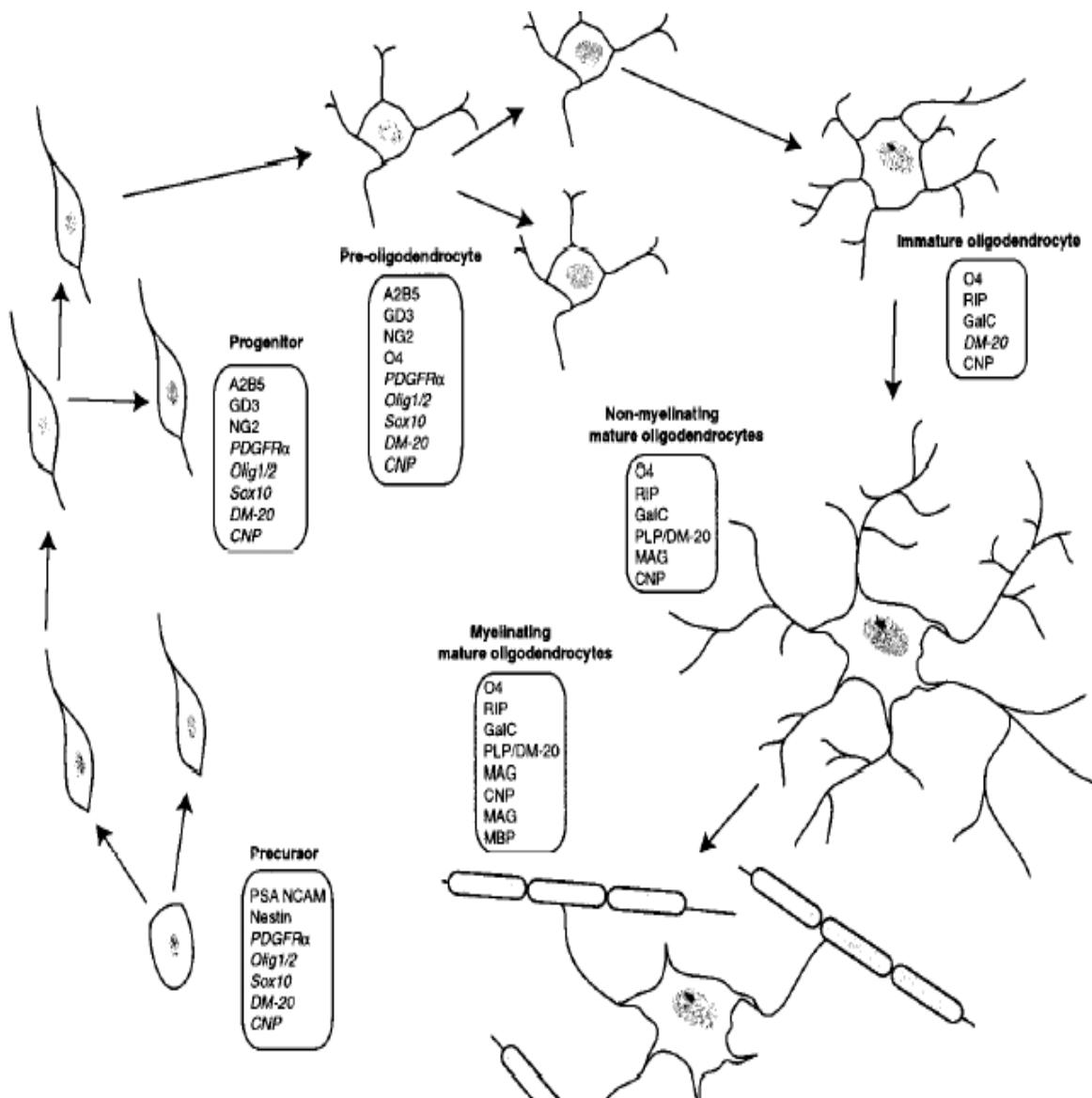
**Fig. 5: Schematic representation of oligodendrocyte development:** Schematic drawing of the morphological and antigenic progression from precursor cells to myelinating matures oligodendrocytes, through progenitors, pre-oligodendrocytes, and immature non-myelinating oligodendrocytes in the rat. Stage-specific markers are boxed. RNA is in italics. Scheme was adapted from Baumann and Pham-Dinh, 2001.

In all cases, at the progenitor stages, oligodendrocytes express different cell surface or intracellular markers like gangliosides, which are recognized by the A2B5 antibody (Eisenbarth et al. 1979), ganglioside GD3, platelet-derived growth factor α-receptor and polysialylated neural cell adhesion molecule (PSA-NCAM) for example (Grinspan and Franceschini, 1995; Hardy and Reynolds, 1991).

During the next phase of differentiation, the progenitors loose their migratory capacity and some intracellular markers such as A2B5, ganglioside GD3

(Rettig and Old, 1989) and finally are not more able to react with growth factors like FGF and PDGF (Fok-Seang and Miller, 1994). At this stage of differentiation, oligodendrocytes are called pre-oligodendrocytes (Hardy and Reynolds, 1993), which are morphologically characterized by the loss of bipolar shape, acquisition of multi-process shape and also featured by the expression of new kinds of antigenic markers which are important for their maturation and survival. The cellular markers appearing at this stage are O4, RIP, GalC, DM-20 and CNPase. Following this stage of differentiation, oligodendrocytes are characterized by an increase in the process number and the expression of the terminal markers such MBP, PLP, MAG, which are important in the synthesis of the myelin membrane.

## 4.4 Myelination

Myelination is a developmentally regulated process involving the co-ordination of expression of genes encoding both myelin proteins and the enzymes involved in myelin lipid metabolism (Campagnoni and Macklin, 1988). This process is undertaken by oligodendrocytes and Schwann cells in the CNS and PNS, respectively. It also includes the process of neuron-glia cell recognition, molecular assembly of myelin components (lipids and proteins) and compaction of membranes to form lamellar structures called myelin (Fig. 6).

During the nervous system development, myelinogenesis starts in rodents after birth and within a couple of days large amounts of plasma membranes are synthesized by oligodendrocytes and Schwann cells, respectively, in the CNS and PNS (Frank et al., 1999). The myelinating cells extend processes to recognize neuronal axons by cell surface receptors. The receptors generate intracellular signals in oligodendrocytes (Umemori et al., 1999) and Schwann cells, which enable them to wrap around axons to form myelin. The mechanism of myelin formation comprises sequential steps involving migration of oligodendrocytes to the axons that are to be myelinated, the adhesion of the oligodendrocyte process to the axon and the spiraling of the membrane

around axons, with a predetermined number of myelin sheaths and the recognition of the space not to be myelinated (the node of ranvier).
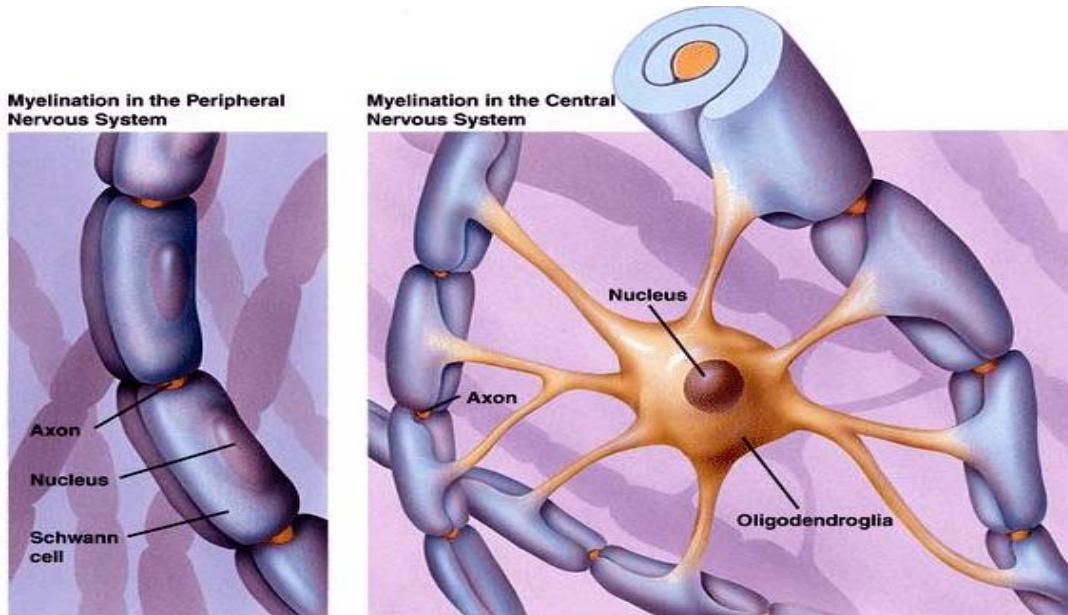


**Fig. 6: Myelination of PNS and CNS axon**. The principal function of oligodendrocytes is to provide support to axons and to produce the myelin sheath, which insulates axons. Myelin consists of 80% lipid and 20% protein and allows for the efficient conduction of action potentials down the axon. Oligodendrocytes unlike Schwann cells of the PNS, form segments of myelin sheaths of numerous neurons simultaneously. As can be seen in the above illustration, the processes of a given oligodendrocyte wrap themselves around portions of the surrounding axons. As each process wraps itself around, it forms layers of myelin. Each process thus becomes a segment of the axon's myelin sheath (Schematic diagram from J. Martin Collinson., School of Medical Sciences, University of Aberdeen, Scotland, UK. m.collinson@abdn.ac.uk).

The signal indicating which axon should be myelinated remains unclear. Studies in the CNS support the idea of a critical diameter for myelination, but individual axons are not myelinated along their entire length simultaneously, indicating that other factors are involved (Suzuki and Raisman, 1994). Axons probably participates in the regulation of this event, since it is known that axons regulate myelin thickness and that single oligodendrocyte myelinates, simultaneously, axons with different diameters (Waxman and Sims, 1984). The relation of astrocytes with myelination has been described by studying mice carrying a null mutation for the glial fibrilary acidic protein (GFAP) (Liedtke et al., 1996). Investigators have demonstrated that these mice display abnormal myelination, and non-myelinated axons are numerous in the optic nerve and spinal cord. The altered white matter vascularization, possibly linked to the abnormal astrocytic processes, may be related to the dysmyelination

observed. Moreover, transgenic mice carrying several copies of the human GFAP gene die by the second postnatal day from a fatal encephalopathy (Brenner et al., 2001). These data and others show that astrocyte as well as neuron and other oligodendrocyte markers represent factors that regulate the myelin formation.

## 4.5 Myelin components and functions

Differentiated oligodendrocytes synthesize large amounts of myelin membrane, which is made up of proteins and lipids. In contrast to most plasma membranes, myelin has a specialized lipid composition and contains a restricted set of proteins. The lipid contents of the myelin membrane represents about 70 to 80% of the myelin dry weight (Dupree et al., 1998) and is constituted mostly cholesterol, complex phospholipids and glycosphingolipids.

### 4.5.1 Myelin sphingolipids and their functions

The lipid molecules that show the most striking and consistent asymmetry in their distribution in the plasma membranes of vertebrate cells are some oligosaccharide-containing lipid molecules called glycosphingolipids. Glycolipids are glycosyl derivatives of lipids such as acylglycerols, ceramides and their sulfated derivatives. They are collectively part of a large family of substances known as glycoconjugates. A subclass of glycolipids called glycosphingolipids which is synthesized from ceramide exists in animals. These glycosphingolipids have a general structure that is similar to that of the glycerol-based lipids, having a polar head group and two hydrophobic fatty acid chains. One of the fatty acid chains is initially coupled to serine to form sphingosines, to which a second fatty acid chain is then ligated to form ceramide (Hakamori, 1986) by a reaction catalyzed by sphinganine synthases and acyl-CoA transferase, respectively.

Sphingolipids are typically found in eukaryotic cells, where they comprise a small but vital fraction of the membrane lipids. Based on the type of head-group attached to the C1, sphingolipids are classified as phosphosphingolipids or glycosphingolipids. The phosphosphingolipid sphingomyelin (SPM) in animals and inositol phosphoceramide (IPC) in plants and fungi carry the polar head group's phosphocholine and phosphoinositol, just like the major glycerolipids phosphatidylcholine (PC) and phosphatidylinositol (PI). In glycosphingolipids, the head group can contain a variety of monosaccharides linked by glycosidic bonds.

The function of sphingolipids has been investigated by *in vitro* and *in vivo* studies using cell transfection experiments or knockout mice. It is in this way that yeast and Chinese hamster ovary cell mutants lacking the first committed enzyme in sphingolipid biosynthesis, serine palmitoyl-transferase, die in the absence of externally added sphingoid base (Hanada et al., 1992; Wells and Lester, 1983). Sphingomyelin fulfill a vital role in mammalian cells, since the mutant could be rescued by exogenous sphingomyelin (Hanada et al., 1998; Hanada et al., 1992). *In vivo* studies using gene knockout mice have also provided substantial insight into the importance of the sphingolipids in the mammalian kingdom. Hence, mice lacking GlcCer and all complex glycosphingolipids were found to be embryonically lethal at the gastrulation stage just after the formation of the primitive germ layers (Yamashita et al., 1999). Furthermore, knockout mice lacking a functional CGT were not able to breed and displayed a compromised nerve function (Bosio et al., 1996; Coetzee et al., 1996), indicating a function of glycolipids in the spermatogenesis and myelin structure. Analysis of epithelial cells lining the gastrointestinal and part of the urogenital tract (Simons and van Meer, 1988) shows high concentration of GlcCer (murine) and/or GalC (bovine, human) and derivatives in the apical plasma membrane domain, indicating the implication of glycosphingolipids in the mechanical stability of the plasma membrane, especially in the gut, protection against harmful, hydrolytic enzymes such as phospholipases. Other data indicate that glycosphingolipids could be involved in specific recognition events between cells and between

cells and the extracellular matrix via their carbohydrate moiety and the modulation of plasma membrane signal processing (Sheikh et al., 1999; Takamiya et al., 1996).

### 4.5.2 Myelin specific proteins and their functions

Myelin proteins are among the most abundant in the nervous system, and generally, they have been considered to be expressed only in myelin-forming cells. The major myelin proteins, representing 70 to 80% of the protein content of the membrane are separated into two classes: the basic proteins and the proteolipid proteins. Many researchers have attempted to determine the patterns of myelin protein gene expression in the developing brain from several species. *In vivo* studies indicate that the developmental profile of PLP synthesis peaks a few days later than that of MBP synthesis in the mouse brain, i.e., 21 or 22 days for PLP against 18 for MBP (Campagnoni and Hunkeler, 1980). These proteins classes consist of multiple polypeptide chains derived from alternative splicing of a single gene (Campagnoni and Macklin, 1988). In mice, the myelin basic proteins are composed of at least six isoforms in mice (deFerra et al., 1985; Newman et al., 1987a, b) with a molecular weight of 14, 17, 18.5, 20, 21.5 kDa, and four in humans (Kamholz et al., 1986; Roth et al., 1986, 1987). Other names such as SBP (for the 14 kDa MBP), LBP (for the 18.5 kDa), prelarge (for the 21.5 kDa) and presmall (for the 17 kDa) also appear in the literature. MBP is hydrophilic, membrane associated protein with isoelectric point greater than 10.6, making them more basic than histones (Lees and Brostoff, 1984). MBP is localized to the major dense line (MDL) of myelin, which is formed by apposition of the cytoplasmic surfaces of the extruded oligodendroglial plasma membrane during myelinogenesis, and appears to be associated with the cytoplasmic side of the unit bilayer (Campagnoni et al., 1980; Omlin et al., 1982). Functionally, MBP plays a crucial role in the compaction of the opposing cytoplasmic surfaces of the plasma membrane (Omlin et al., 1982; Campagnoni and Skoff, 2001).

In contrast to MBP, PLP is constituted of two isoforms: the proteolipid protein with a molecular mass of 30 kDa and the DM20 with a molecular mass of 26 kDa (Spörkel et al., 2002). DM20 differs from PLP by an internal deletion of 35 amino acids (Trifilieff et al., 1986) and genetic studies established the location of these amino acids deletion in exon 3B of the PLP gene (Nave et al., 1987). The amino acid sequence of PLPs has been deduced from their corresponding cDNA in many species, and their strong conservation among species was noted by many researchers (Macklin, 1992; Hudson, 1992). The proteolipid proteins are integral membrane proteins, constituting about 50% of the total protein content of myelin. They are extremely hydrophobic and aggregate easily under a variety of experimental manipulations (Agrawal and Hartman, 1980; Lees, 1982). Functionally, PLP has been shown to have a structural role in the myelin sheath.

Several other proteins and enzymes are associated to myelin, making up the remainder of 20 to 30 % of its protein content (Lees and Sapirstein, 1983). MAG is the glycoprotein associated with CNS, has a molecular mass of around 100 kDa on SDS gels and constitutes nearly 1 % of the total myelin proteins (Quarles, 1979; Quarles et al., 1983). MAG expression occurs in a time-specific manner and yields the L-MAG (72 kDa) isoform predominantly expressed at an early and S-MAG (67 kDa) isoform at a late stage of myelination (Lai et al., 1987; Tropak et al., 1988; Inuzuka et al., 1991; Pedraza et al., 1991). A significant portion of MAG is localized at the extracellular surface of the membrane and shares a carbohydrate determinant with a number of molecules such as NCAM, L1, J1, which mediate cell-cell interactions in the nervous system. MAG is also known to mediate axon-glial contact during myelin assembly (Holley and Yu, 1987; 1987; Trapp, 1990).

CNPase is a myelin minor protein that catalyses the hydrolysis of several 2′, 3′cyclic nucleotide monophosphates. The activity of this enzyme is very high in the CNS and is mostly localized in myelin (Olafson et al., 1969). Structurally, CNPase is composed of two polypeptide chains (Sprinkle et al., 1980a) with a molecular weight between 46 and 48 kDa. This protein was also found in mammalian photoreceptor cells, testis and lymphocytes. Although the

biological function of CNPase is unknown, it is thought to play a significant role in the maintenance of axon-glia interactions at nodes of Ranvier in the CNS, where it comprises 4% of total protein (Kozlov et al., 2002; Rasband et al., 2005).

### 4.5.3 Myelin structure and functions

Myelin is a tightly compacted multilamellar sheath that surrounds axons to promote saltatory conduction of nerve impulses, thus increasing the speed of the nerve conduction. This membrane, which is produced by oligodendrocytes in the CNS and Schwann cells in the PNS, is a specialized extension of the plasma membrane of these two glial cell types (Wright et al., 1997). Myelin, as well as many of its morphological features, such as nodes of Ranvier, can be seen readily in light microscopy. However, much of our understanding of the organization of the myelin sheath has been derived from biophysical techniques (polarized light, X-ray diffraction and electron microscopy). Myelin, examined by polarized light, exhibits both a lipid-dependent and a protein-dependent birefringence (Raine, 1984).
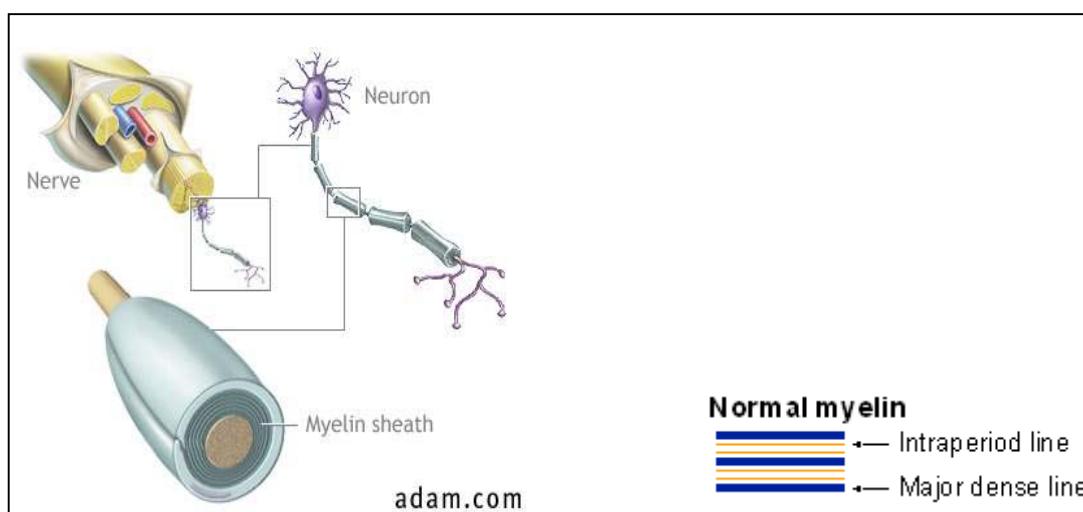


**Fig. 7 Schematic diagram of a nerve and myelinated axon**. Pictures show a neuron with its myelinated axon and a detailed structure of the myelin displaying intraperiod lines and major dense lines. For reference, see www.thirdage.com/adam/ency/article/000737trt.htm

This suggests that myelin is build up of layers where lipid components are oriented radially to the axis of the nerve fibers (Hirano and Dembitzer, 1967). X-ray diffraction analysis suggests a repeated unit of dark and clear lines in the myelin structure (Norton, 1977). Taken together, these results suggest that proteins and lipids have an alternative "protein-lipid-protein-lipid-protein" disposition. During the recent years, the myelin structure has been investigated and is known to be compatible with the "fluid mosaic" model of the membrane structure, including the intrinsic transmembrane proteins as well as extrinsic proteins (Kirchner and Blaurock, 1991). Electron microscopic analysis of the myelin sheath, visualizes myelin as a series of alternating dark and less dark lines (protein area), separated by unstained areas (lipid area) (Morell at al., 1994) (fig. 7). Furthermore, Myelin segments are separated by uncovered regions: the so called nodes of Ranvier. At these regions, Hirano and Dembitzer (1967) have demonstrated that the cytoplasmic surfaces of myelin are not compacted, and Schwann cells or oligodendrocyte cytoplasm is included within the sheath.

## 4.6 Myelin-related diseases

Diseases of myelination, whether acquired or inherited, are severe disorders of nervous system. The integrity of myelin sheaths is dependent on the normal functioning of myelin-forming oligodendrocytes in the CNS and Schwann cells in the PNS as well as on the viability of the axons that they wrap. Deficiencies of myelin can result from multiple causes, including viral infections, inherited disorders, toxic agents, malnutrition, and mechanical trauma that affect myelin, myelin-forming cells, or myelinated axons (Quarles et al., 1994). In some acquired disorder of myelin, the causes are external. In most of the cases, the lesions are disseminated in the nervous system and are characterized by periventricular demyelination and inflammation, macrophage activity, sudanophilic deposits consisting of myelin degradation products, and relative sparing of axons (Morell, 1984; Vinken et al., 1985).

The most commonly acquired disorder of myelin is multiple sclerosis (MS), causes of which are not well established. Nevertheless, researchers believe the combination of heredity, immune system, and possibly a virus may play a role in a person developing MS (http://www.bandagainstms.org/msinfo_cause.html). The clinical aspects of MS are highly variable both in symptoms and clinical course. The most typical form of the disease begins during the third or fourth decade of life, and characterized by exacerbations, and remissions over many years (Morell, 1984; Martin et al., 1992; Rodriguez, 1989). Structurally, patients show lesions in the white matter with a breakdown of the blood brain barrier (BBB). Biochemical analysis of MS patients shows an increase of catabolic enzymes and a severe loss of myelin proteins and lipid components (Morell et al., 1984).

Storage diseases or lysosomal enzymopathies are rare degenerative disorders which, in the majority of cases result from a genetically-determined defect of a specific lysosomal enzyme. Most storage diseases have an autosomal recessive mode of inheritance, affecting both males and females. The onset of the disease manifests diffuse neurological dysfunction, and have progressive, inexorable course, leading to death.

Among the disorders of myelin, leukodystrophies are a large group of inherited disorders of the CNS and are characterized by a severe deficiency of myelin. Biochemically, some leukodystrophies are characterized by a sphingolipidosis in which some specific lipid accumulates, due to a genetic lesion in an enzyme that is involved in its catabolism, as already described in the Metachromatic leukodystrophy (MLD: demyelinating disease) and Krabbe´s disease (Globoid Cell Leukodystrophy: dysmyelinating disease) which are two classic genetic myelin disorders.

MLD is a recessively inherited disease characterized by intralysosomal storage of sulfatide resulting from a complete or partial deficiency of arylsulfatase A (ASA) activity. A number of clinical variants of MLD have been described, including late-infantile, juvenile, and adult forms (Kihara et al., 1982; Gieselmann et al., 1991). Genetic heterogeneity within MLD is indicated by both absence and presence of ASA polypeptides in fibroblast from patients

(von Figura et al., 1983; Bach and Neufeld, 1983). The mutation in MLD can affect the apparent rate of synthesis, stability and the catalytic properties of ASA (von Figura et al., 1986). In some cases of MLD, ASA is normal and the impaired degradation of sulfatide results from a deficiency of the activator protein saposin B (Stevens et al., 1981).

Krabbe's disease is a rare, inherited degenerative disorder of the nervous system in which a specific enzyme deficiency (Galactosylceramide beta-galactosidase) leads to the destruction of myelin. Two types based on the age of onset are recognized: (a) Infantile-onset Krabbe disease is featured by the appearance of symptoms at 3 to 6 months of age and (b) the adult type. The biochemical characteristic is the abnormal turnover of the myelin sheath. Enzyme deficiency blocks degradation of cerebrosides and its deacylated derivative galactosylsphingosine (psychosine), resulting in their increased concentration, which contributes to degeneration of the white matter of the brain, and the elevation the protein level of the cerebrospinal fluid (Kolodny et al., 1991).

# 5   <u>MATERIALS AND METHOS</u>

## 5.1 Generation of the targeting constructs

### 5.1.1 Generation of the rat CGT and PST-1/ST8SialV cDNA

pcDNA3/CGT (10 ng) (a kind gift of Dr. Popko) were mixed with 10 U Pfu polymerase (Qiagen. Hilden, Germany) in the presence of a mixture containing 0.2 mM dNTPs, 1X Pfu buffer [20 mM Tris-HCl pH 8.8, 2 mM $MgSO_4$, 10 mM $(NH_4)_2SO_4$, 10 mM KCl, 0.1% Triton X-100, 1 mg/ml BSA]. The following nucleotide sequences, harboring the AscI and PacI restriction sites, respectively, were used as primers: (forward) 5´-CATG<u>GGCGCGCC</u>ATGAAGTCTTACACTCC-3´ and (reverse) 5´-CATGA<u>TTAATTAA</u>TCATTTCACTTTCTTTTCATG-3´ (Sigma, Germany). Amplification was performed using the following conditions: 1 cycle at 94°C for 2 min.; 35 cycles (94°C 30 seconds, 55°C 30 seconds, 68°C 2minutes) 1 cycle 68°C 7 minutes. PCR products were separated from the primers by gel isolation.

Polysialyltransferase (PST-1/ST8SialV) cDNA was released from a recombinant pBS (SK)-PST using HindIII and XbaI and treated with Klenow enzyme (fill in reaction).

### 5 1.2 Ligation, transformation and sequencing

The rat UDP-galactose:ceramide galactosyltransferase (CGT) PCR fragment was ligated into the PacI/AscI sites present in the PLP promoter cassette using a mixture containing 10 ng of the rat CGT cDNA, 2.5 ng of the PacI/AscI linearized PLP promoter cassette in the presence of 5U T4 DNA ligase (MBI Fermentas, Germany) at 16°C overnight.

For the mouse PST-1/ST8SialV, PLP promoter cassette was linearized with PmeI enzyme, blunt ended as described above and dephosphorylated using alkaline phosphatase. Finally, the blunt ended PST-1/ST8SialV cDNA was

ligated in the PLP promoter cassette as described above and the orientation determined by sequencing and restriction digestion.

4 µl of the ligation solution were used to transform the DH5α bacterial strain. Colonies were picked, cultured overnight and screened for the presence of the recombinant plasmid.

Automatic Taq DyeDeoxy Terminator Cycle sequencing of both strands of rat CGT and mouse PST-1/ST8SiaIV cDNA was performed on plasmid templates and an ABI Model 310 prism system (Applied Biosystems) was used to read the sequence. Primers listed in the table below were used for sequencing (PLP-CGT) and the PCR program was: 2 min. at 96°C, 25 cycles (10 sec. 96°C, 5 sec. 50°C, 4 min. 60°C).

| Primer name | Rat CGT |
|---|---|
| HCGT6 | 5´-CGCTGTCCATCAGATCTCC-3´ |
| Rat CGT2 | 5´-AACTGTGCTGTGCGTACTCC-3´ |
| CGT AscI | 5´-CATGGGCGCGCCATGAAGTCTTACACTCC-3´ |
| Hu CGT3 | . 5´-CTTCTGGTAGTGGGCTGG-3´ |
| RatCGT1 | 5´-ATGTACTGACGTAGCACTGG-3´ |
| RatCGT2 | 5´-AACTGTGCTTGTGGGTACTCC-3´ |
| RatCGT3 | 5´-AGGGTCAACCAGTAGCAGG-3´ |
| RatCGT4 | 5´-CCTCTCTCGTGCAAGGC-3´ |
| RatCGT5 | 5´-AATGGAATCCTCAATGGCAG-3´ |
| RatCGT6 | 5´-CAGCCCTTGCTATTCCAACA-3´ |
| RatCGT7 | 5´-CCTGCCTAACGTTGTATATG-3´ |
| RatCGT8 | 5´-GTGATTTGGAGGTTTTCTGG-3´ |
| RatCGT9 | 5´-ACTACATTCTTCGCCACGAC-3´ |

**Table 1. Primers list used to sequence the rat CGT cDNA.**

## 5.2 Activity test of the PCR amplified rat CGT cDNA.

The activity test of the PST/ST8Sia IV cDNA was performed during the generation of the Thyl/PST/STSia IV transgenic mice.

### 5.2.1 Sub-cloning of the rat CGT into pcDNA 3.1

In order to determine if the PCR amplified rat CGT cDNA generated is active, CGT cDNA was released from the PLP-CGT plasmid using the PacI/AscI enzymes, blunt ended using the Klenow enzyme and ligated into the HindIII site in the pcDNA3.1 vector. The orientation of CGT insert in the pcDNA3.1 vector was 5´→3´and was determined both by sequencing and restriction digestion of the generated pcDNA3.1-CGT plasmid. A large amount of the recombinant plasmid was prepared according to Qiagen DNA MIDI preparation method and the concentration determined spectrophotometrically (Beckman).

### 5.2.2 Cell culture and transfection

The day before the transfection, cells (CHO wild type and stably transfected CHO-CGT) were trypsinized and seeded on poly-L-lysine (0.1 mg/ml) coated coverslips at a concentration of 40,000 cells per coverslip. After 24 hours, transfection was performed as follows: 2 μg of the plasmid DNA was mixed to 50 μl NaCl (150 mM). At the same time, 6.6 μl Exgen500 reagents were mixed to 43.4 μl sterile NaCl (150 mM). DNA and Exgen500 solutions were then mixed and incubated for 10 min. at RT. During RT incubation of the previous mixture, cells were washed with phosphate buffered saline (PBS) in order to deplete the cells from the FCS. Transfections were finally undertaken by incubating the cells with 250 μl of the Exgen500-DNA complex per ml serum free RPMI medium for 3 hours at 37°C and under 5% $CO_2$. The transfection was terminated by changing the medium to DMEM supplemented with 5%

serum, 2 mM glutamine, and 100 U/ml penicillin 100 U/ml streptomycin and cultured for 48 hours at 37°C under 5% $CO_2$.

### 5.2.3 Analysis of the transfected cells.

48 hours after transfection, the cells grown on the poly-L-lysine coated coverslips were washed with phosphate-buffered saline (PBS: 137 mM NaCl, 2.7 mM KCl, 4.3 mM $Na_2HPO_4$ $7H_2O$, 1.4 mM $KH_2PO_4$ pH 7.4), treated for 7 min. at -20°C with 100% methanol, and fixed in 4% PFA for 30 min. at RT. Non specific binding sites were blocked using 1% BSA in PBS for one hour at RT. Cells were finally labeled using the rabbit anti-GalC diluted (1/200) in PBS containing 1% BSA for 2 hours at RT, followed by 3 times 5 min. washing with PBS. Immunofluorescence analysis was terminated by incubating the cells with a FITC-labeled goat anti-rabbit antiserum for 1 hour at RT and followed by 3 times washing as described above. Coverslips were mounted on the microscopic slide using gelatin and positive cells documented by fluorescence microscopy on an Axiovert M instrument (Carl Zeiss, Halbergmoos, Germany).

## 5.3 Generation and identification of the founder mice

### 5.3.1 Purification of DNA for microinjection

Recombinant bluescript plasmid (30 µg) was linearized at 25°C for 12 hours in the presence of 25 U ApaI in 20 mM Tris-acetate pH 7.9 containing 10 mM magnesium acetate, 1 mM dithiothreitol and 1% BSA. After 12 hours of digestion, linearized plasmids were further digested in the presence of 25 U NotI at 37°C for 12 hours. DNAs fragments were separated onto 0.8% agarose gel in TAE (40 mM Tris-acetate pH 8.5, 2 mM $Na_2EDTA$ $2H_2O$) buffer at 80 volts for 2 hours. The band of interest was visualized (UV light 360 nm) and excised. DNA was extracted from the gel by electroelution at 100 volts for 45 min. in dialysis bags [preparation of the bag: (1) boil the bag for 10 minutes in 2% (w/v) $Na_2CO_3$ containing 1 mM EDTA, (2) wash with distilled water, (3) boil in 1 mM EDTA solution for 10 minutes, (4) wash with water and store it at 4°C],

using 0.2X TBE (2.2 g of Tris, 1.1 g of Boric acid, 0.8 ml of 0.5 M EDTA pH 8.0. add 1000 ml $H_2O$) as elution buffer. Eluted DNA was further precipitated as described [mix DNA solution to 1/10 (v/v) 3 M NaAc, add 2.5 volumes of 100% ethanol, mix it and incubate at –20°C overnight]. The pellet collected by centrifugation (20,800 xg at 4°C) was dissolved in low salt buffer (20 mM Tris-HCl pH 7.4, 0.2 M NaCl, 1 mM EDTA).

For Elutrap (Schleicher & Schuell, Germany) purification, DNA previously re-suspended in low salt buffer was bound to the mini column by passing it through the activated matrix (Activation of the matrix: wash matrix two times with 5 ml of the low-salt buffer through a matrix at approximately 0.5-1.0 ml/min.) at approximately 1-2 drop/second. Matrix was washed twice with 2 ml of the same buffer and DNA eluted using 0.5 ml high salt buffer (1.0 M NaCl, 20 mM Tris-HCl, and 1.0 mM EDTA). Finally, DNA was precipitated as described above, resuspended in the microinjection buffer (10 mM Tris-HCl pH 7.5, 0.1 mM EDTA and sterilize by filtration using a 0.2 µm filter) and quantified by comparing the band intensity on an ethidium bromide (0.5 µg/ml) agarose gel to the one of the lambda HindIII marker (MBI Fermentas, Steinheim, Germany).

### *5.3.2 Microinjection and oocytes transfer*

PLP-CGT and PST-1/ST8SiaIV transgenic mice were generated at the Karolinska Center for transgene technology (Stockholm, Sweden). Briefly, a 11.362 kb (PLP-CGT) or 10.86 kb (PLP-PST) ApaI-NotI (New England Biolabs, Frankfurt, Germany) fragments containing the PLP promoter fused to the rat CGT cDNA or mouse PST was gel isolated, purified using the Elutrap system (Schleicher & Schuell, Germany) and injected into the fertilized mouse eggs from F2 C57BL/6xCBA strain.

### 5.3.3 Southern blot identification of the transgenic founder mice

In order to determine which founder mouse carry the transgene, southern blot analysis of genomic DNA extracted from mouse tail was performed. After overnight digestion of the mouse tails at 56°C using 100µg proteinase K solution [proteinase K solution: 10 µg/µl in 10 mM Tris-HCl (pH 8.0), 25 mM EDTA, 150 mM NaCl and 1% SDS (Roche Diagnostic, Mannheim, Germany)], genomic DNA was extracted by the phenol/chloroform method, followed by precipitation of DNA with 100% ethanol, washing in 70% ethanol, drying at RT and re-suspension in water. DNA fragments generated by SspI (1.9 kb for PLP-CGT) and AccI (0.8 kb for PLP-PST) digestions of genomic (10 µg) DNA, were separated on 1% agarose gel and transferred onto HybondN+ (Amersham Pharmacia Biotech., Germany) nylon membranes. After transfer, DNA was immobilized on the membrane by heating for 2 hours at 80°C.

A 2.4 kb of the rat CGT and 1 kb of the mouse PST-1/ST8SiaIV cDNA fragments were used as template for the synthesis of the $^{32}$P-labeled DNA, as follows:

| | |
|---|---|
| DNA | 25 ng |
| Random primers | 5 µl |

Water to a final volume of 50 µl was added, incubated at 100°C for 5 min. and at RT for 10 min.

| | |
|---|---|
| Buffer (5X) | 10 µl |
| [$^{32}$P]dCTP (10µCi) | 5 µl |
| Klenow (1U/µl) | 2 µl   incubate the mixture for 10 |

min. at 37°C. Labeled-probes were purified using G-25 sephadex column by centrifugation for 5 min.at 240 xg.

Membranes were prehybridized for one hour at 42°C using a mixture of 50% formamide, 4.8X SSC, 10 mM Tris HCl pH 7.5, 1% SDS, 1X Denhardt´s solution, 10 % Dextransulfate (Sigma-Aldrich, Steinheim, Germany) supplemented with 100 µg/ml heat denatured salmon sperm DNA (Sigma-Aldrich, Steinheim, Germany). Following prehybridization, hybridization was carried out overnight in the same solution and at the same temperature, using

2 x 10$^6$ cpm/ml heat denatured $^{32}$P-labeled DNA probes. Membranes were washed twice for 10 min. at RT with 2X SSC containing 0.1% SDS and twice for 20 min. at 65°C using 0.2X SSC containing 0.1% SDS. Membranes were finally packed in plastic bags and exposed Membranes were exposed to pre-flashed Fuji Bioimager screen and subsequently to X-ray film at -80°C.

## 5.4 UDP-galactose:ceramide galactosyltransferase assay

The CGT activity assay used was based on the protocol described by Sprong et al. (2000) with some modifications. Briefly, brains were homogenized in 250 mM sucrose, 10 mM Hepes/NaOH (pH 7.2), 1 mM EDTA, and 1 mM PMSF. A postnuclear supernatant was prepared by centrifugation at 500×g for 10 min. at 4°C and stored at –80°C. Protein concentration was determined using the DC protein assay (Biorad, München, Germany). The homogenate was adjusted to a protein concentration of 4 mg/ml and incubated with 0.4% saponin on ice for 30 min. One volume (30 µl) of the homogenate was mixed with one volume of the reaction buffer containing 200 µM [14C]-UDP-galactose (30 kBq/ml) (Amersham Bioscience, Freiburg, Germany), 30 µM C6-ceramide (Biomol, Hamburg, Germany), 2% bovine serum albumin, 4 mM MgCl$_2$, 4 mM MnCl$_2$, 250 mM sucrose, 10 mM Hepes (pH 7.2), 1 mM EDTA and incubated at 37°C for 30 min. Control reactions were done in the absence of C6-ceramide. Reactions were stopped by addition of 500 µl chloroform/methanol (2:1) and 100 µl, 150 mM NaCl. The aqueous phase was washed once with chloroform and the combined organic phases were dried and separated by TLC on silica gel 60 plates using chloroform/methanol/water (70:30:4) as the solvent system. Radioactivity was detected using a Fuji Bioimager BAS 1000. Differences were tested for significance using Student's t-test.

## 5.5. Northern blot analysis

### 5 5.1 RNA isolation by CsCl and trizol solutions

All solutions are prepared in diethylpropyl pyrocarbonate treated water (DEPC. Sigma-Aldrich, Steinheim, Germany) prepared as follows: mix overnight 1 ml DEPC per ml double distilled water was mixed overnight at RT and autoclave. Mouse brains at different ages (PLP-CGT: 2, 4, 12 weeks; PLP-PST: 2, 4, 24 weeks) from transgenic and wild type littermates mice were collected, frozen in liquid nitrogen, and stored at –80°C. Total RNA was purified by the cesium chloride (CsCl) method as described by Chirgwin et al. (1979). Briefly, frozen mouse brain was homogenized in GIT buffer [4 M guanidiniumisothiocyanate (Sigma, Germany), 25 mM sodium acetate pH 4.8, 0.1 M β-mercaptoethanol] for 1 min. at 4°C using the Ultra Turrax (IKA T25). Homogenate was depleted from tissue debris by centrifugation (30,000 xg at 4°C for 30 minutes; SS34 rotor). Supernatant was then laid onto 3 ml 5.7 M CsCl and centrifuged at 92,500 xg (SW41 Ti) overnight at 12°C. The supernatant was carefully removed and the RNA pellet was re-suspended in DEPC-treated water. RNA solution was depleted from proteins by phenol/chloroform precipitation [mix one volume of RNA solution to 0.5 volume of phenol/chloroform and centrifuge at 15,700 xg (Eppendorf centrifuge 5415 D) for 5 minutes at RT. Mix one volume of the previous supernatant to one volume chloroform and centrifuge at the same speed and conditions]. RNA was finally precipitated in alcohol as described above, dried at RT, re-suspended in DEPC-treated water, quantified at 260 nm and stored at –80°C.

Alternatively, Trizol (sigma, Germany) solution was used for RNA isolation and the protocol is described by the manufacturer.

### 5.5.2 Description of the northern blot

### 5.5.2.1 Separation and transfer of RNA on the nylon membrane

Purified RNA (20µg) was denatured (65 °C), separated on 1% agarose gel containing 20 mM MOPS (pH 7.0), 5 mM sodium acetate, 1 mM EDTA, and

2.2 M formaldehyde and transferred overnight to HybondN$^+$ nylon membranes (Schleicher & Schuell, Germany) using 20X sodium citrate buffer (SSC) according to standard protocols (Sambrook et al., 1989). RNA was immobilized on the membrane by heating at 80°C for 2 hours.

### *5.5.2.2 Detection of the expressed mRNA*
### *5.5.2.2.1 Preparation of DNA templates*

A 223 bp mouse CGT specific DNA of the 3´-noncoding region of the mouse CGT was generated by RT-PCR follows:

5 µg of total RNA was mixed to 100 pmole RNase free oligo-dT primer (5´-AACCCGGCTCGAGCGGCCGCTTTTTTTTTTTTTTTT-3´) and denatured for 5 min. at 70°C. Single strand DNA was generated at 42°C for 1 hour by incubating the denatured RNA mixture with 1 mM dNTPs in 25 mM Tris-HCl pH 8.3 supplemented with 25 mM KCl, 4 mM MgCl$_2$, 10 mM DTT, 20U of ribonuclease inhibitors and 40 U reverse transcriptase (MBI Fermentas, Steinheim, Germany). RNA was depleted from the mixture by hydrolysis in the presence of 5U RNAse H for 20 minutes at 37°C. 1µl of the single strand DNA solution was used to generate the 223 bp double strand fragment of the rat CGT cDNA as previously described using the following reagents: forward (5´-AAATGATCCAACAGCCCAGGTG-3´) and reverse ( 5´-GGCTTCTAAATGGTTCACTGCC-3´). PCR conditions were : 2 min. at 94°C, 30 cycles (30 s. at 94°C, 30 s. 55°C, 1 min. 70°C) and 10 min. 70°C. PCR product was gel purified, quantified using lambda HindIII marker as reference and used as template for the synthesis of radioactive probe for the detection of endogenous mouse CGT mRNA.

The rat CGT cDNA was obtained by PCR as described above. The mouse PST/ST8Sia IV (1.09 kb) was released from the plasmid Bluescript using HindIII/XbaI. The mouse MBP (1.3 kb) cDNA was released from a pCMV-sport6 plasmid using BstxI enzyme. HindIII/BamHI enzymes were used to digest the PLP (800 bp) cDNA from a pEGFP plasmid and the MAL (600 bp) insert was removed from a dsRed2 plasmid using EcoRI/SalI. The CST coding

region (1.3 kb) was amplified by PCR using the following primers: forward: (5´-ATGACTCTGCTGCCAAAGAAGC-3´) and Reverse: (5´-CCACCTTAGAAAGTCCCTAAGG-3´). PCR conditions were: 2 min. 94°C, (30 seconds 94°C 30 seconds 55°C 1 min. 72°C) 35 cycles, 10 min. 72°C.

### 5.5.2.2.2 Synthesis of $^{32}$P-labeled probes and detection of the expressed mRNA

The synthesis of $^{32}$P-labeled DNA probes was carried out as follows:

| | |
|---|---|
| DNA | 25 ng |
| Random primers | 5 µl |

Add water to a final volume of 50 µl. incubate at 95°C for 5 min. and at RT for 10 min.

| | |
|---|---|
| Buffer (5X) | 10 µl |
| [$^{32}$P]dCTP (10µCi) | 5 µl |
| Klenow (1U/µl) | 2 µl |

incubate the mixture for 10 min. at 37°C. Labeled-probes were purified using G-25 sephadex column by centrifugation at 1500 rpm for 5 minutes. Labeled DNA fragments were denatured at 95°C for 5 min., ready for membrane hybridization.

Membranes were pre-hybridized for 1 hour at 42°C (0.2 ml hybridization solution per cm² of the membrane) in the presence of 100 µg heat denatured salmon sperm DNA per ml hybridization solution and hybridized overnight at the same temperature and in the same solution supplemented with 2 million cpm/ml hybridization solution of $^{32}$P-labeled mouse CGT 3´-UTR, rat CGT, PST, MBP, MAL or CST. Following hybridization, membranes were washed twice for 10 min. at room temperature in 2X SSC/0.1% SDS and twice for min. at 65°C in 0.2X SSC/0.1% SDS. Membranes were packed in plastic bags and exposed on pre-flashed Fuji Imager screen (Fuji Photofilm Co., Kanagawa, Japan), and when higher sensitivity was required, X-ray films were used at –80°C. Before re-probing, the membranes were stripped for 30 minutes at 65°C in 0.1 M Tris-HCl, pH 8.0, 1% SDS and 50% formamide.

## 5.6 Purification of myelin

Myelin was prepared from mouse brains at different age (2, 4, 8, 12 and 32 weeks old for PLP-CGT and 2, 4 12 and 24 weeks old for PLP-PST) as described by Norton and Poduslo (1973). Briefly, brains were homogenized for 1 min. at 4°C in 10.5% sucrose using the ultra-turrax T25 (IKA), and centrifuged for 45 min. at 17,000 xg. The resulting pellet was homogenized in 30% sucrose, overlaid with 10.5% sucrose and centrifuged for 50 min. at 68,000 xg. Myelin was collected from the 10.5%:30% inter-phase and washed twice with cold water to remove axolemma. After a second 10.5%/30% sucrose gradient centrifugation, the myelin fraction was washed twice with cold water to remove sucrose, frozen at –80°C and lyophilized overnight. The myelin powder obtained was weighed, resuspended in 500 µl ice-cold ddH$_2$O and stored at –80°C.

## 5.7. Lipid extraction and thin layer chromatography

Lipids were isolated from brain or purified myelin as described (van Echten-Deckert, 2000). Briefly, brains or myelins were homogenized in 10 volumes of chloroform/methanol (2:1; v/v) and lipids extracted for 4 hours at 50°C under constant stirring. Insoluble material was removed by filtration and lipids were dried at 45°C under a stream of nitrogen. Lipids were dissolved in chloroform/methanol (1:1; v/v) and stored at –80°C. In some experiments, glycerophospholipids were removed by mild alkaline hydrolysis for two hours at 37°C using 100 mM NaOH in methanol. Lipids were separated by thin layer chromatography on silica gel 60 HPTLC plates (Merck) in chloroform/methanol/water (60:27:4). Lipid standards were obtained from Sigma (galactosylceramide, sulfatide, sphingomyelin) and Matreya (monosialo- and disialo-gangliosides), respectively. Lipids were visualized by spraying TLC plates with cupric sulfate in aqueous phosphoric acid as described (Yao and Rastetter, 1985). Quantification of lipid bands was

performed by densitometry using Advanced Image Data Analyser (AIDA) (Raytest, Straubenhardt, Germany) and lipid standards as reference and the results of three independent experiments are given as an average ±SEM.

## 5.8 Preparation of mixed cells from new born mouse brains

Primary culture of mixed brain cells was performed as described by Pesheva et al. (1997). Briefly, mouse brains (PND 1 or 2) were removed from the cranial cavity and the forebrain cut in small pieces and incubated in trypsin-DNAseI (Sigma) solution for 10 min. at RT. Cell homogenate was mixed to Hank balanced salt solution (HBSS) and pelleted by centrifugation at 4°C at 600 xg for 10 minutes. Pellet was further dissociated in DNAse I solution on ice bath using flamed Pasteur pipette. Dissociated cells were mixed with 7 ml HBSS and pelleted as described above. Pellet was re-suspended in DMEM containing 10% fetal calf serum, 2 mM Glutamine, 100 U/ml penicillin 100 U/ml streptomycin and plated at a concentration of 50,000 cells per 18 mm poly-L lysine (0.1 ml/ml) coated coverslip and cultured for 24 hours in the same medium at 37°in the presence of 5% $CO_2$ as described by Bansal et al. (1999). Differentiation of oligodendrocyte progenitors were induced by culturing the cells in SATO medium [DMEM containing 10 µg/ml insulin, 16.1 µg/ml putrescine, 62 ng/ml progesterone, 0.34 µg/ml TIT, 6,66 µg/ml Selenium, 0.4 µg/ml L-Thyroxin, 0.1 mg/ml transferrin, 0.1% BSA, 25 µg/ml Gentamycin, 2 mM L-glutamine, 100 units/ml penicillin, 100 units/ml streptomycin supplemented with 4.5 g/l glucose] supplemented with 1% fetal calf and 1% horse serum for 10 and 20 days at 37°C and 5% $CO_2$.

## 5.9 *In vitro* differentiation of oligodendrocytes

Primary cultured cells from transgenic [line 2615 (n=5), line 2620 (n=3)] and wild type littermates (n=5) were analyzed for oligodendrocyte differentiation at 10 and 20 days of culture. Cells were washed twice with PBS and fixed for 7 minute at -20°C in 100 % methanol, followed by fixation at RT 10 minutes in 4

% (w/v) paraformaldehyde. After incubating with 50 mM NH$_4$Cl in PBS for 20min, non-specific binding sites were blocked with 1% (w/v) BSA in PBS. To detect intracellular antigens, cells were permeabilized using 0.1% (v/v) Triton X- 100. Cells were stained with rabbit anti-MBP (1/200) monoclonal antibody, followed by anti-rabbit Ig–Cy3 (1/300). Nucleus was detected using DAPI (1/500). MBP positive cells and nucleus were counted and the percentage of MBP positive cells calculated. The result of is given as an average ±SME. Differences were tested for significance using Anova.

## 5.10 Delayed extraction matrix-assisted laser desorption ionization-time-of-flight analysis (DE MALDI-TOF)

Myelin lipids were separated on the HPTLC plate and regions containing the lipid of interest were cut out from TLC plates and extracted with chloroform/methanol (2:1), dried under nitrogen, and dissolved in chloroform/methanol (1:1). One µl of the sample was mixed with one µl of 2,5-dihydroxybenzoic acid (10 mg/ml in 70% acetonitril). One µl of the mixture was loaded into a well of a 100-well sample plate. Mass spectra were recorded with a Voyager-DE STR mass spectrometer (PE Biosystems) in positive (detection of monogalactosyldiacylglycerol, galactosylceramide and sphingomyelin) or negative (sulfatide) ion mode/reflector mode.

## 5.11 Psychosine assay.

The measurement of psychosine contents in tg2615 line and wild type littermates was performed at the Group of Dr. Marie Vanier in Lyon (France). Briefly, adult mice were killed by cervical dislocation and the brain was removed and frozen at –80°C. Brain psychosine (galactosylsphingosine) was determined on aliquots of tissue homogenates corresponding to 2-2.5 mg of protein using a HTPLC procedure. The extraction procedure and the general conditions have been previously described (Rodrigue-Lafrasse et al. 1994;

Matsumoto et al. 1997). The analysis of the orthophtalaldehyde derivatives was conducted on a 20 cm Spherisorb 5 µm OSD2 C18 column with a 5 cm Spherisorb OSD2 C18 guard column. The mobile phase was methanol/5 mM sodium phosphate buffer (89:11), pH 7.0 with 50 mg/l sodium octylsulphate as an ion-pairing agent.

## 5.12 SDS-PAGE and Western blot analysis

Brains or myelin were homogenized in 20 mM Tris-HCl pH 8.0, 5 mM EDTA, 1 mM PMSF, 20 µg/ml aprotinin, 1 µg/ml leupeptin, 50 mM NaCl, 0.5% SDS. Protein content was determined using the Biorad DC protein assay. Protein samples from brain or myelin and homogenates were denatured at 95°C for 5 min. in Laemmli sample buffer in (4X: 4% SDS, 0.5% bromophenol blue, 1% β-mercaptoethanol, 50 % glycerol, 0.5 M Tris-HCl pH 6.8), separated on 12.5% SDS-PAGE and blotted onto nitrocellulose membranes using the semidry blotting technique. Bound proteins were detected using the following primary antibodies: mouse monoclonal anti-MBP (1/5000)(Serotec, Düsseldorf, Germany), rabbit polyclonal anti-MBP (1/5000) (Chemicon, Hofheim, Germany), mouse anti-PLP (1/10,000) (a kind gift of J. Trotter, Heidelberg), mouse anti-2',3'-cyclic nucleotide 3'-phosphohydrolase (1/200) (CNPase; Chemicon), mouse anti-fyn kinase (1/400) (Chemicon), rabbit anti-L-MAG (1/500) (Erb et al., 2003), and mouse anti-GFAP (1/1000) (Sigma, Taufkirchen, Germany). Secondary antibodies used were peroxidase-labeled anti-mouse Ig (Amersham Bioscience, Freiburg, Germany) and anti-rabbit Ig (Dianova, Hamburg, Germany). Bound antibodies were visualized using chemiluminescence. Membranes were incubated for 1 min in 2.7 mM $H_2O_2$, 1.25 mM 3-amino-pthalhydrazide, 0.2 mM p-coumaric acid, 100 mM Tris-HCl (pH 8.5) and exposed to X-ray film. The anti-MAL rabbit antiserum was raised against a recombinant GST-coupled polypeptide comprising the 53 N-terminal amino acids of MAL and affinity purified. For immuno-detection of MAL, SDS-PAGE was performed in 15% acrylamide gel and Western blot analysis was carried out as described previously (Erne et al., 2002).

## 5.12.1 Western blot of NCAM and PSA

For NCAM western detection, myelin samples (50 µg) was diluted in sodium acetate buffer (50 mM sodium acetate pH. 5.5, 1 mM EDTA, 20 µg/ml Aprotinin, 1 µg/ml leupeptin, and 1 mM PMSF) and incubated at 37°C for 4 hours in the presence of 1 µl of 11.7 U/ml neuraminidase (*Vibrio Cholerae* Type II) (Sigma, St. Louis, USA). The reaction was stopped by adding SDS at final concentration of 0.5 %. Proteins were finally extracted, quantified, and separated on 7.5 % SDS-PAGE. NCAM expression was investigated by Western blot analysis using rat anti-NCAM (1/200) (Chemicon) as described above. To investigate the expression PSA, proteins were extracted as described above and 50 µg of protein from brain or myelin homogenate was separated on 7.5 % SDS-PAGE and and blotted onto nylon membrane. PSA was finally detected using the mouse anti-PSA (2.5 µg/ml) (a kind gift of Dr Gerardy-Schahn University of Hannover, Germany) as described above.

## 5.13 *In situ* hybridization analysis

### 5.13.1 Synthesis of DIG-labeled probes

A 760 bp rat CGT cDNA fragment (harboring 50 bp of the 5'-untranslated region and 710 bp of the coding region), a 1 kb mouse PST (containing the whole coding region) or a 800 bp mouse PLP cDNA (containing the coding region of the PLP gene) or PDGF α-R ORF was cloned into pBluescript SK(-) (Stratagene) and used as the template for transcription of digoxigenin-11-UTP-labeled (0.35 mM) antisense and sense CGT, PST, PLP or PDGF alpha-receptor cRNA probes using T3 and T7 RNA polymerase (Roche Diagnostic, Mannheim, Germany). Transcription efficiency of cRNAs was controlled on DNA-agarose gel.

## 5.13.2 Preparation of the mouse brain

Mice were anaesthetized using 2.5 % tribromoethanol (Fluka, Germany) diluted in 0.9% NaCl and the skin cut in a T-shaped form at the middle abdomen to the cervix and at the caudal edge to both sides. The peritoneum below the lower thoracic aperture and the thoracic cage was opened. Mice were then perfused by inserting a sharp needle (26G X ½") into the left ventricle, first using the Ringer's solution (140 mM NaCl, 2.7 mM KCl, 11.9 mM NaHCO$_3$, 1.5 mM CaCl2) for the time and the rate given below, then with fixative (4 % paraformaldehyde). Brains were separated from the cranial cavity and post fixed for the time given below. Brains were washed as described in the table below, dehydrated in an increasing concentration of ethanol (30%, 40%, 50%, 70%) for 1 to 2 hours per alcohol concentration at RT. Brains were finally paraffinated, and embedded.

| Age | Amount anesthetics µl | Perfusion rate (ml/min) | Perfusion time, Ringer (min) | Perfusion time, fixative (min) | Time of post fixation | Time of tap water washing |
|-----|-----|-----|-----|-----|-----|-----|
| P0 | 50 - 100 | 7 ml/min | 1 min | 2 min | 16 hours | 2 days |
| P3 | 100 | 8 ml/min | 1 min | 2 min | 24 h | 2 d |
| P5 | 100 | 8 ml/min | 1 min | 2 min | 24 h | 2 d |
| P7 | 150 | 10 ml/min | 1 min | 2 min | 24 h | 2 d |
| P9 | 150 | 10 ml/min | 1 min | 2 min | 36 h | 3 d |
| P11 | 200 | 10 ml/min | 1 min | 2 min | 36 h | 3 d |
| P15 | 300 | 12 ml/min | 1 min | 2 min | 48 h | 3 d |
| Adult | 500 | 17 ml/min | 1 min | 5 min | 48 h | 3 d |

**Table 2 Schematic protocol for the perfusion of mice**

### 5.13.3 General description of the hybridization

In situ hybridization analysis of mice brains was performed as described by Baader et al. (1998). Briefly, brain slices were deparaffinated in xylol (Merk), rehydrated, fixed in 4% PFA and permeabilized at RT in proteinase K (10 µg/ml) and triton X-100 (0.25%). Hybridization was performed with 1/500 diluted Digoxigenin-11-UTP-labeled antisense or sense cRNA probes at 65°C in 50 % formamide, 1 % Denhardt´s solution, 0.2 % SDS, 0.25 mg/ml ssDNA, 0.25 mg/ml tRNA and 10 % hybridization salt (3 M NaCl, 0.1 M PIPES, 0.1 M EDTA) overnight in humid chamber. To remove unspecific hybridized probes, sections were washed twice with 2X SSC for 5 and 30 min. and 0.1X SSC for 45 min. The sections were finally equilibrated in maleic acid buffer (100 mM maleic acid, 150 mM NaCl, pH.7.5) before blocking the unspecific binding sites using the same buffer containing 2% blocking reagent (Boehringer-Mannheim) for 1 hour at room temperature and then incubated overnight in the blocking buffer containing 1/5000 diluted anti-DIG-alkaline phosphatase (Roche Diagnostic GmbH, Mannheim, Germany) at 4°C in a humid chamber. After incubation, sections were washed with Tris buffer (100mM Tris-HCL pH 9.5, containing 100 mM NaCl, 50 mM $MgCl_2$) at room temperature for 5 hours and stained using 165$\mu$g/ml BCIP and 330$\mu$g/ml Nitro Blue Tetrazolium (NBT) in 100mM Tris/HCl, pH9.5, containing 100mM NaCl, 5mM $MgCl_2$. Staining was 12 hours for CGT and PST mRNA, 1 hour for PLP mRNA and 4 days for PDGF α-receptor mRNA. Positive cells were documented as described above. Concerning PLP and PDGF alpha receptor staining, positive cells were counted and normalized to the $mm^2$ of the counted region. Differences were tested for significance using Anova.

### 5.14 Immunohistochemical analysis

Immunohistochemical analysis was performed as described by Baader et al. (1998). Briefly, transgenic and wild type littermates mice were perfused and post fixed in paraformaldehyde as describe above. After washing, brains were

stored at 4°C in PBS. 40 µm vibratome (Leica HM 355 S) slices were fixed in paraformaldehyde for 30 min. at RT before permeabilization in the same conditions using PBS containing 0.5 % triton X-100. Permeabilized slices were washed three times 5 min. with PBS and unspecific binding sites were blocked for 30 min. at RT using 2 % goad serum prepared in PBS. Blocking binding sites were followed by overnight incubation of slices at 4°C in PBS containing 2 % goad serum and antibodies [anti GFAP (sigma) and anti MBP (1/1000)]. Unbound antibodies were removed by washing the slices three times 5 min. at RT in PBS. After washing, sections were incubated for 2 hours at RT with cy3-labelled goad anti mouse IgG antibody, washed and the nucleus stained with DAPI (4, 6-diamidino-2-phenylindole) for 2 min. at RT and mounted on the microscopic slide with gelatin. Sections were finally imaged with a Zeiss Axiophot 2 fluorescence microscope (Carl Zeiss, Oberkochen, Germany).

## 5.15 Electron microscopy

Electron microscopic analysis was performed by the group of Professor Büssow at the Institute of anatomy of the University of Bonn. Briefly, four and twelve weeks old transgenic and wild type littermates from 2615 and 2620 mice line were perfused with 6% glutaraldehyde via left cardiac ventricle. The optic, cervical, spinal cord and sciatic nerve were isolated and post fixed in phosphate-buffered $O_SO_4$ in sucrose, and embedded in Epon 812. The semi thin sections were stained with toluidine/pyronin and the ultra thin sections were contrasted with uranyl acetate and lead citrate and examined as previously described (Büssow, 1978).

## 5.16 Rotarod

Rotarod test was performed as described by Kuhn et al. (1995) and Uschkureit et al. (2000). Briefly, animals (8 male transgenic mice of the transgenic line tg2615 and 8 wild-type mice) 4 weeks of age were trained on two consecutive days by placing them on a rotating rod (10 rpm) for 180 sec. Thereafter, mice

were tested at 4, 6, and 8 weeks at 6 and 10 rpm. The test was performed on four consecutive days by placing the mice on the rotating rod and the time the mice stayed on the rod was recorded (cut-off time 180 sec). The percentage of mice able to stay on the rotating rod for 180 sec was calculated and differences in the time interval during their stay on the rod were tested for significance using Kolmogorov-Smirnov test.

# PART I

Reversal of non-hydroxy:alpha-hydroxy galactosylceramide ratio and demyelination in transgenic mice overexpressing UDP-galactose:ceramide galactosyltransferase

# PART I

## 6.1 Activity test of CGT transgenic construct and genotyping the founder mice

### 6.1.1 Activity test of the transgenic construct.

Before the generation of transgenic mice, the CGT cDNA of the transgenic construct was investigated by transfection experiments for enzymatic function to exclude cloning artifacts. Rat CGT cDNA (2.4 kb) harboring the open reading frame (ORF), 50 bp of the 5´-untranslated region and 689 bp of the 3´-untranslated regions was excised from the transgenic cassette using PacI/AscI restriction enzymes and inserted in the pcDNA3.1 expression vector. The recombinant plasmid constructed was then used for transient transfection of CHO cells.
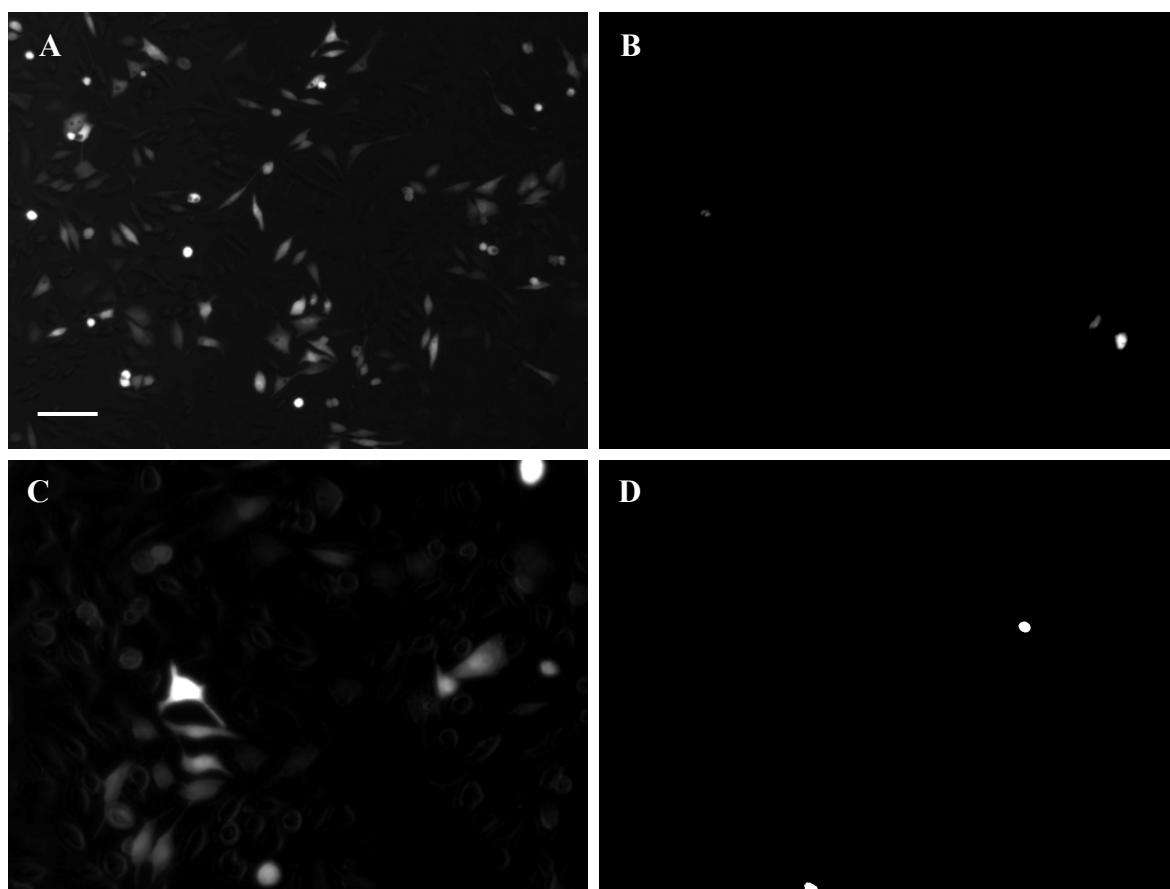


**Fig. 8 GalC expression in CGT-transfected CHO cells**. The rat CGT cDNA was introduced into the CHO wild type cells (**C** & **D**) using Exgen500. Both transiently (**C** & **D**) and stably (A & B) CGT transfected CHO cells were labeled with (**A** & **C**) or without (**B** & **D**) anti-GalC antibody. (**A**) CGT stably transfected CHO labeled with rabbit anti-GalC antibody and FITC-conjugated goat anti rabbit antiserum, (**B**) CGT transiently transfected CHO labeled with rabbit anti-GalC antibody and FITC-

conjugated goat anti rabbit antiserum, (**B**) stable and transient (**D**) transfected CHO only labeled with FITC-conjugated goat anti-rabbit antiserum. GalC positive cells are documented using fluorescence microscopy on an Axiovert M instrument (Carl Zeiss, Hallbergmoos, Germany).  Scale bar 50 µm

Following transfection, cells were inmmunofluorescently labeled using an antibody against galactosylceramide. Results show a membrane staining of the cells (fig. 8). This result indicates that the CGT fragment used to generate transgenic mice can be transcribed and translated to an active protein.

### 6.1.2 Identification of PLP-CGT transgenic founder mice

To target the expression of CGT in the CNS, we have exploited the PLP expression cassette (Fig. 9A) developed by Fuss et al. (2001), which contains a 2.4 kb PLP promoter, exon1, intron1 (8.5 kb), the first 37 bp of the exon2, where the translation start site was mutated in order to allow the transcription to start at the transcription start site present in the rat CGT cDNA and the SV40 polyadenylation site. By inserting a 2.4 kb rat CGT cDNA between the PacI and AscI sites, the PLP-CGT recombinant plasmid was constructed (fig. 9A). Following the micro-injection of 11.362 kb DNA fragment into the fertilized mouse oocytes obtained by the crossing of CBA and C57/Bl6 mouse strains, twenty mice (12 females and 8 males) were obtained. Founder mice were screened for the presence of the transgenic construct both by PCR (data not shown) and Southern blot (fig.9B) analysis of the genomic DNA isolated from mouse tail. Results indicate four transgenic mice [one female (2604) and three males (2615, 2619, 2620)]. One founder mouse (2619) died at three months of age. Among the three remaining lines, two transmitted the transgene in the Mendelian fashion (2604, 2620) and the third one did not (2615), indicating a multiple integration site.
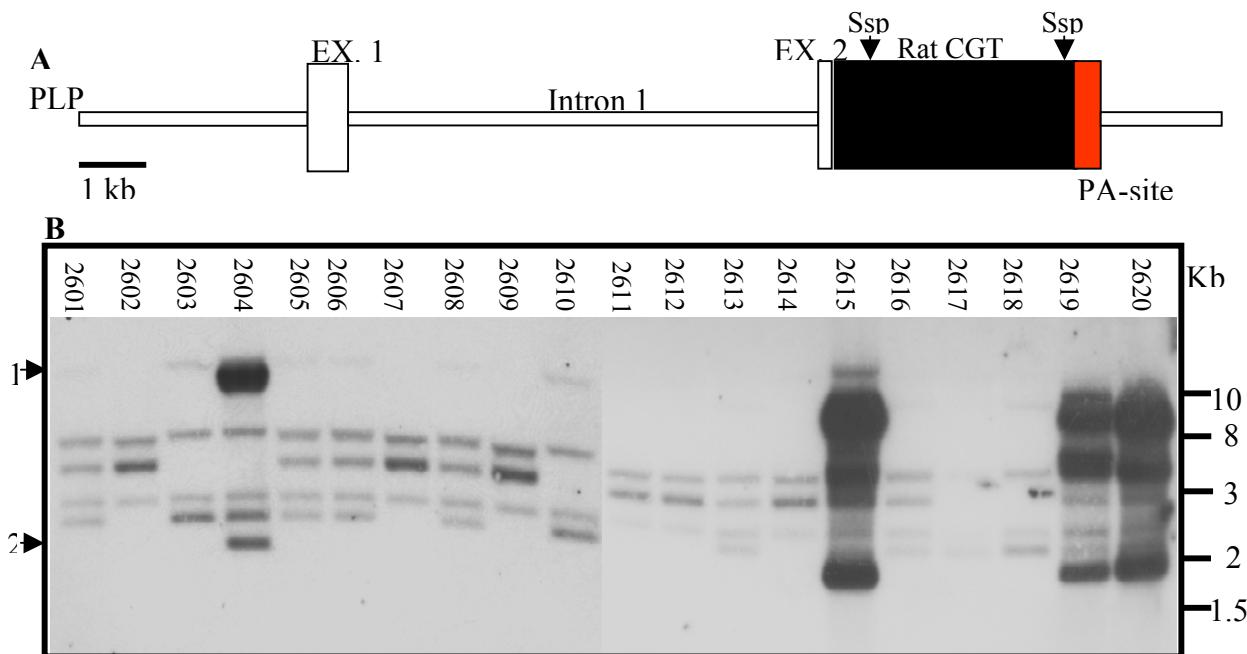
**Fig.9 Diagram of PLP-CGT transgene construct and Southern blot analysis of founder mice**. **(A)** The diagram represents the DNA region derived from the PLP promoter gene (2.4 kb) including the transcription start site as well as the whole PLP intron1. The white boxes represent the PLP exon1 and 37bp of the exon2. The black box represents the rat CGT cDNA including 50bp 5´-untranslated region, the whole ORF and 689bp 3´-untranslated region. Finally, the red box represents the SV40 polyadenylation signal. **(B)** Southern blot analysis of the founder mice. Genomic DNA (10 µg) was digested overnight using the Ssp1 enzyme (Ssp1 generates a 1.9 kb fragment by digesting the rat CGT cDNA at nucleotides 343 and 2280), separated onto 1% agarose gel, transferred to the HyBondN[+] membrane. The membranes were finally hybridized with [32P]-labeled DNA probe generated by using the whole rat cDNA as template. Bands were visualized on phosphoimager after exposure on pre-flashed Fuji Imaging plate. (1) Transgenic fragments generated by partial digestion of the inserted rat CGT. (2) 1.9 kb fragment generated from the rat CGT cDNA by the SspI enzyme.

## 6.2 Down regulation of endogenous CGT mRNA expression in PLP-CGT transgenic mice

CGT mRNA overexpression was assessed by Northern blot analysis of total RNA from mouse brains. Total RNA was extracted from the brain of 6 weeks old transgenic and wild type littermate mice. Total RNA (20 µg) was separated in a formaldehyde agarose gel, transferred onto HybondN+ membrane and hybridized with [32P]-labeled DNA probe using the whole rat cDNA as template. Fig. 10A demonstrates that CGT transgenic mRNA was overexpressed in mice brains and that the amount was different among the different transgenic lines (2604<2620<2615).

Using a probe specific for the mouse CGT mRNA, Northern blot analysis demonstrates in contrast that the endogeneous CGT mRNA was reduced.

Reduction was only observed in the lines 2615 and 2620 (Fig. 10A), whereas no change of the expression was observed in the line 2604 (Fig. 10A). This observation is reminiscent of the down regulation of CGT mRNA in twitcher mice (Taniike et al., 1998), indicating a feedback inhibition of CGT expression. Also, down regulation of CGT mRNA expression was found in twitcher mice (C57BL/6J-twi: twi/twi), which is an authentic murine model for the genetic demyelinating disease, globoid cell leukodystrophy (Suzuki et al., 1995) and is characterized by the deficiency of the lysosomal enzyme, galactosylceramidase, which catalyzes the degradation of galactosylceramide. To determine whether the increase of transgenic mRNA (Fig. 10A) induces the increase of the activity of CGT, an activity assay was performed using mouse brain extracts and C6-ceramide as acceptor of $[^{14}C]$-labeled galactose as described by Sprong et al. (2000). As expected, CGT activity in transgenic mice was significantly elevated ($p<0.01$, t-test). A 2.5-fold (25 days of age) and 4-fold (6 months of age) increase was observed in the line 2615, compared to wild-type mice (Fig. 10B). In the transgenic line 2604, CGT activity was significantly increased by about 40% ($p<0.01$, t-test) in 6 months old animals. This results correlate to the Northern and Southern blot results.
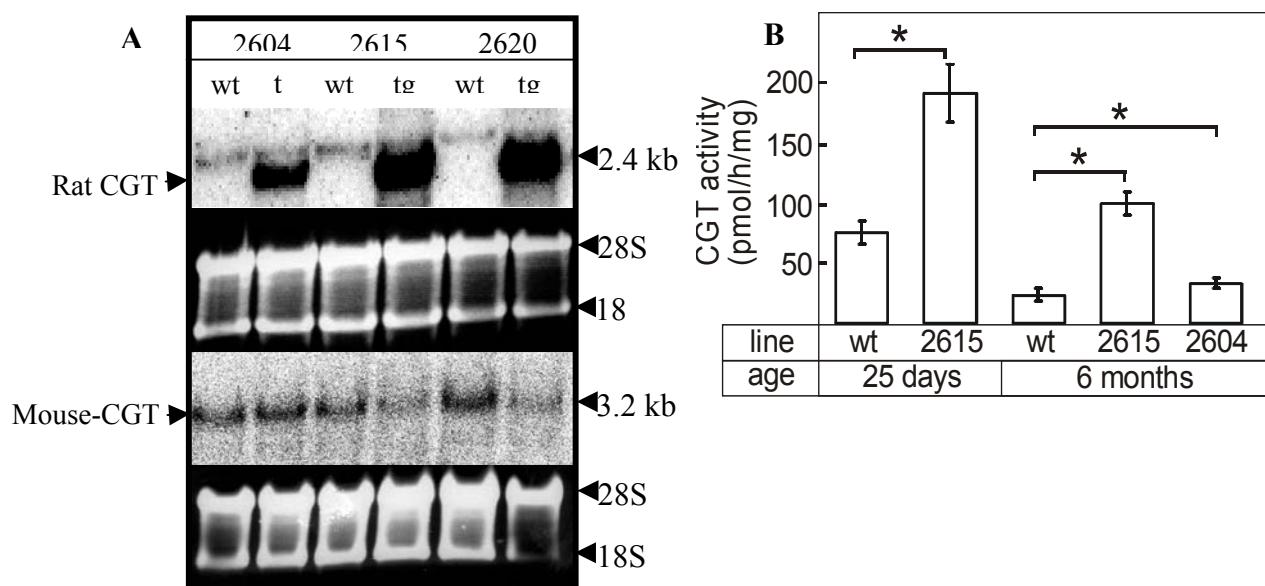


**Fig. 10 Assessments of CGT overexpression and enzyme activity in PLP-CGT transgenic mice**. The transgene expression in the mouse brain was assessed by Northern blot analysis of total RNA. Total RNA (20 μg) was separated on a 1 % agarose gel, transferred onto HybondN+ membrane. CGT mRNA was detected on the membrane by hybridization using the $[^{32}P]$-labeled rat CGT and mouse 3´-UTR CGT (**A**). Quantity and integrity of mRNA present on the membrane was verified by the ethidium

bromide staining. (**B**) Determination of CGT activity using C6-ceramide as acceptor of the [$^{14}$C]-galactose. One volume of the brain homogenate was mixed to one volume reaction buffer containing [14C]-UDP-galactose and C6-ceramide and incubated for 30 min. at 37°C. Lipids were extracted in chloroform/methanol (2:1), separated on silica gel plates using chloroform/methanol/water (70:30:4) and quantified. The transgenic lines 2615 and 2604 showed 4-fold and 1.4-fold, respectively, increase in activity in adult mice and a 2.5-fold increase in mouse line 2615 at 25 days of age. Asterisks indicate significant differences between transgenic and wild-type mice (p<0.01; t-test).

## 6.3 Overexpression of the CGT mRNA is restricted to the white matter regions of brain

Myelin formation starts around birth in the brainstem and the ventral and dorsal funiculi of the cervical spinal cord (Rozeik and Von Keyserlingk, 1987; Schwab and Schnell, 1989). To determine the localization of CGT mRNA and its expression pattern in the brains of transgenic mice, *in situ* hybridization on paraffin sections of ten (PLP-CGT) weeks old mice brains have been performed. 8 μm slices from transgenic and wild type littermate mouse brains were hybridized using the DIG-labeled sense and antisense rat CGT cRNA.

Fig. 11 shows that transgenic mRNA overexpression was restricted to the white matter regions of the brain, indicating that the targeted cells might be oligodendrocytes present in the white matters of cerebellum and corpus callosum. mRNA overexpression as evaluated by in situ hybridization also correlates with the transgene copy number inserted in the chromosome. Hence, CGT mRNA is higher in the line 2615 (Fig. 11C & D) than in line 2620 (fig. 11E & F) which expresses a higher amount of CGT mRNA than the line 2604 (Fig. 11A & B).

The expression pattern described in this study correlates to the one already demonstrated by Schulte and Stoffel (1993) and Dong Hong et al. (1999) in the developing rat brain, indicating that the overexpression of the rat CGT is restricted to the oligodendrocytes.
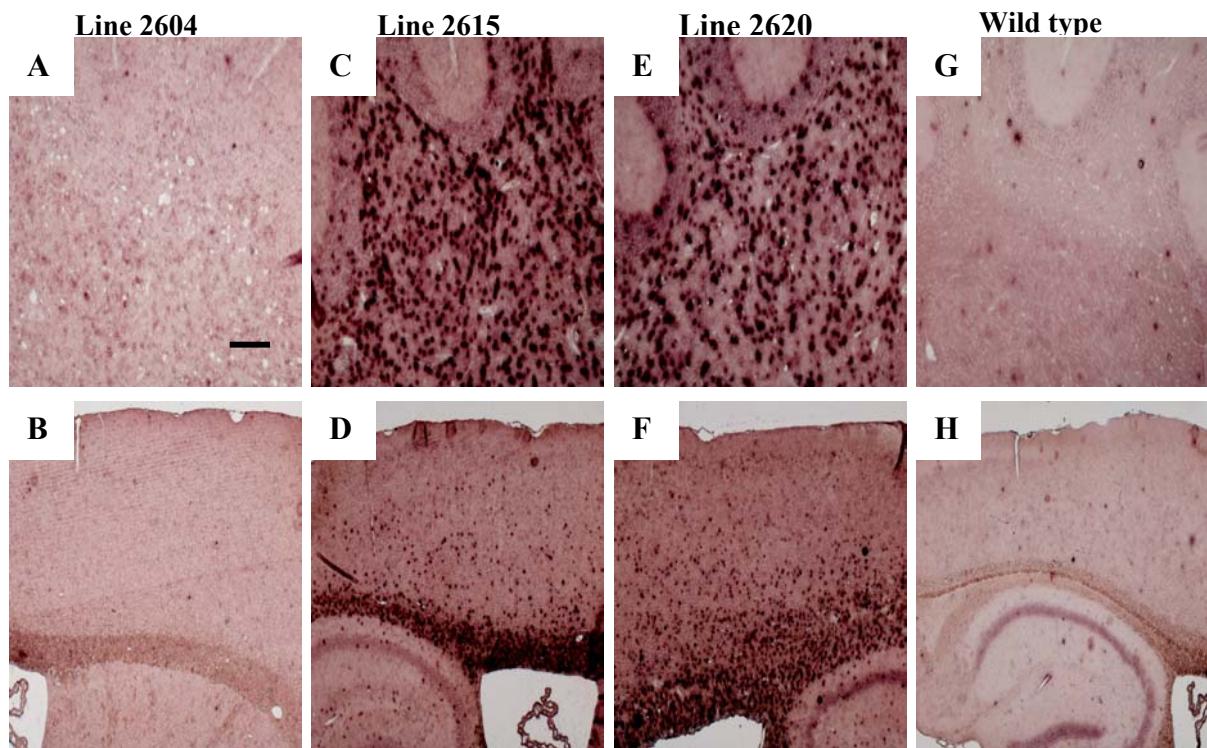
**Fig. 11. White matter specific expression of CGT mRNA in mouse brains**. In situ hybridization in brain sections (8 µm) of transgenic mice. Sagittal brain sections (10weeks of age) of the transgenic lines 2604 (**A**, **B**), 2615 (**C**, **D**), 2620 (**E**, **F**), and wild-type mice (**G**, **H**) were hybridized with a digoxigenin-labeled rat CGT cRNA probe and the mRNA expression documented using microscopic analysis on an Axiovert M instrument (Zeiss, Jena, Germany). Hybridization signals revealed strong transgene expression in the white matter of the forebrain (**C**, **E**) and cerebellum (**D**, **F**) in transgenic lines 2615 (**C**, **D**) and 2620 (**E**, **F**), and relatively weak expression in 2604 mice. Scale bar 50 µm.

## 6.4 Expression of the myelin and oligodendrocyte specific proteins in PLP-CGT mice: up-regulation of MAL expression

To investigate the impacts of CGT overexpression on the expression of myelin and oligodendrocyte proteins, Northern and Western blot analysis of proteins and total RNA from mouse brains were performed. Western blot analysis of proteins from purified myelin and brain did not reveal any reduction of the levels of PLP, L-MAG, CNPase, and Fyn kinase in PLP-CGT mice compared to wild-type controls (Fig. 12A & B). In contrast to the previous proteins cited, a dramatic reduction in the amount of MBP protein in purified myelin (Fig. 12A & B) and in total brain homogenates (data not shown) was observed in the transgenic line 2615. MBP levels were, however, normal in lines 2620 and 2604 (Fig. 12A) at 12 weeks of age. Because MBP down regulation was only observed in one line, it can not be excluded that it is the result of a transgene

insertion artifact. Northern blot analysis did not reveal differences in the MBP mRNA level in transgenic mice and wild type controls at 6 weeks of age (Fig. 13C), although MBP protein was reduced from 2 to 12 weeks of age (Fig. 12B). Thus, decrease of MBP in transgenic mice (2615) occurred posttranscriptionally. In contrast to MBP, the MAL protein was increased in the myelin of 12 week old animals in lines 2615 and 2620 but not in the line 2604 (Fig. 12A). Although the MAL mRNA concentration was unchanged at 6 weeks of age in all lines of PLP-CGT transgenic mice (Fig. 13C), Northern blot hybridization showed 50% increase of MAL mRNA level in 12 week old 2615 and 2620 mice lines (Fig. 13A & B). Thus, increase in MAL protein occurs at least in part at the transcriptional level.
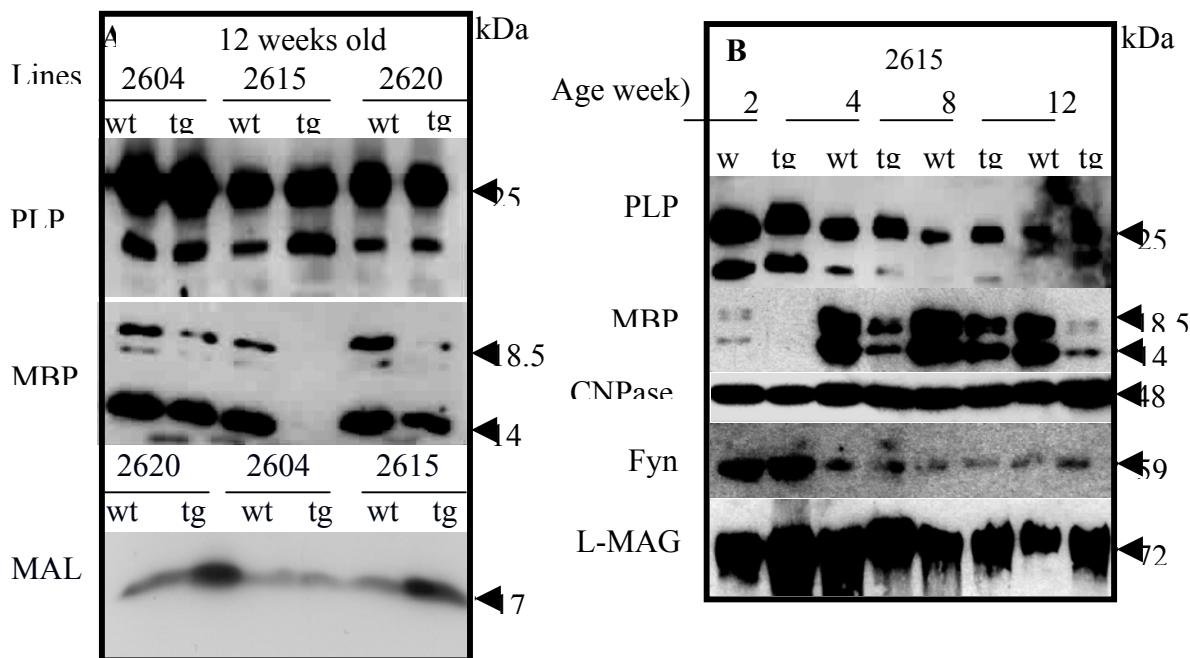


**Fig.12 Expression of myelin/oligodendrocyte proteins in PLP-CGT transgenic mice.** Wild type littermates were used as control mice in all experiments. Myelin protein fraction was extracted in buffer containing 0.5% SDS and separated onto 12.5%. For the MAL Western blot, myelin samples were treated as described by (Erne et al., 2002), separated onto 15% (MAL) polyacrylamide gel (MAL Western blot was performed by the group of Dr. Schaeren-Wiemers). In all cases, separated proteins were blotted onto nitrocellulose membrane using a semidry blotting technique. Bound proteins were detected using anti-MBP, anti-Fyn, anti-L-MAG, PLP, CNPase, and MAL sera. PLP, MBP and MAL expression in the line 2604, 2615 and 2620 at 12 weeks of age (**A**) and age dependent PLP, MBP, CNPase, Fyn, and L-MAG levels in the line 2615 (**B**).
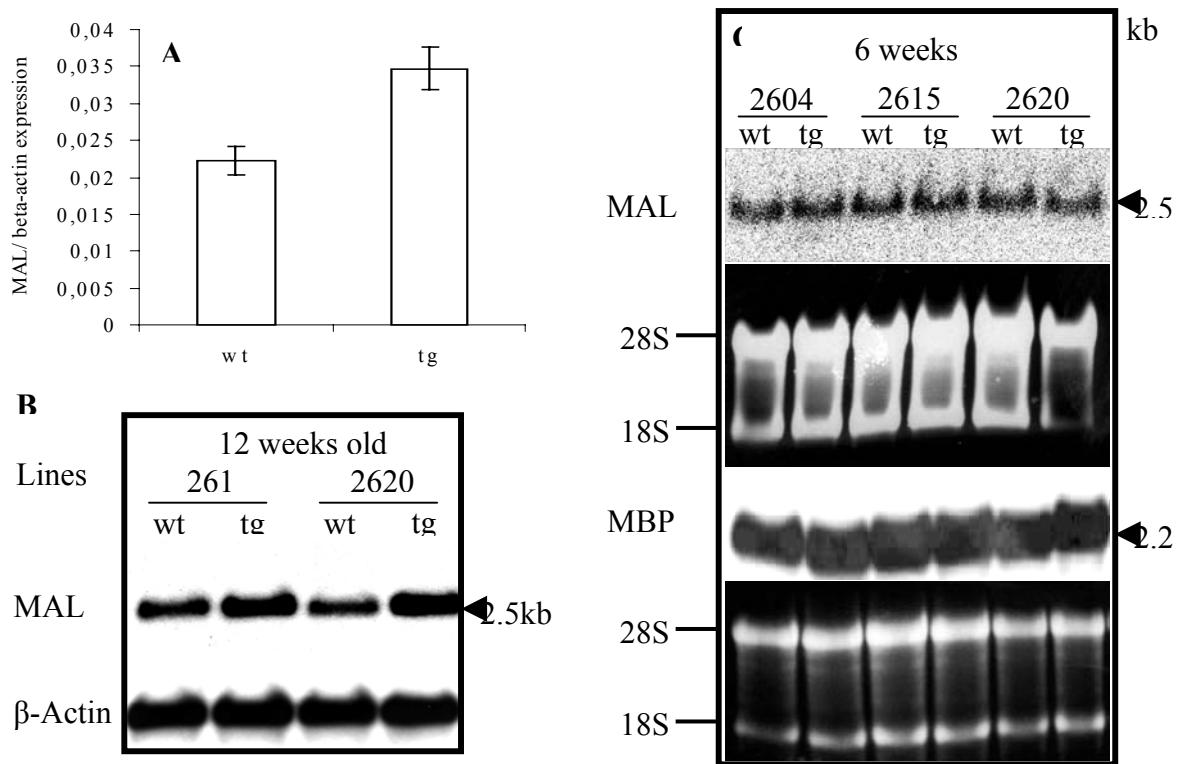
**Fig.13 Expression of MBP and MAL mRNA in PLP-CGT transgenic mice**. The expression of MBP and MAL mRNA in transgenic mice (n=3 per line) and wild type littermate (n=3) mouse brain was assessed by Northern blot analysis of total RNA at 6 and 12 weeks of age. Total RNA was purified from mouse brains by CsCl and 20 µg were separated in 1% RNAse free agarose gel and transferred onto HybondN[+] membrane. Membranes were hybridized using [32P]-labeled 600 bp MAL or 1.3 kb MBP cDNA fragments. Visualization of the bands was performed by exposing the membrane to pre-flashed Fuji Bioimager screen and subsequently to X-ray films. MAL expression was quantified using AIDA software. MAL mRNA signals in 12 weeks old wild-type and transgenic mice (**B**) were normalized to β-actin. The same increase in mRNA expression was observed in both lines (2615 and 2620), therefore quantification data from 2615 and 2620 mice were combined (**A**). The observed difference is statistically significant (p<0.05; t-test). (**C**), MBP and MAL mRNA expression at 6 weeks of age in PLP-CGT transgenic and wild type littermate mouse brains.

# 6.5 Consequences of the CGT overexpression on the lipid metabolism in the nervous system of PLP-CGT mice

It has already been shown that CGT is responsible for the synthesis of the two isoforms (NFA and HFA-GalC) of GalC (Schulte and Stoffel, 1993; Stahl et al., 1994). Furthermore, it has also been demonstrated *in vitro* that CGT has a high affinity for the hydroxy-fatty acid substituted ceramide (HFA-ceramide). Therefore, explaining the differences in the concentration of hydroxy-fatty acid GalC (HFA-GalC) and non-hydroxy-fatty acid GalC (NFA-GalC) observed, respectively (Schaeren-Wiemers et al. 1995).

## 6.5.1 Reversal of non-hydroxy:α-hydroxy fatty acid galactosylceramide in the brain of PLP-CGT mice

To examine the influence of CGT overexpression on lipid metabolism in the CNS, lipids from myelin and whole brain were analyzed by HPTLC and quantified densitometrically. GalC and GalC isoform levels were quantified in myelin samples using the AIDA software. We noticed on one hand, an increase of NFA-GalC concentration in both myelin (Fig. 14A) and saponified brain lipid extracts (Fig.14B). In the other hand, a decrease of HFA-GalC level was observed in both lipid homogenates (Fig. 14A & B). Quantitatively, the decrease of HFA-GalC was approximately 0.3 fold in both lines (Fig. 15A & D), whereas the increase of NFA-GalC was around 0.4 and 1.3 fold (Fig. 15B & E), in myelin from lines 2620 and 2515, respectively at 12 weeks of age. In lines 2615 and 2620, the increase or decrease in GalC isoforms was developmentally observed.
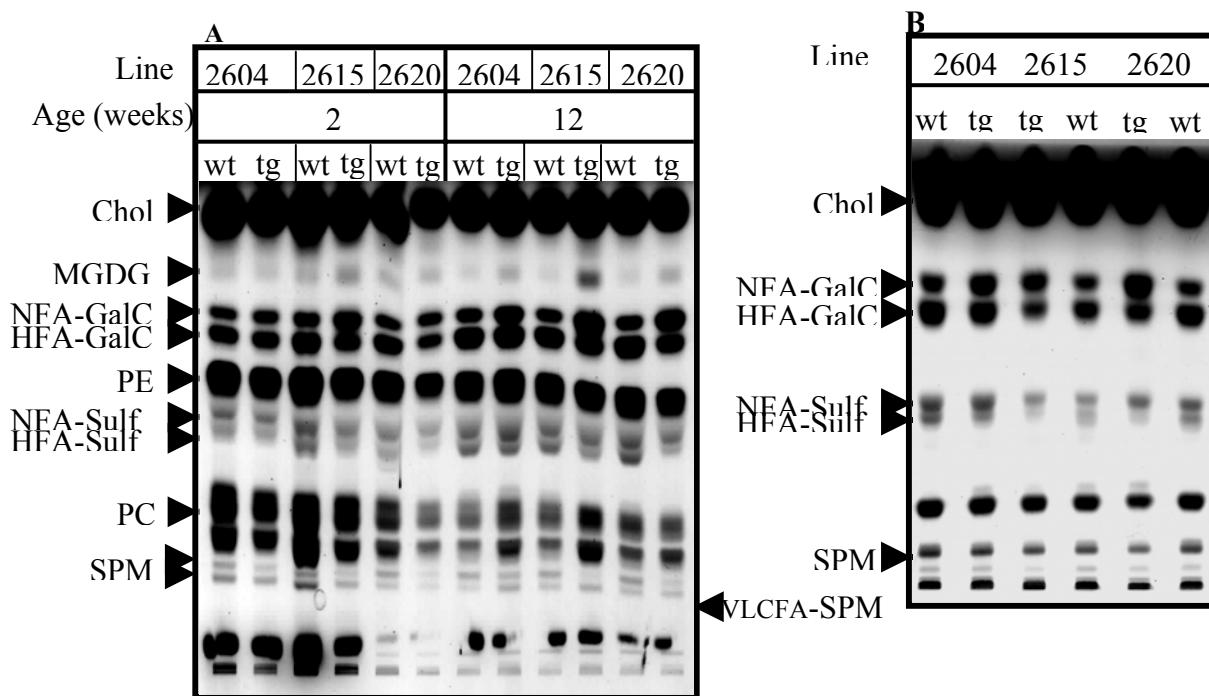


**Fig. 14 HPTLC analysis of lipids from transgenic mouse brains.** Myelin was purified from transgenic and wild type littermate mouse brains at different ages according to Norton and Poduslo (1973). Myelin and brain lipids were extracted using C/M (2:1). Lipid quantity corresponding to 100µg myelin dry weight or brain wet weight was spotted, separated on HPTLC plates using C/M/W (60:27:4) as mobile phase. Lipid bands were visualized on the $CuSO_4/H_3PO_4$ sprayed plate by heating at 170 °C for 2 minutes. (**A**) HPTLC profile of transgenic and wild type littermates from the three lines at 2 and 12 weeks of age. (**B**) HPTLC analysis of total brain lipid extracts at three months of age. NFA-Sulf (non hydroxy-fatty acid sulfatide), HFA-Sulf (hydroxy-fatty acid sulfatide), SPM (sphingomyelin), VLCFA-SPM (very long chain fatty acid containing-sphingomyelin), Chol (cholesterol), MGDG

(monogalactosyldiacylglycerol), NFA-GalC (non hydroxy-fatty acid galactosylceramide), HFA-GalC (hydroxyl-fatty acid galactosylceramide), PC (phosphatidyl choline), PE (phosphatidyl ethanolamine).

In general, GalC concentration in PLP-CGT transgenic mice was significantly increased only in the line 2615 (0.5 fold), whereas in the other lines (2604 and 2620) no significant increase was be observed (Fig. 15C & F).
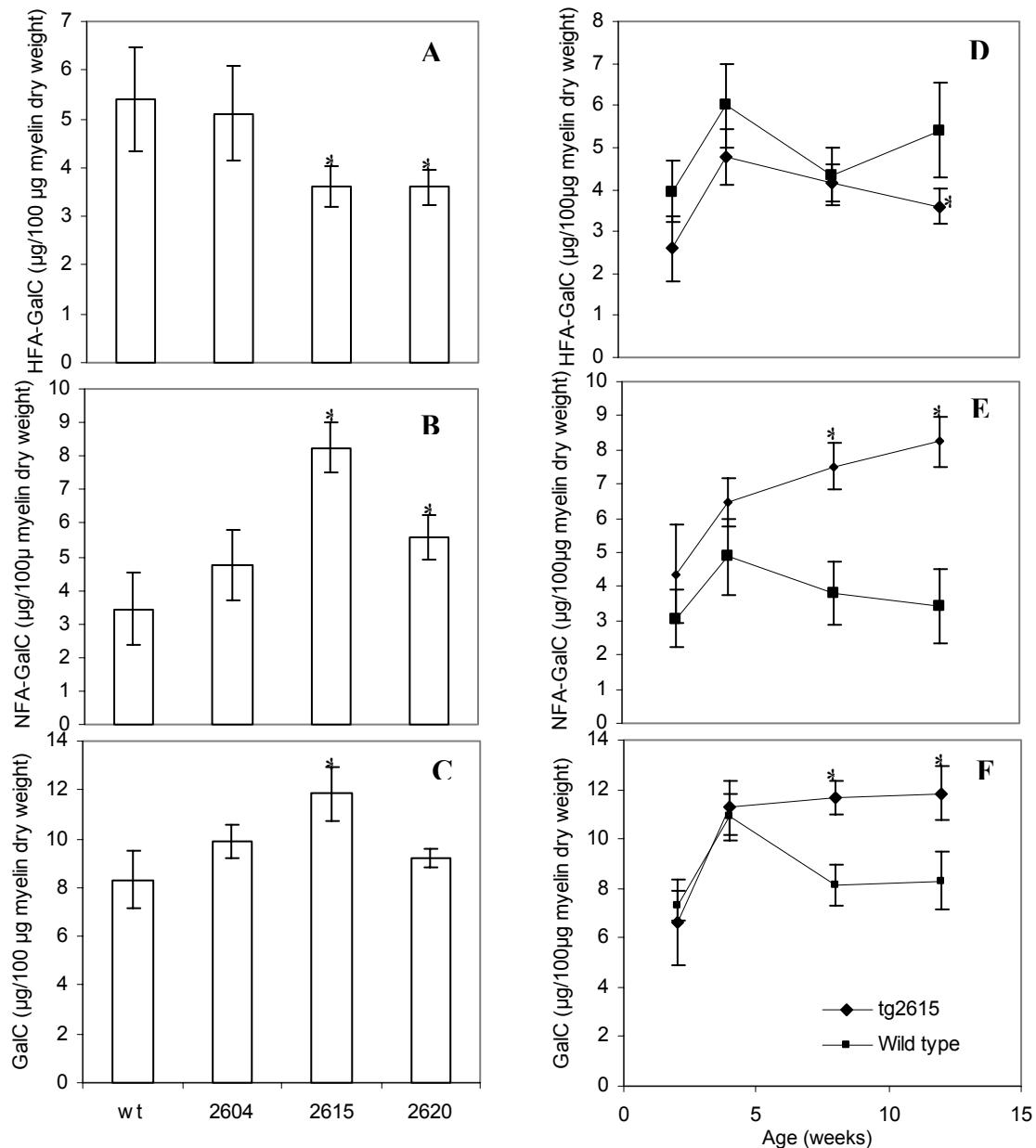


**Fig. 15 Levels of GalC and its isoforms in PLP-CGT transgenic mice**. Total lipid was isolated independently from myelin from 3 transgenic mice per line and 9 wild type mice using chloroform/methanol (2:1). The volume of the lipid solution corresponding to 100µg myelin dry weight was spotted and separated on the HPTLC plate and separated using C/M/W (60:27:4) as mobile phase. Plates were finally stained as described and the lipid concentrations determined, using lipid standards as reference. Each lipid sample was analyzed 5 times independently by TLC. The results of five independents experimentation [2604 (n=3), 2615 (n=6), 2620 (n=3), and wild-type (n=9)] are given as an average ±SME. Asterisks indicate that differences are statistically significant (t-test; $p < 0.05$) compared to wild type mice. (**A**) Comparison of HFA-GalC level at 12 weeks of age between the three lines and wild type littermates, (**B**) comparison of NFA-GalC levels at 12 weeks of age in the three lines and wild type littermates, (**C**) comparison of GalC level in the three lines and wild type littermates

at 12 weeks of age (**D**) age dependent HFA-GalC level in the line 2615 and wild type littermates, (**E**) age dependent NFA-GalC level in the line 2615 and wild type littermates, and, (**F**) age dependent GalC level in the line 2615 and wild type littermates.

## 6.5.2 Increase of the monogalactosyldiacylglycerol level at the adult age in the CNS of PLP-CGT transgenic mice

CGT is not only involved in the synthesis of GalC, but also in the conversion of sphingosine to psychosine (galactosylsphingosine) and 1,2-diacylglycerol to monogalactosyldiacylglycerol (Inoue et al. 1971). For this reason, we confirmed the identity of the monogalactosyldiacylglycerol (MGDG) by MALDI-TOF analysis (Fig. 17) and quantified it using the AIDA software. It is known that in the rat brain, MGDG expression is almost undetectable before 10 days of age, and then reaches a peak at 17 or 18 days of age and finally decreases to lower levels with increasing age (Wenger et al., 1968; Wenger et al., 1970). In the present study, we noticed an increase of MGDG (for TLC analysis see Fig. 14A) in the myelin fraction, which reaches a peak at 12 weeks of age and slightly decreases at 32 weeks (data not shown). Quantitatively, increase in MGDG levels were almost 0.6, 4.8 and 2 fold when compared to the wild type littermates and for the lines 2604, 2615 and 2620, respectively (Fig. 16B & D). Furthermore, MGDG signal was not detectable in saponified lipid fraction from the whole brain (Fig. 14B).

## 6.5.3 Decrease in sulfatide level in the CNS of PLP-CGT transgenic mice

Since lipid metabolisms (synthesis and degradation) are closely related in a living organism, we looked also for the level of other brain lipids involved in the myelination. In the CNS, sulfatide and GalC metabolisms are closely related. GalC is synthesized by CGT and is used as a substrate for the synthesis of sulfatide. HPTLC analysis (Fig. 14A & B) and densitometric quantification (Fig. 16A & C) of sulfatide shows a decrease in sulfatide content at 12 weeks of age in lines 2615 and 2620. Surprisingly, overexpression of the NFA-GalC does not lead to an increase of NFA-sulfatide concentration, indicating that factors

other than NFA-GalC limit the synthesis of NFA-Sulf in the Golgi apparatus. Moreover, only the HFA-sulfatide level was decreased, a phenomenon which is logical, since the HFA-GalC level was also decreased.
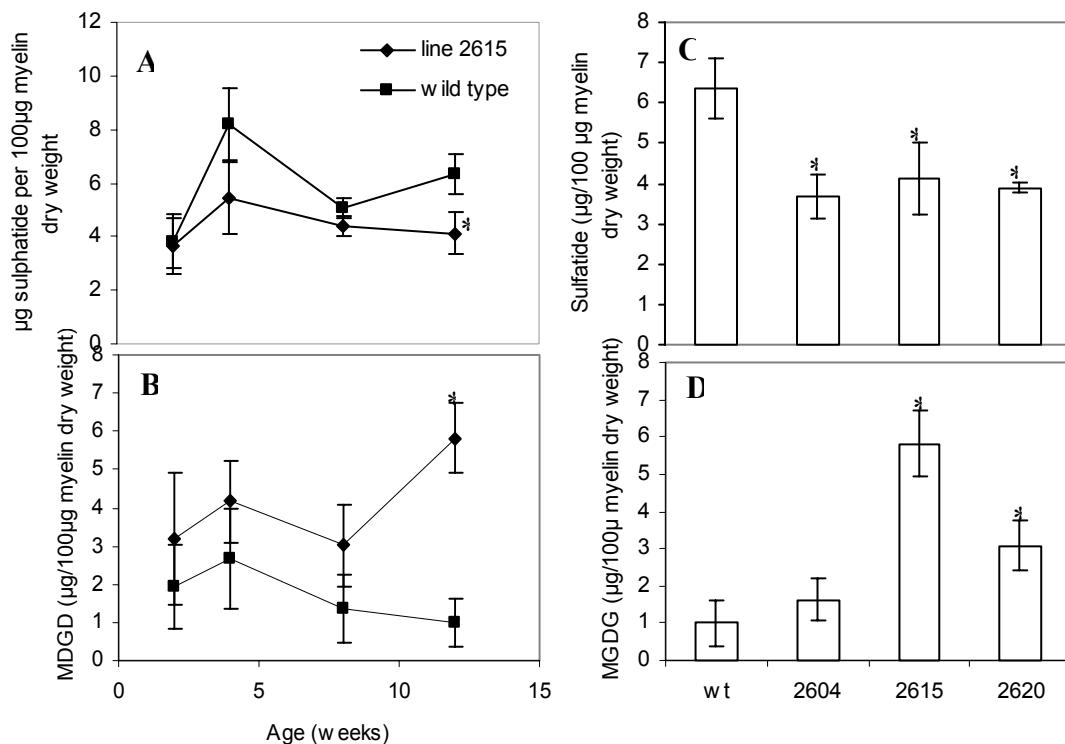


**Fig. 16 Level of sulfatide and MGDG in PLP-CGT transgenic mice**. Myelin and brain lipids were extracted using C/M (2:1). Lipid quantity corresponding to 100µg myelin dry weight was spotted, separated on HPTLC using C/M/W (60:27:4) as mobile phase. Plates were finally stained as described and the lipid concentration determined, using lipid standards as reference. The results of five independent experiments [2604 (n=3), 2615 (n=6), 2620 (n=3), and wild-type (n=9)] are given as an average ±SEM. Asterisks indicate that differences are statistically significant (p<0.05, Anova) compared to wild type mice. (**A**) Age dependent sulfatide level in the line 2615, (**B**) age dependent MGDG level in the line 2615, (**C**) comparison of sulfatide level in the three lines and wild type littermates at 12 weeks of age, (**D**) comparison of MGDG level in the three lines and wild type littermates at 12 weeks of age
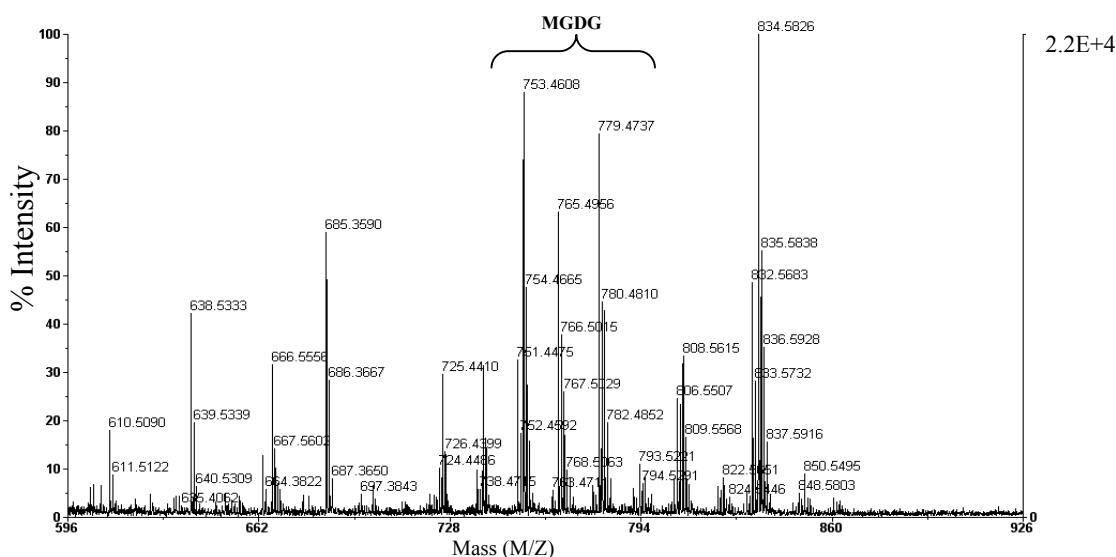
**Fig. 17 DE MALDI-TOF mass spectrum of the myelin lipid fraction**. Myelin lipid was extracted using C/M (2:1). Lipid quantity corresponding to 100µg myelin dry weight was spotted, separated on HPTLC using C/M/W (60:27:4) as mobile phase. The position of MGDG was identified, cut and re-extracted using C/M (1:1). Extracted sample was finally analyzed by DE MALDI TOF and the MGDG peaks identified by reference to the one already published (Tamotsu et al., 2001). Note the expanded mass spectrum between m/z 610 and 5495 and the MGDG peaks.

## *6.5.4 Psychosine is not responsible for the demyelination observed in PLP-CGT mice*

Galactosylceramidase is the enzyme that catalyze the degradation of galactosylceramide and psychosine (D-galactosyl-β-1,1´-sphingosine) to ceramide and galactose and to sphingosine to and galactose respectively (Austin et al., 1970; Kobayashi et al., 1985). The deficiency of galactosylceramidase leads in the accumulation of psychosine (essentially not detectable in healthy brain) in the brain of patient suffering from globoid cell leukodystrophy (Suzuki and Suzuki, 1978). Furthermore, accumulation of psychosine correlates with apoptosis of oligodendrocytes, globoid cell formation by microglia, and degeneration of axons (Suzuki et al., 1995). Cytotoxicity of psychosine in vitro and the fatal effect of injected psychosine led to the conclusion that progressive accumulation of psychosine is the critical biochemical pathogenetic mechanism of cell death in krabbe brain (Sweet, 1986; Luzi et al., 1996; Sugama et al., 1990; Tanaka et al., 1993: Ida and Eto, 1990). Because PLP-CGT transgenic mice show a loss of axons and oligodendrocytes, it was not clear, whether demyelination was caused by the loss of oligodendrocytes due to the increase of the level of psychosine or a defect in myelin function. For this reason, psychosine concentration was measured in the brain extract of transgenic mice and wild type littermates. HPLC results indicate no change of the psychosine concentration in transgenic mouse brains extract when compared to the wild type littermates. Psychosine values in transgenic mice were ranged between 25 and 31 pmole/mg protein compared to 31 pmole/mg proteins in wild type littermates. These values are in accordance with the one of Matsuda et al. (2001). These data indicate that psychosine is not responsible for the loss of oligodendrocytes observed by electron microscopy analysis of brain and optic nerve.

## 6.5.5 Specific down-regulation of the very long chain fatty acid (VLCFA)-containing sphingomyelin

In addition to cerebrosides, the other myelin lipids such as cholesterol and sphingomyelin have been analyzed. Sphingomyelin is synthesized by the transfer of phosphocholine from phosphatidylcholine to ceramide backbone, yielding diacylglycerol as a side product (Futerman et al., 1990; Jeckel et al., 1990). Since this reaction uses the same substrate as CGT, it was of great importance to look for its metabolism when CGT is overexpressed. VLCFA-sphingomyelin was identified in the myelin lipid homogenate by MALDI-TOF (data not shown). HPTLC analysis of myelin lipids (Fig. 14A) shows decrease in its level in the transgenic mouse lines 2620 and 2615. No change in sphingomyelin was observed in the line 2604. Cholesterol and phospholipids were also unchanged.

## 6.5.6 Reversal of non-hydroxy:α-hydroxy fatty acid galactosylceramide level of the spinal cord and PNS in PLP-CGT transgenic mice

The nervous system is composed of the CNS (brain and spinal cord) and PNS. Spinal cord was isolated from the vertebral column of transgenic mice and wild-type controls and total lipid extracted. The peripheral nerve was the sciatic and pectoral nerve and lipids were extracted as previously described. Results from HPTLC analysis (Fig. 18A) of lipids from the spinal cord and PNS shows the same reversibility in the HFA:NFA-GalC ratio as the one already observed the brain of PLP-CGT mice (Fig. 18A & B). As in the brain of PLP-CGT mice, sulfatide and the very long chain fatty acid sphingomyelin levels were also reduced in the spinal cord (Fig. 18A).
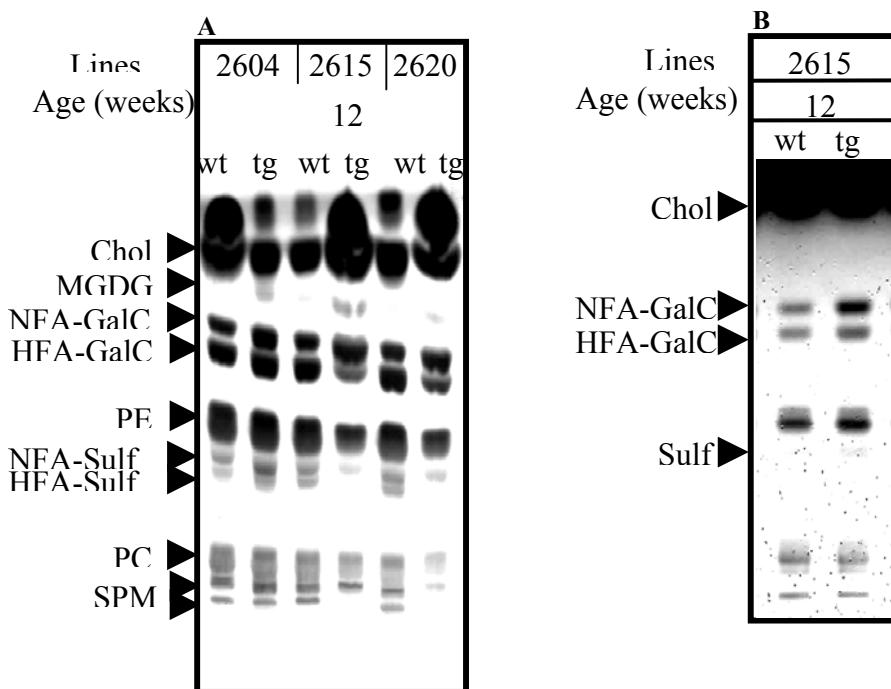
**Fig. 18 HPTLC analysis of spinal cord and PNS lipid extracts.** Lipids were extracted from spinal cord and PNS of transgenic and wild type littermate at 12 weeks of age according to Norton and Poduslo (1973). The volume of lipid corresponding to 100 µg (wet weight) spinal cord or PNA tissues lipids was spotted and separated on HPTLC plates using C/M/W (60:27:4). Lipid Bands were visualized on the $CuSO_4/H_3PO_4$ sprayed plate by heating at 170 °C for 2 minutes. (**A**) HPTLC profile of transgenic and wild type littermate from the three lines at 12 weeks of age in the spinal cord. (**B**) HPTLC profile of transgenic and wild type littermate from the three lines at 12 weeks of age in the PNS. For abbreviations, see Fig. 15.

# 6.6 Functional effects of transgenic overexpression of CGT on the development of oligodendrocytes

The high percentage of the galactolipids GalC and its sulfated form in the myelin sheath suggest that these lipids play an important role in oligodendrocyte and myelin physiology. During development, OL progenitors are characterized by changes in their morphology, proliferation and migratory capacities and the regulated expression of myelin-specific proteins and lipids such as GalC and sulfatide (Pfeiffer et al, 1993).

## 6.6.1 Increase in MBP and PLP positive cells in PLP-CGT transgenic mice

Previous studies have shown that GalC and sulfatide appears at the immature stage during oligodendrocyte differentiation (Bansal et al., 1992; Bauman and

Pham-Dinh, 2001). It was previously demonstrated that GalC and sulfatide plays important role in the regulation of oligodendrocyte differentiation (Bansal et al., 1988, 1999; Boggs and Wang, 2001; Hirahara et al., 2004). For this reason, it was logic to ask whether increased activity of CGT have an effect on the differentiation of oligodendrocyte. In present study, we did not examine the intermediate markers that appear during oligodendrocyte development, but only the MBP expression which is the marker of the mature oligodendrocyte. Oligodendrocyte maturation in wild type and PLP-CGT mixed culture was analyzed as the function of time by immunofluorescence microscopy (Fig. 19 and 20). The expression of MBP was assayed as the marker for oligodendrocyte maturation *in vitro*. The results indicate that a significant increase of MBP positive cells number in the mixed culture of brain cells from PLP-CGT transgenic mouse compared to wild type after 10 and 20 days of culture (Fig. 21A). In addition, less MBP positive cells from the PLP-CGT culture exhibited the morphology of a mature oligodendrocyte after 20 days of culture (Fig 21B). In contrast, an elevated number of MBP positive cells in PLP-CGT culture did exhibited the morphology of an immature oligodendrocyte, compared to the cells from the wild-type culture (Fig. 21C). The morphological classification in this study was similar to the one already published by Baumann and Pham-Dinh (2001) (for schematic classification, see Fig. 5). In our study, any MBP positive cell having a morphology resembling to the one of the pre-oligodendrocyte or immature oligodendrocyte stages was classified in one group as immature oligodendrocyte.

To test further the impact of CGT overexpression on the development of oligodendrocytes, MBP immunolabeling was performed on vibratome sections from PLP-CGT transgenic mice and wild type controls. As observed *in vitro*, an increase of the MBP immunostaining was observed in the striatum (Fig. 22A) and the corpus callosum (Fig. 22B) of PLP-CGT mouse brains, compared to the wild-type controls (Fig. 22C and D), respectively.
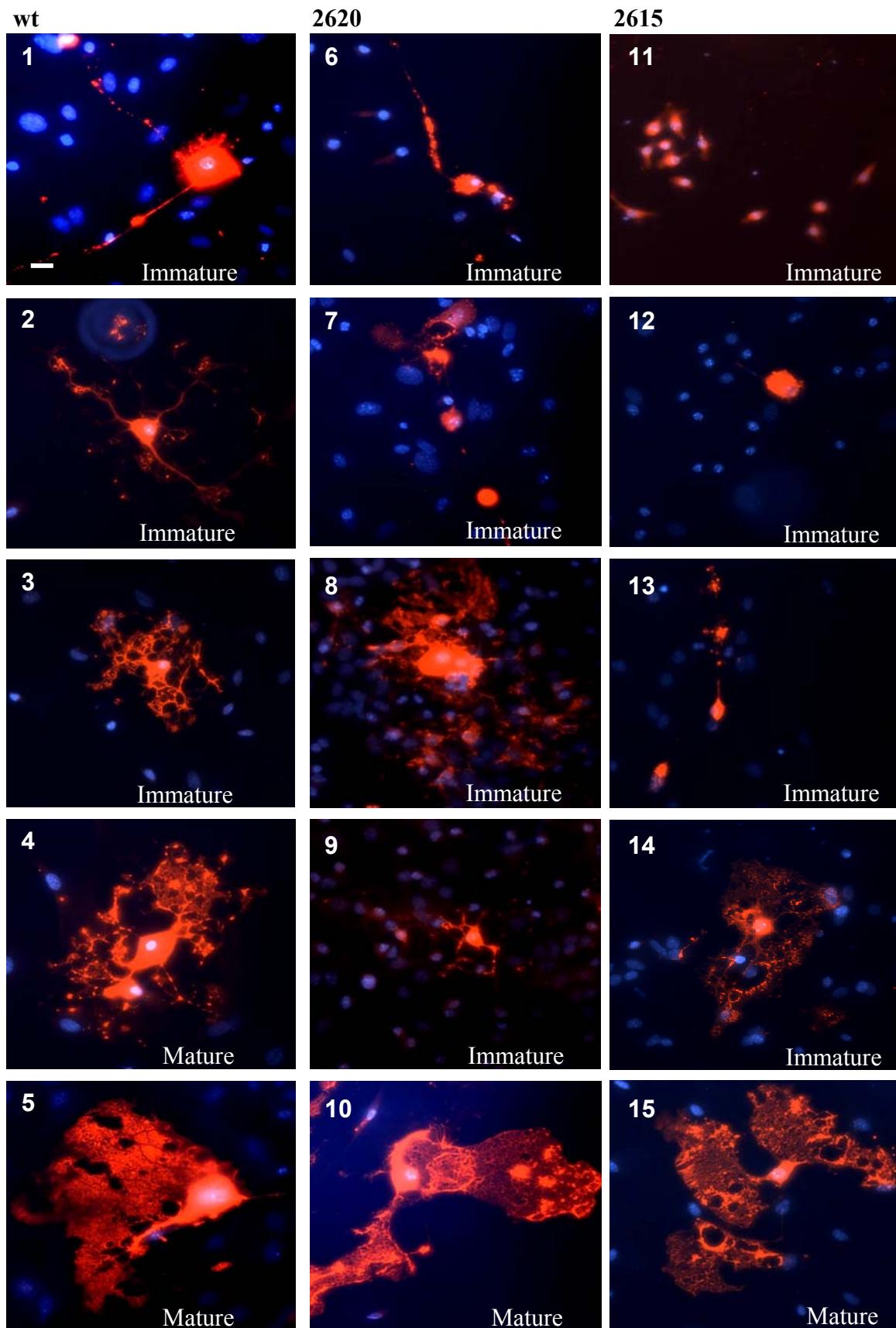
**Fig.19 Morphology of oligodendrocytes after 10 days of the culture of cells from PLP-CGT mouse brains**. Mixed primary cultures of neonatal mouse brain (PND 1-2) were prepared from transgenic lines [line 2620 (6-10), line 2615 (11-15)] and wild type littermates (1-5) as described by Pesheva et al. (1997) and culturte as described by Bansal et al. (1999). Differentiated cells were visualized by immunofluorescence after the labeling of the cells with rabbit anti-MBP and anti-rabbit

Cy3-labelled second antibody. Nucleus was visualized by DAPI staining. Note that some cells expressing MBP do not have the morphology of a mature oligodendrocyte. Scale bar 20µm.
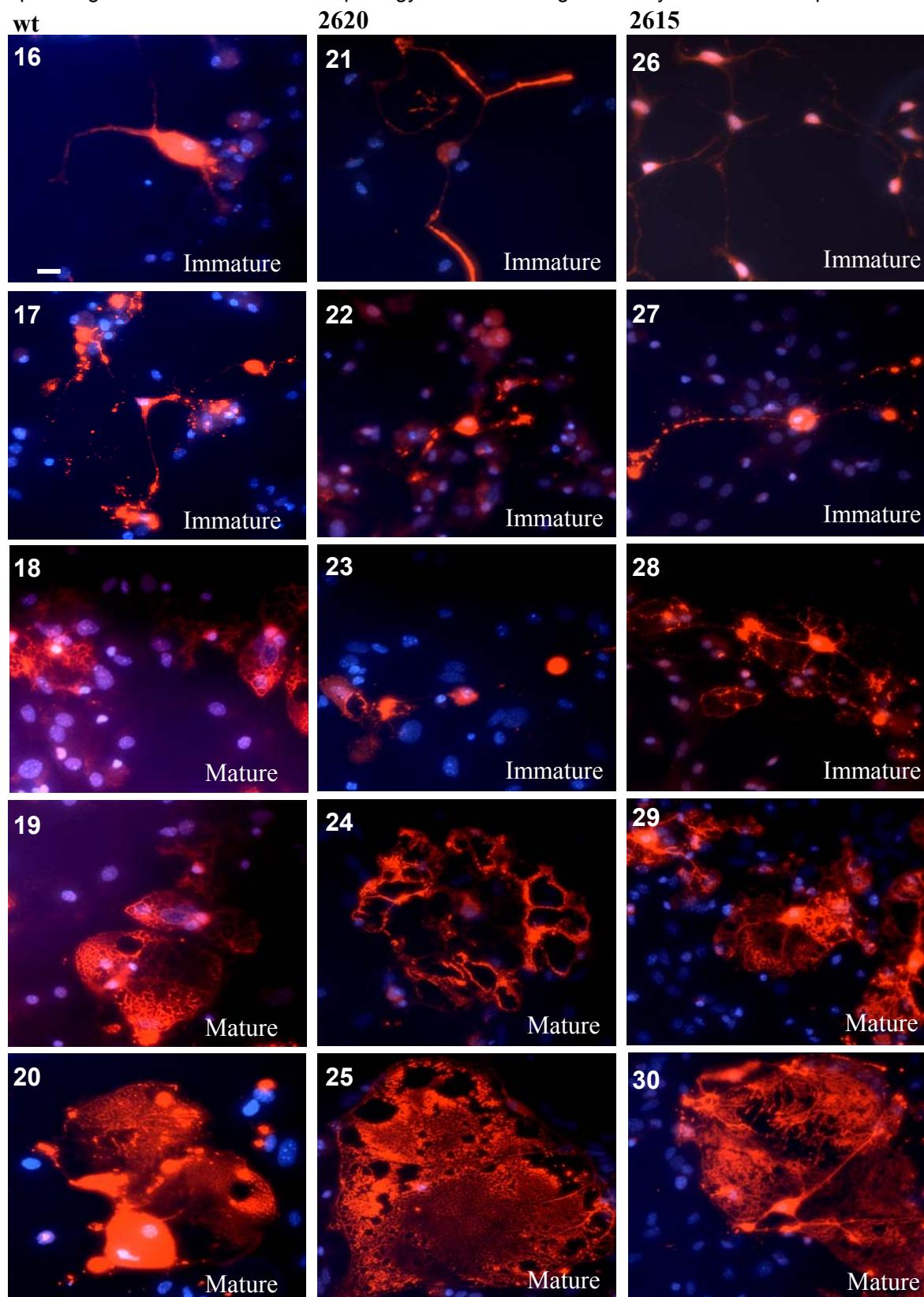


**Fig.20 Morphology of oligodendrocytes after 20 days of the culture of cells from PLP-CGT mouse brains**. Mixed primary cultures of neonatal mouse brain (PND 1-2) were prepared from transgenic lines [line 2620 (21-25), line 2615 (26-30)] and wild type littermates (16-20) as described by Pesheva et al. (1997) and culturte as described by Bansal et al. (1999). Differentiated cells were visualized by immunofluorescence after the labeling of the cells with rabbit anti-MBP and anti-rabbit

Cy3-labelled second antibody. Nucleus was visualized by DAPI staining. Note that some cells expressing MBP do not have the morphology of a mature oligodendrocyte. Scale bar 20µm.
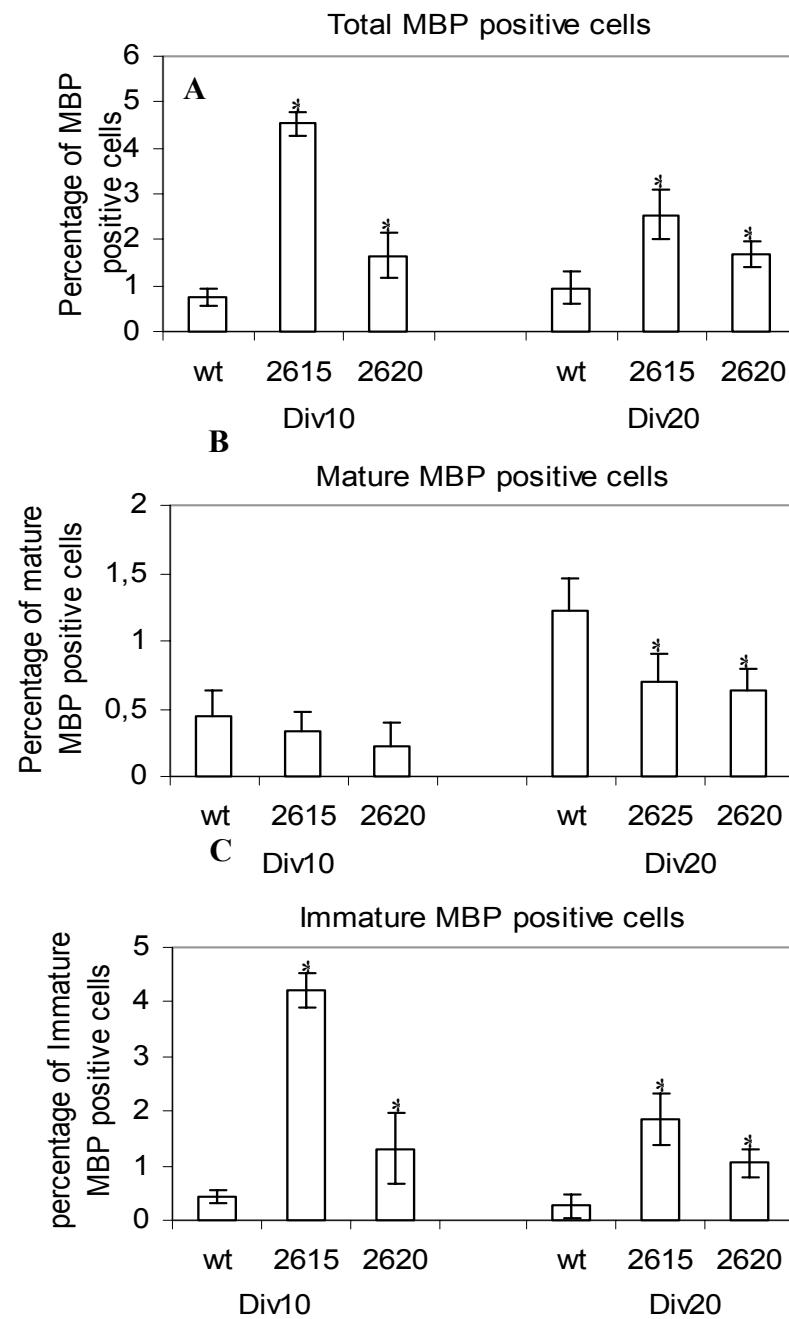


**Fig. 21 Enhencement of MBP positive cells in the primary cultures from PLP-CGT Transgenic mouse brains**. Mixed primary culture of neonatal mouse (PND 1-2) fore brains were prepared from transgenic lines 2615, and 2620 and wild-type controls. After 10 and 20 days of culture, cells were analyzed for the expression of MBP by immunofluorescence microscopy. Cells probed with antibody against MBP were visualized using Cy3-labelled anti-rabbit antiserum. Total number of the cells was visualized by the nuclear staining (DAPI). Total (700-30000) and MBP positive cells were counted and the percentage of the MBP positive cells calculated. Cells were classified as total MBP positive cells (**A**), mature OL (**B**) and immature OL (**C**) according to their morphology. Error bars represent SEM (n=3-5). Asterisks indicate significant differences between transgenic mice and wild type controls. (p<0.01; ANOVA). In our study, any MBP positive cell having a morphology resembling to the one of the pre-oligodendrocyte or immature oligodendrocyte stages was classified in one group as immature oligodendrocyte.
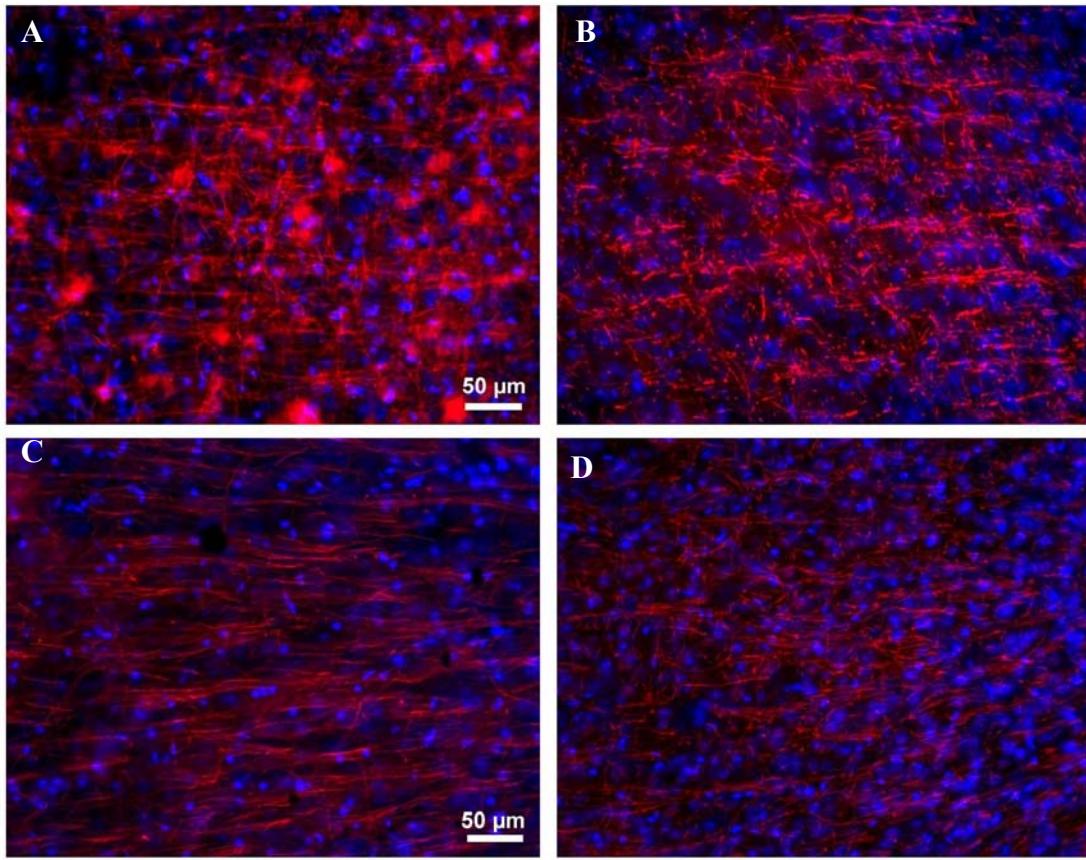
**Fig. 22 MBP expression in PLP-CGT transgenic mice**. Vibratome slices were prepared from 6 weeks old transgenic mice and wild-type controls as described by Baader et al. (1998). Slices were probed with anti-MBP antibody and finally with the appropriated Cy3-labeled second antibody. Positive cells were documented by microscopic analysis. (B) MBP staining in the striatum of the line 2615 of PLP-CGT mice. (B) MBP staining in the corpus callosum of the line 2615 of PLP-CGT mice, (C) MBP staining in the striatum of wild type littermate, and (D) MBP staining in the corpus callosum of wild-type mouse.

During *in vivo* analysis of oligodendrocytes differentiation, a reliable quantification of MBP positive cells in the vibratome slices was impossible because of a highly immuno-labeled fiber. This problem was overcome by counting PLP positive cells obtained by in situ hybridization of microtome brain slices from transgenic and wild type controls at 4 weeks of age. When parallel sections from control and transgenic mice were counted, no significant difference was observed in the brainstem of transgenic mice compared to controls, except the line 2615 where a significant reduction of cells expressing the PLP mRNA was observed (Fig.23A-C, for quantification see Fig 23G). In contrast to brainstem, a significant increase in PLP mRNA-positive cells was

noticed in the corpus callosum of the two line at 4 weeks of age (Fig. 23D-F, see Fig. 23G for quantification).
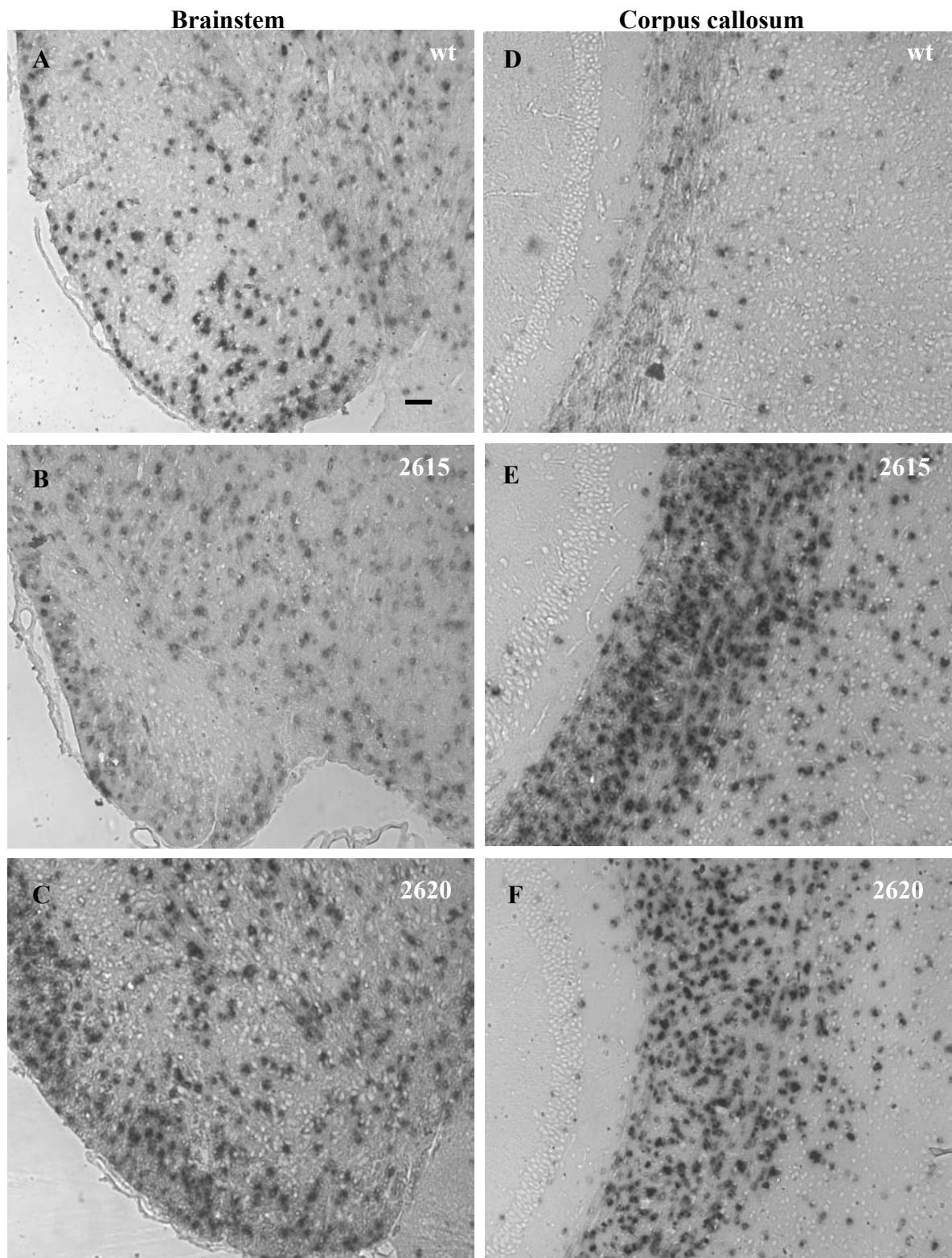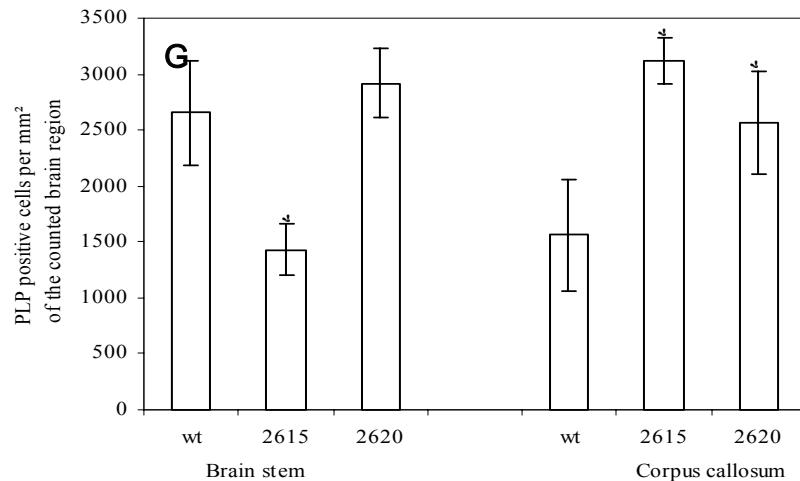
**Fig. 23 Enhancement of oligodendrocyte in vivo in the corpus callosum of PLP-CGT transgenic mice**. Expression of PLP mRNA, as marker of the mature oligodendrocyte was assessed by in situ hybridization in the sagittal sections of the PND 28 brains taken from parallel regions from PLP-CGT transgenic and wild type littermate mice. PLP mRNA positive cells in the brain stem (**A-C**) and corpus callosum (**D-E**) are shown. Sections show a significant higher number of PLP mRNA positive cells in the corpus callosum (**E & F**) of PLP-CGT transgenic mice and a significant reduction in the brainstem of the line 2615 (**B**) , but no for the line 2620 (**B & C**) when compared to the wild type littermates (**A & D**). Difference between transgenic mice and wild type littermates were obtained by counting the cells (**G**). The result is given as a number of PLP positive cells per mm² of the counted regions. Each value represents the mean ± SEM of 3 animals per group. Asterisks indicate significant differences between transgenic mice and wild type controls. ($p < 0.01$; ANOVA). Scale bar 50 μm.

## 6.7 Behavioral deficits in PLP-CGT transgenic mice

Three lines of transgenic mice overexpressing CGT in the CNS were produced. One of these lines expresses only low doses of transgene and did not show any clinical or morphological changes (Line 2604). In contrast, the two other lines (Lines 2615 and 2620), carry several copies of transgene per haploid genome (Fig. 9B). Hemizygous PLP-CGT mice develop severe behavioral abnormalities. At around 8 weeks of age, offspring mice from the line 2615 start to display uncoordinated gait and splaying of the hind limbs during locomotion, which continuously aggravate over time. Mice of the line 2620 later showed the same phenotype. At the adult age, transgenic mice displayed a complete paralysis of the hind limbs and were incapable of movement. Mice presenting this phenotype were unable to live more than one year.

To reveal exactly the time of the onset of motor impairments in PLP-CGT transgenic mice, mice of the line 2615 (n=8) and wild type littermates mice

(n=8) were subjected to rotarod analysis at different age (4, 6 and 8 weeks), at two different speeds (6 and 10 rpm), respectively. Results show no difference between transgenic and wild type littermate at 4 weeks of age, both at 6 and 10 rpm (fig. 24A & B). At 10 rpm, and at 6 weeks of age, only 40% of transgenic mice were able to stay on the rotating rod compared to the 80% of wild type controls (fig. 24B), whereas at 6 rpm transgenic mice scored the same performance as wild type (fig. 24A). At 8 weeks of age and at both speeds, a clear difference was observed (see Fig. 24). Taking together, these results indicate that the onset of the motor impairment started at around 8 weeks of age.
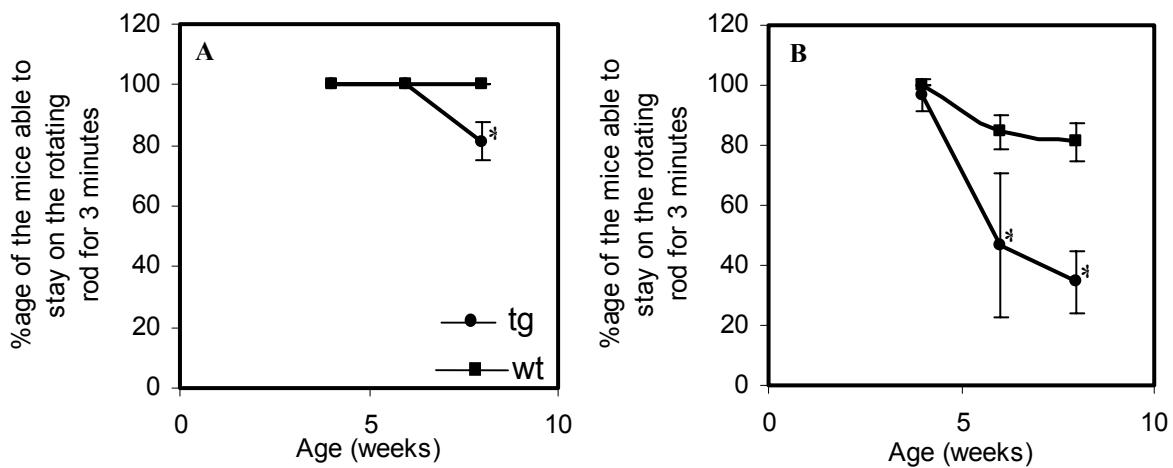


**Fig. 24 Motor-coordination capacities of PLP-CGT transgenic mice**. Animals (n=8 per group) at different age were placed on a rotating rod at 6 and 10 rpm. The time interval during that the mice stayed on the rod was measured. A maximal time of the staying on the rod was fixed to 180 second. The test was one time a day over a period of 5 days. The percentage of animals able to stay on the rotarod in a maximal time of 180 second. Results are given as an average ± SD. (A) Rotarod experiment at 6 rpm and (B) 10 rpm. Asterisks indicate significant differences between transgenic and wild type mice ($p<0.01$; t-test).

## 6.8 Astrogliosis in PLP-CGT transgenic mice

Astrogliosis is a generalized response of glial cells to CNS injury and trauma (Mucke and Eddleson, 1993). In multiple sclerosis (MS), reactive astrocytes are found in the scar-like regions of demyelinated axons (Mckhann, 1982). The sign of the reactive astrocytes is the increase of the glial fibrilary acidic protein level (GFAP), the major glial intermediate filament protein. In order to determine if reactive gliosis occurs in the CNS of PLP-CGT mice, GFAP levels were examined both by Western blot and immunohistochemistry. Western blot

analysis of proteins homogenate from the brains of transgenic mice and wild type controls showed a marked increase in the GFAP level in PLP-CGT transgenic mice (Fig. 25B).

Immunohistochemical analysis on sagittal sections from brains of 6 weeks old mice also revealed a significant increase in GFAP immunoreactivity signals in cerebellum, hippocampus, forebrain and brainstem of transgenic mice compared to wild type controls (Fig. 25A).



| Line | 2615 | | | | | |
|------|------|------|------|------|------|------|
| Age (weeks) | 4 | | 8 | | 19 | |
| | wt | tg | wt | tg | wt | tg |
| GFAP | | | | | | |

**Fig. 25 GFAP immunoreactivity in the CNS of PLP-CGT transgenic mice.** Astrocyte reactivity was determined both by immunuhistochemical and Western blot analysis using antibody directed to GFAP. GFAP immunoreactivity of Vibratome slices of the line 2615 of PLP-CGT mice and wild type littermates at 6 weeks of age (**A**) and Western blot analysis of total brain protein from the line 2615 of PLP-CGT transgenic and wild type controls at different age (4, 8 and 19 weeks) (**B**). Scale bar 50 µm.

## 6.9 Consequences of CGT overexpression on the myelin structure

A myelinated fiber appears as myelinated membrane segments, termed internodes, separated by regions of ensheathed nerve membrane (Allard et al., 1998). It is this disposition by segments that induces the major characteristic of the so-called "saltatory conduction" of nerve impulses in myelinated tracts. The normal myelin sheath has a high resistance and low

capacitance that makes the current tend to flow down the fiber to the next node rather than leak back across membrane.

### 6.9.1 Demyelination and myelin destabilization in PLP-CGT transgenic mice

The optic nerve and spinal cord from transgenic mice were examined for structural changes by electron microscopy. At 5 weeks of age, transgenic mice from the three lines showed apparently normal myelination as revealed by the cross section of the optic nerve of the line 2615 (fig. 26A). Between 4 and 6 months, transgenic mice display a massive loss of myelin membranes as shown in Fig. 26C and 26E. Hence, in relation to the severe pathological behavior observed in the transgenic line 2615, axonal demyelination occurred earlier in the line 2615 than in the line 2620 of the PLP-CGT transgenic mice. No demyelination was observed in the line 2604 that expresses a low amount of GalC mRNA, has a low CGT activity, and shows no deficit of the motor locomotion.

Electron microscopy analysis of the optic nerve from the line 2615 at 18 weeks of age show an almost complete depletion of axons of the myelin sheath (Fig. 26C), whereas a substantial number of myelinated axons were still found at 28 weeks of age in the transgenic mouse line 2620 (Fig. 26E). Similar results were obtained by electron microscopic analysis of the spinal cord (Fig. 26D). Transgenic mice exhibited vacuolation in the optic nerve (Fig. 26 see arrow in E) and more extensive decompaction in the spinal cord (Fig. 26 see arrow D). Electron microscopy analysis also show thinner and less compacted myelin sheath in the line 2615 at 5 weeks of age (Fig. 26A) and 2620 (Fig. 26E) when compared to the wild type littermate (Fig. 26B). Axonal degeneration was also observed in the optic nerve of transgenic mice of adult age (Fig. 26 see arrow in A) and the spinal cord (data not shown).

In contrast to the CGT-/- mice, the electron micrographs of a longitudinal section from the spinal cord tissue of PLP-CGT mice, show no abnormal formation of the paranodal junction (Fig 27B low magnification, Fig. 27A

enlarged area) when compared to the wild type littermates (data no shown). Beside the abnormal structure of myelin observed in the CNS, PNS axons are correctly ensheathed by compacted peripheral myelin in all transgenic mice, with no sign of demyelination, or degenerating Schwann cells (data not shown).
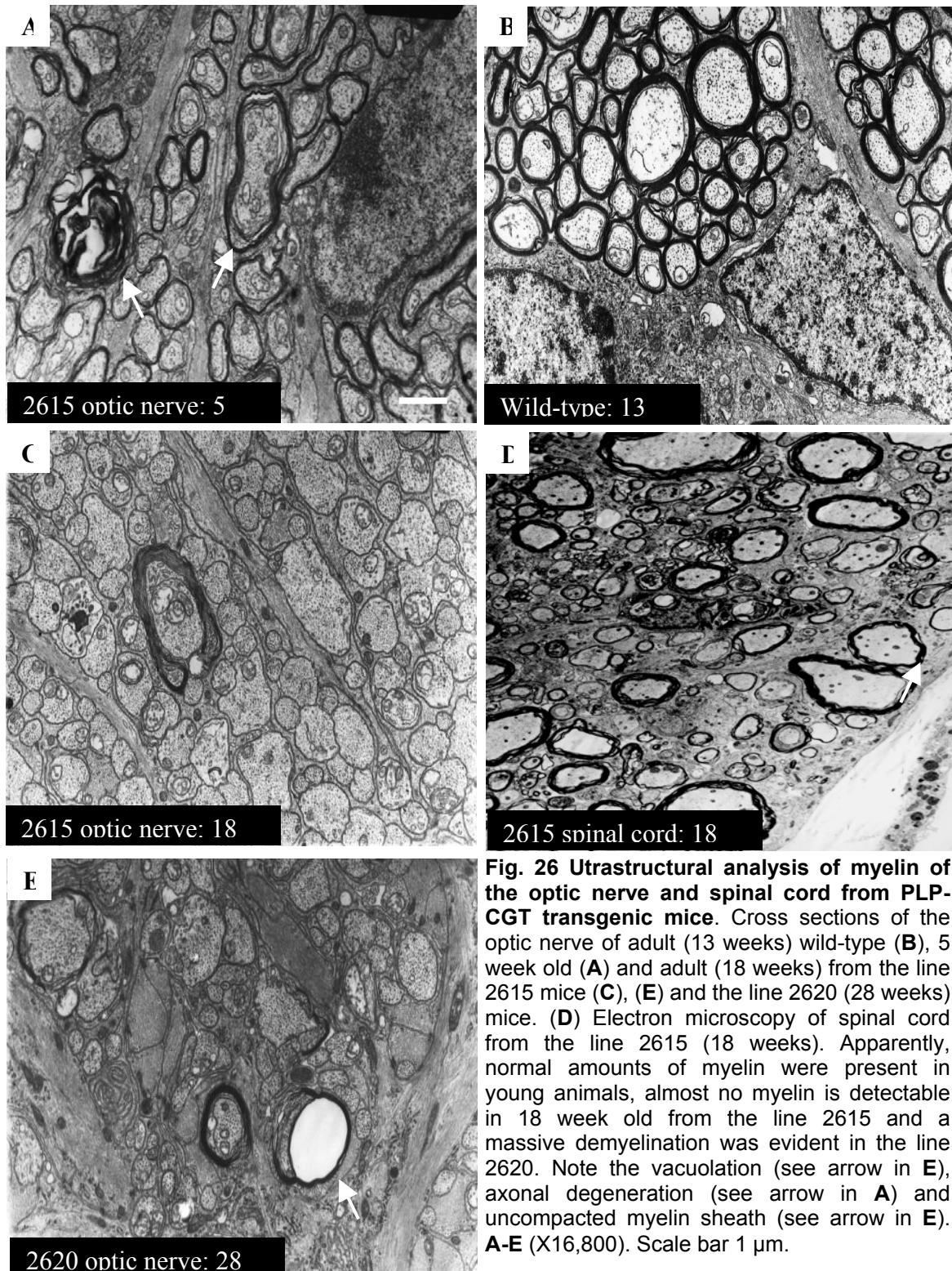


**Fig. 26 Utrastructural analysis of myelin of the optic nerve and spinal cord from PLP-CGT transgenic mice**. Cross sections of the optic nerve of adult (13 weeks) wild-type (**B**), 5 week old (**A**) and adult (18 weeks) from the line 2615 mice (**C**), (**E**) and the line 2620 (28 weeks) mice. (**D**) Electron microscopy of spinal cord from the line 2615 (18 weeks). Apparently, normal amounts of myelin were present in young animals, almost no myelin is detectable in 18 week old from the line 2615 and a massive demyelination was evident in the line 2620. Note the vacuolation (see arrow in **E**), axonal degeneration (see arrow in **A**) and uncompacted myelin sheath (see arrow in **E**). **A-E** (X16,800). Scale bar 1 µm.
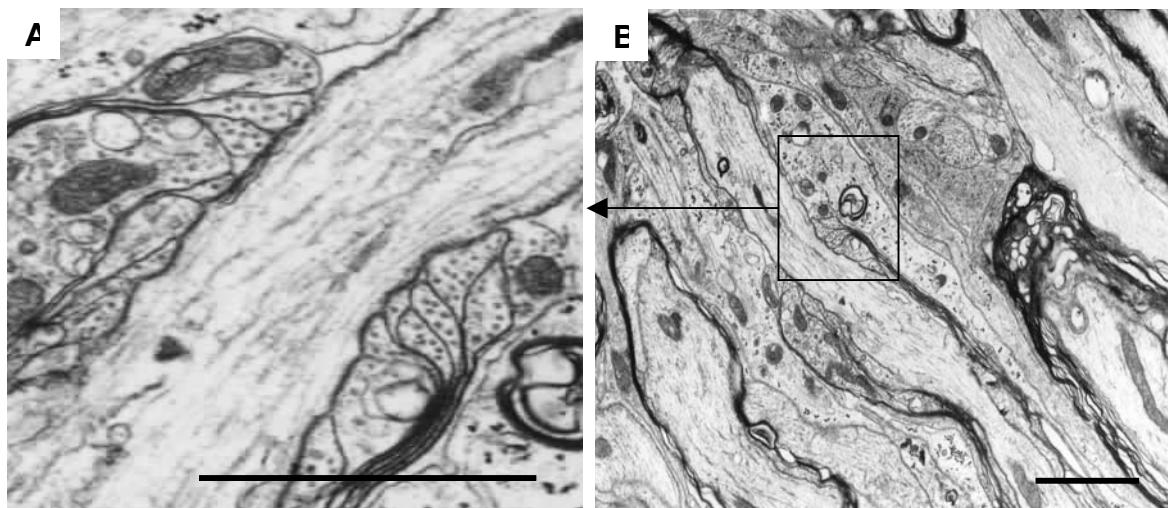
**Fig. 27 Utrastructural analysis of the paranode in the spinal cord of PLP-CGT transgenic mice**. Longitudinal sections from 18 weeks old transgenic mice from the line 2615 of the PLP/CGT transgenic mice. The node paranodal junction appears to be normal. **B** (X5,600) and (**A**) area enlarged. Scale bar 1 µm.

# 7    <u>DISCUSSION</u>

One aim of this study was to increase GalC and sulfatide synthesis by transgenic overexpression of CGT, in order to study the effect of increasing levels of these lipids on oligodendrocyte lipid metabolism and myelin stability. Surprisingly, despite a significant increase in CGT enzyme activity, there was only a marginal increase in total GalC in one out of three transgenic lines, moreover, sulfatide levels were reduced. Increase in MGDG, which is an alternative product of CGT, indicates that CGT activity was indeed increased *in vivo* and that the supply of UDP-galactose probably was not limiting galactosylation of ceramide. While NFA-GalC increased in good correlation with the increased CGT activity, we unexpectedly observed a decrease in the major GalC species, HFA-GalC. α- hydroxylation occurs in the microsomal fraction though it is not clear whether the free fatty acid, ceramide, or an unidentified intermediate product is the substrate for the mammalian fatty acid 2-hydroxylase (FA2H) (Singh and Kishimoto, 1979). The mammalian FA2H is a 42.8 kDa protein, located in the endoplasmic reticulum and that catalyzes the hydroxylation of the fatty acid present on the ceramides (Eckhardt et al., 2005). Nevertheless, strong evidence has been obtained for direct α-hydroxylation of ceramide in lower eukaryotes (Kaya et al., 1984; Haak et al., 1997: for contrary view see Anderson et al., 2004). Therefore, competition between α-hydroxylation and galactosylation of ceramide is likely being responsible for the decrease in HFA-GalC in CGT transgenic mice. In line with this, absence of GalC and sulfatide in CGT deficient mice is accompanied by a dramatic upregulation of HFA-glucosylceramide and HFA-sphingomyelin, which become the major sphingolipids in purified myelin (Coetzee et al., 1996; Bosio et al., 1996). The reduction of HFA-ceramide upon increased galactosylation of NFA ceramide suggests that ceramide availability may be limited. This is also in accordance with the finding that total GalC levels do not significantly increase and allows the conclusion that ceramide availability and not CGT activity limits GalC synthesis in vivo. Predominance of HFA-GalC in

myelin of wild type mice has been attributed to an increased activity of CGT towards HFA-ceramide. Our results demonstrate that the differential affinities of CGT for HFA and NFA-ceramide (Schaeren-Wiemers et al. 1995a) are not the only determinant of the ratio of these two lipid species in vivo. In fact, predominantly the level of CGT activity may determine how much of the ceramide is galactosylated and thus unavailable for hydroxylation. Thus, the predominance of HFA-GalC in vivo may be due to the low level of CGT relative to ceramide hydroxylation. Interestingly, whereas HFA-sulfatide was reduced in parallel with HFA-GalC in transgenic mice, NFA-sulfatide was not increased, leading to an overall decrease of sulfatide. Thus, HFA-GalC levels limit HFA-sulfatide whereas NFA-GalC is not limiting NFA-sulfatide synthesis. In the mammalian brain, more than 50% of the GalC and sulfatide contain α-hydroxylated fatty acids. α-hydroxylase activity reaches a maximum during the active period of myelination (Svennerholm and Stallberg-Stenhagen, 1968; Nonaka and Kishimoto, 1979), similar to the expression of CGT and other myelin-related genes, e.g. MBP, PLP, and MAL (Garbay and Cassagne, 1994; Muse et al., 2001; Frank et al., 1999; Schaeren-Wiemers et al., 1995b; Sorg et al., 1987; Gardinier et al., 1986). α-hydroxylation of sphingolipids has been implicated in the stability of the myelin sheath (Shah et al., 1995; Koshy et al., 1999; Graf et al., 2002). There is, however, no direct experimental evidence for a functional role of sphingolipid α-hydroxylation in vivo. Transgenic mice overexpressing CGT have essentially normal levels of GalC. In myelin, the only major alteration of lipid composition is the significantly reduced HFA:NFA-GalC ratio. At the same time there seem to be no major changes in protein composition of myelin of transgenic mice. Thus, it seems likely the HFA:NFA-GalC ratio is responsible for unstable and uncompacted myelin, suggesting an important role of sphingolipid α-hydroxylation in the stability and maintenance of the myelin membrane. The total amount of HFA-sphingolipids was reduced to a similar degree in CGT transgenic and deficient mice. The massive myelin decompaction, however, observed in CGT transgenic mice was not observed in the CGT knockout mice (Bosio et al., 1998a; Coetzee et al., 1996; Coetzee et al., 1998). This suggests that destabilization of the myelin in CGT transgenic

mice is not due to reduced levels in HFA-sphingolipids, but that the HFA:NFA-GalC ratio is the relevant factor in the stabilization of the myelin sheath. α-hydroxylation of sphingolipids might increase lateral interaction between sphingolipids and it could facilitate formation of ion complexes (Graf et al., 2002) and therefore stabilize the membrane by increasing lateral interactions within the compact myelin. In the absence of GalC in CGT knockout mice, the distribution of several proteins between lipid-rafts and non-raft fractions is affected (Kim and Pfeiffer, 2002). Thus, GalC is important in the formation of myelin lipid rafts and it is tempting to speculate that alterations in the HFA:NFA-GalC ratio might interfere with the assembly of functional rafts in the myelin membrane. An indication for alterations in myelin microdomain structure is the accumulation of MAL in CGT transgenic mice. Although we observed upregulation of MAL mRNA levels in PLP-CGT transgenic mice, upregulation of MAL protein was much more pronounced. This raises the possibility that there is also an accumulation of MAL in the myelin membrane. MAL is a four transmembrane domain protein, which also has been identified in epithelial cells of kidney and stomach (Schaeren-Wiemers et al., 1995; Frank et al., 1998). Thus, MAL is expressed in tissues with exceptionally high amounts of GalC and sulfatides. In line with this, Frank et al. (1998) showed that MAL binds sulfatide. Expression of MAL correlates with myelination and the protein is found in compact myelin, where it associates with sphingolipid-rich membrane microdomains or rafts (Frank et al., 1998, 1999; Erne et al., 2002). MAL is required for efficient vesicular transport to the apical surface in MDCK cells (Cheong et al., 1999; Martin-Belmonte et al., 2001). Recently, it has been shown that MAL is also an important factor in the clathrin-mediated endocytosis at the apical surface in MDCK cells (Martin-Belmonte et al., 2003), and its presence in the Schmidt-Lanterman incisures (Erne et al., 2002) suggests that MAL might be involved in the turnover of myelin membrane components as well. Thus apparent accumulation of MAL protein in the myelin of CGT transgenic mice (lines 2615 and 2620) might be explained by impaired recycling of MAL via the endosomal pathway (Martin-Belmonte et al., 2003). Other myelin proteins e.g. PLP or MAG, however, are not enriched in the

myelin of CGT transgenic mice, indicating that their turnover is not affected. This suggests localization of MAL and PLP in different membrane microdomains. In line with this, differences in detergent solubility between MAL and PLP and other membrane proteins suggest the existence of different types of membrane microdomains (Erne et al., 2002; Kim and Pfeiffer, 2002; Taylor et al., 2002). Interestingly, we recently observed that sulfatide accumulation in arylsulfatase A deficient mice leads to severe reduction in MAL mRNA and protein level as well as mistargeting of MAL (Saravanan et al., 2004). In sulfatide storing kidney cells, MAL was redistributed to the endosomal/lysosomal compartment, supporting the hypothesis that altering the sphingolipid composition affects MAL protein transport.

Overexpression of transgenic CGT led to a specific decrease in the endogenous murine CGT mRNA, suggesting feedback inhibition. Whether this occurs at the transcriptional or posttranscriptional level remains to be determined. Negative regulatory elements have been found in the promoter region of both human and mouse CGT gene, though their functional relevance in vivo has not been investigated (Yonemasu et al., 1998; Tencomnao et al., 2001). Similar to CGT transgenic mice, downregulation of CGT mRNA has been observed in twitcher mice (Taniike et al., 1998). Twitcher mice lack a functional galactosylceramidase and are unable to degrade GalC and psychosine (Wenger et al., 2001). Interestingly, these mice as well as humans suffering from globoid cell leukodystrophy (Krabbe disease) do not accumulate substantial amounts of GalC (Wenger et al., 2001), which at least in part may be explained by the reduced CGT mRNA level. Similarly, in metachromatic leukodystrophy and in arylsulfatase A deficient mice accumulation of sulfatide is accompanied by a significant reduction in GalC, although it has not been investigated whether this is due to downregulation of CGT expression (Von Figura et al., 2001). Psychosine is dramatically increased in globoid cell leukodystrophy (Igisu and Suzuki, 1984) and could potentially be the signaling molecule responsible for CGT mRNA downregulation. This can, however, be excluded in the case of CGT transgenic mice, where psychosine concentration was normal. Our data shows that the HFA:NFA-GalC ratio is an indicator of

CGT activity. Changes in this ratio might affect membrane micro domain organization and consequently signal transduction in oligodendrocytes, resulting in CGT mRNA reduction. Alternatively, the reduction in VLCFA-sphingomyelin might affect the formation of ceramide, sphingosine or sphingosine-1-phosphate and thereby modify signal transduction processes leading to CGT mRNA downregulation. In any case, the existence of a feedback control of CGT expression emphasizes the necessity of a tight control of CGT expression/activity in formation and maintenance of a functional myelin sheath. Further, the apparent devastating consequences of altering the HFA:NFA-GalC ratio without altering GalC concentration in myelin is remarkable, and supports the crucial role that these lipids have in myelin stability and maintenance.

Understanding the mechanisms that regulated differentiation of oligodendrocytes is important for an understanding the myelin formation and maintenance processes. GalC and sulfatide synthesized in the ER and Golgi, respectively, are transported to the outer leaflet of oligodendrocyte plasma membrane at a specific time during differentiation (Raff et al., 1978; Hardy and Reynolds, 1991). Antibody perturbation studies demonstrated that GalC and sulfatide plays critical role in oligodendrocytes differentiation (Bansal and Pfeiffer, 1989). GalC-/- and sulfatide knockout mice shows increase of oligodendrocyte differentiation both *in vivo* and *in vitro*, suggesting that GalC and sulfatide are important factors of oligodendrocyte development and myelin formation (Bansal et al., 1999; Hirahara et al. 2004).

Mature oligodendrocytes are characterized by the expression of MBP and PLP, which therefore serve as markers for terminal differentiation. Moreover, differentiated oligodendrocytes are characterized by a change in their morphology. In the present study, we found *in vitro*, an increase of MBP positive cells in the primary culture of cells from PLP-CGT transgenic mouse brains. Furthermore, a significant increase of PLP positive cells was observed *in vitro* in the corpus callosum of transgenic mice (lines 2615 and 2620). This increase could not be due to the overexpression of CGT in the mouse brain, but to the decrease of sulfatide content observed in PLP-CGT transgenic mice,

since sulfatide is known as a negative regulator of oligodendrocyte differentiation (Hirahara et al. 2004). Morphologically, low amount of MBP positive cells from PLP-CGT transgenic mice displays the morphology of a mature oligodendrocyte *in vitro*. This data could suggest an impairment of the terminal stage during the development of oligodendrocytes in PLP-CGT transgenic mice in vitro.

# 8 <u>CONCLUSION</u>

In any event, the observation presented in the first part of this thesis establish a relationship between the ratio of HFA:NFA-GalC and the stability of the myelin sheath in the CNS. Mice with altered ratio of HFA:NFA-GalC demyelinate at the adult age. In addition, myelin in these mice is uncompacted, with signs of vacuolation and axonal degeneration. Furthermore, elevation of the level of NFA-GalC did not induce the increase of NFA-sulfatide level, suggesting that NFA-GalC is not a limited factor for the NFA-sulfatide synthesis. Examination of the longitudinal section of PLP-CGT optic nerve indicates no alteration of the paranode structure. In contrast to CNS, PNS myelin was not altered, suggesting that change of HFA:NFA-GalC ratio have no effect on the stability of PNS myelin. Moreover, increased concentration of the MAL protein in myelin of PLP-CGT mice suggests a possible alteration of the rafts microdomain. Although the HFA:NFA-GalC ratio was altered, and HFA-sulfatide level reduced in these mice, oligodendrocyte numbers were elevated both *in vitro* and *in vivo*. The increase of oligodendrocyte numbers could not be affected to the change of HFA:NFA-GalC ratio, but to the decrease of sulfatide level in PLP-CGT mice, since sulfatide is a negative regulator of oligodendrocytes differentiation. In contrast to increased amount of oligodendrocytes in PLP-CGT mice, an impairment of the terminal stage of oligodendrocytes development was observed, indicating that a normal HFA:NFA-GalC ratio is required for an efficient maturation of oligodendrocytes.

# PART II

## Regional impairment of oligodendrocytes development and demyelination in PLP-PST transgenic mice

# PART II

## 9.1 Identification of the PLP-PST founder mice and their behavior

The transgene (Fig. 28A) was constructed by inserting a 1.09 kb of the mouse PST/ST8Sia IV cDNA into the PmeI site present in the PLP promoter cassette (a kind gift of Dr. Macklin). The PLP promoter cassette contains a 2.4 kb PLP promoter, exon1, intron 1 (8.5 kb), the first 37 bp of the exon 2, where the translation start site was mutated in order to allow the transcription to start at the transcription start site present in the PST cDNA, and the SV40 polyadenylation site. By digesting (ApaI/NotI) a 10.86 kb DNA fragment, the PLP-PST construct was released from the bluescript plasmid and microinjected into the fertilized mouse oocytes obtained by the crossing of CBA and C57/Bl6 mice strain. Sixty founder mice (33 females and 27 males) were obtained. Founder mice were screened for the presence of the transgenic construct both by PCR (data not shown) and Southern blot (fig.28B) analysis of the genomic DNA from mouse tails. Results indicate four transgenic founder mice (224, 244, 266, 281), which transmitted the transgene in the Mendelian fashion.
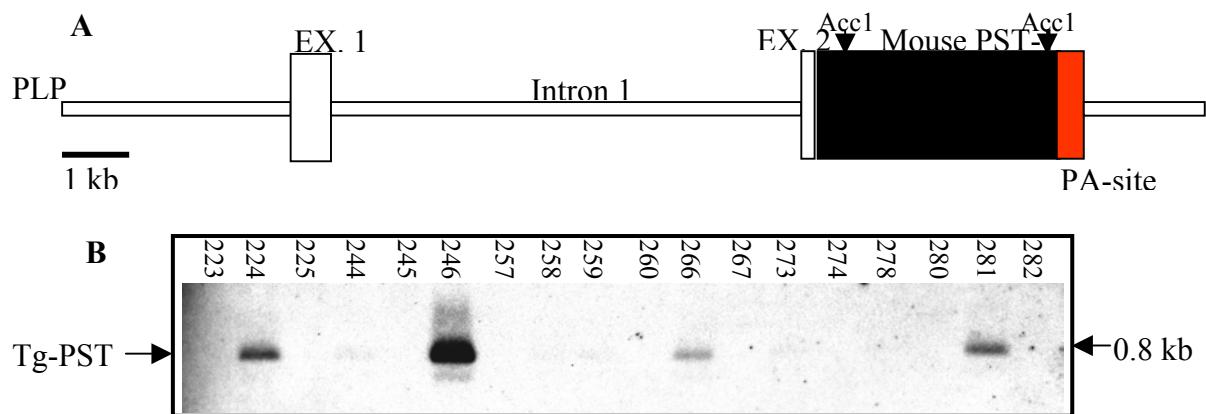


**Fig.28 Transgene construction and identification of the PLP-PST mice**. **(A)** The scheme represents the DNA region derived from the PLP promoter gene (2.4 kb) including the transcription start site as well as the whole PLP intron 1. The white boxes represent the PLP exon1 and 37bp of the exon 2. The black box represents the mouse PST cDNA including the translation start site ATG and the stop codon and the ORF (1095 bp) and the red box represents the SV40 polyadenylation signal. 10 µg of the genomic DNA was digested overnight using AccI [AccI digests the mouse PST cDNA at nucleotide 57 and 868 and generates a 811 bp fragment], separated onto 1% agarose gel, transferred to the HyBondN+ membrane. The membrane was finally hybridized with [$^{32}$P]-labeled DNA probe generated by using the full length mouse PST (**B**) ORF as template. Bands were visualized on phosphoimager after exposure on pre-flashed Fuji imaging plate.

Among the four founder mice produced, only the offspring mice from the line 246 and 281 were fully analyzed. One of these lines displays only a low copy number of transgene (281). In contrast, the second line (246) carries several copies of transgene per haploid genome (Fig. 28B). Less than 5% of the mice from this line develop severe behavioral abnormalities, characterized by tremor and paralysis of the hind limbs. Mice with these phenotypes were not able to live more that eight months.

## 9.2 PST mRNA expression and PSA level in PLP-PST mouse brains

PST mRNA overexpression was investigated by Northern blot analysis of total RNA isolated from mouse brains. Total RNA was purified from 10 weeks old PLP-PST transgenic mice and wild type littermates. RNA (10 µg) was separated on formaldehyde agarose gel, transferred onto HybondN$^+$ membrane and hybridized with [$^{32}$P]-labeled PST cDNA probe. Fig. 29A demonstrates that transgenic mRNA was overexpressed in the brains of transgenic mice and that the expressed amount was related to the transgene copy number inserted to the chromosome (258<273<281<246).

To determine whether the increase in transgenic mRNA induces the increase in PSA concentration, Western blot analysis of 24 weeks old PLP-PST transgenic and wild type littermates were performed. As expected, a significant increase of PSA concentration was observed in transgenic mice brain and myelin (Fig. 29B) when the membrane was probed by the rabbit anti-PSA antibody.

Cell adhesion molecules expressed by both axons and glial cells are known to play a crucial role in the establishment of axon-glial contact and subsequent signaling to oligodendrocyte, driving the process of myelination (Doyle and Colman, 1993; Notterpek and Rome, 1994). Moreover, oligodendrocyte cells adhesion molecule is the NCAM-120 (Bhat and Silberberg, 1988) and is post-translationally modified by the addition of PSA. Because in the normal case the PSA concentration on the NCAM is barely detectable at the adult age, it was of great importance to investigate the level of the NCAM-120 in PLP-PST

mice, since these mice expresses a higher amount of the PSA at the adult age. During myelination, NCAM expression in the myelin fraction from PLP-PST mice was unchanged (Fig. 29C). At the adult age, no change in the concentration of the NCAM-120 was also observed (Fig. 29D: neuraminidase treated myelin samples).
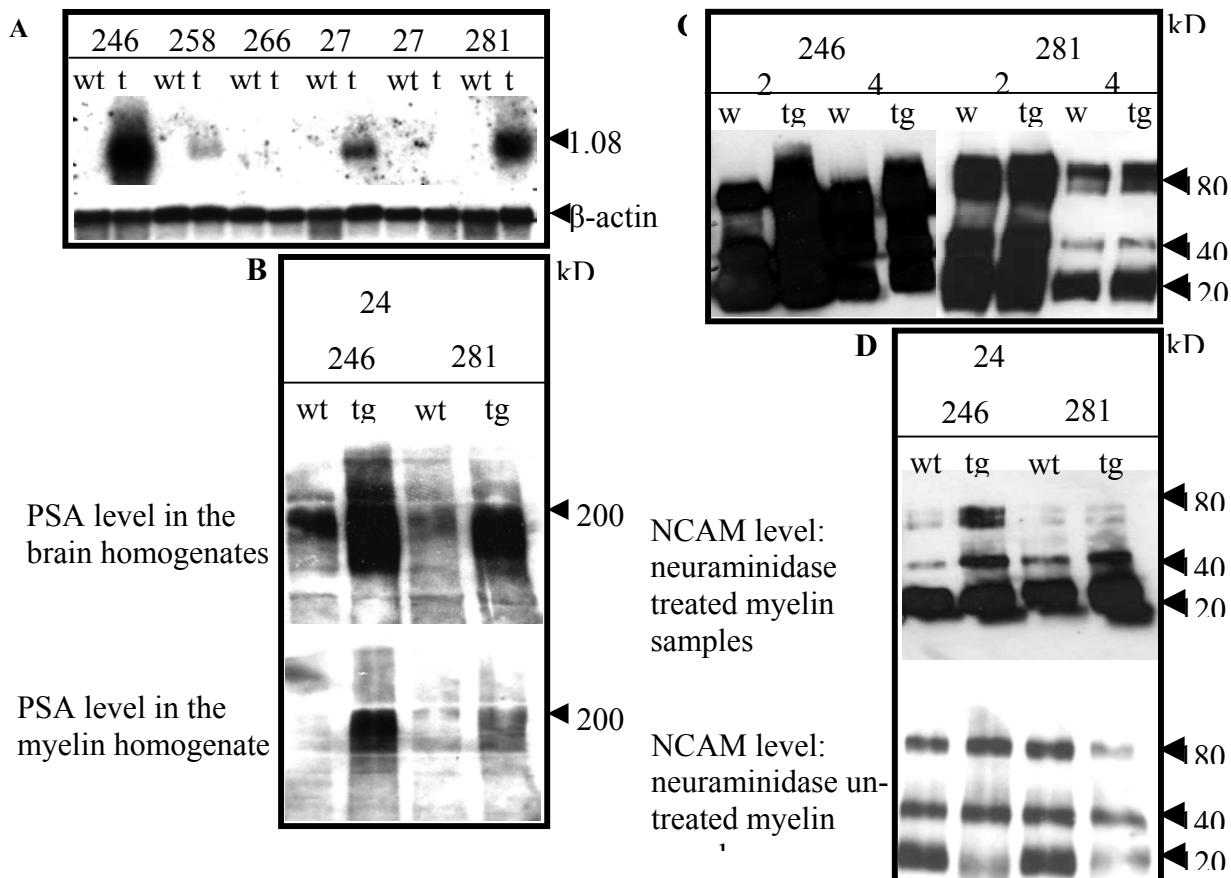


**Fig. 29 Assessment of the level of PST, PSA and NCAM in PLP-PST mice**. The transgene expression in 10 weeks old mouse brains was assessed by Northern blot analysis of total RNA. Total RNA (20 µg) was separated onto 1 % agarose gel, transferred onto HybondN+ membrane. (**A**) PST mRNA expression was detected on the blot by hybridization using the [$^{32}$P]-labeled mouse PST cDNA probe. Quantity and integrity of mRNA was verified by the ethidium bromide staining of the agarose gel and β-actin hybridization. Overexpression was also assessed at the PSA level by Western blot analysis of proteins from myelin and brain homogenates. SDS-extracted myelin and brain proteins were separated on 7.5% polyacrylamide gel and transferred onto nitrocellulose membrane using the semi-dry technique. PSA expression was then detected using mouse anti-PSA antibody and anti-mouse Ig couple to HRP (**B**). To investigate the expression of NCAM, 50µg of myelin was diluted in the buffer and treated for 4 hours using neuraminidase enzyme at 37°C. Proteins were then extracted from the neuraminidase treated myelin samples and investigated for NCAM expression as previously described using anti-NCAM antibody and the appropriate HRP-labeled second antibody. (**C**) NCAM expression in neuraminidase treated myelin samples from PLP-PST mice at 2 and 4 weeks of age. (**D**) NCAM expression in neuraminidase treated and un-treated myelin samples from PLP-PST mice at 24 weeks of age. Note that the low signal of the NCAM-120 is not because of the downregulation of the NCAM-120 expression, but because of the low accessibility of the NCAM antibody to the NCAM-120 molecule, due to the abundance of the PSA molecule at the surface of this NCAM isoform.

To determine whether the PSA overexpression is targeted to the NCAM-120, Western blot analysis of the NCAM expression was performed on neuraminidase untreated myelin samples from 24 weeks old PLP-PST mice. As expected, only the NCAM-120 shows a reduced signal on the blot (Fig. 29D: neuraminidase untreated myelin samples). This reduction of the NCAM-120 signals is not due to the downregulation of its expression, but to the low accessibility of the antibody to the NCAM-120 molecule, due to the abundance of the PSA molecule at the surface of this NCAM isoform.

## 9.3 PST mRNA overexpression is restricted to the white matter regions of brain

Myelin formation starts around birth in the brain stem and the ventral and dorsal funiculi of the cervical spinal cord (Rozeik and Von Keyserlingk, 1987; Schwab and Schnell, 1989). To determine the localization of PST mRNA and its expression pattern in the transgenic mouse brains, in situ hybridization on paraffin sections of 8 weeks old PLP-PST transgenic mice and wild type controls was performed. When the brain slices were hybridized with DIG-labeled PST cRNA, a significant staining was observed in the white matter region of the transgenic mice brain compared to the wild type controls (Fig. 30), suggesting that overexpression of PST mRNA could be restricted to the oligodendrocyte present in the white matter.

In situ hybridization also demonstrated that PST mRNA was not expressed at the same level in each transgenic line. Hence, the line 246 (Fig. 30C & D) was expressing a higher amount than the line 281 (fig. 30E & F) in the white matter of the forebrain and cerebellum.
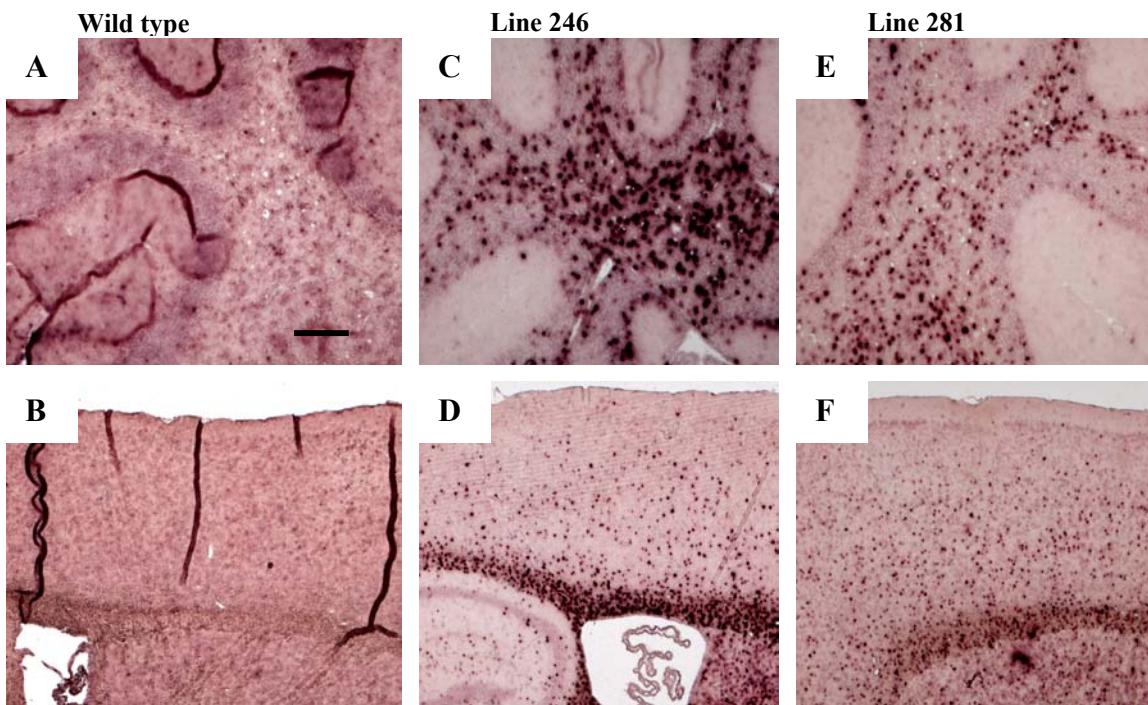
**Fig. 30 White matter specific expression of PST mRNA in mouse brain**. In situ hybridization was performed as described by Baader et al. (1998). Paraffin sections of the brains wild type and transgenic mice (8 weeks old) were hybridized with a DIG-labeled riboprobe for PST transcripts. PST expression was finally documented by microscopic analysis (Zeiss, Germany). Hybridization signals revealed strong transgene expression in the white matter of the forebrain [line 246 (**D**) and 281 (**F**), wild type (**B**)] and cerebellum [line 246 (**C**) and 281(**D**)] of transgenic mice compared to the expression in wild-type mice (A, B). Scale bar 50 µm.

## 9.4 Effects of PST overexpression on the level of myelin and oligodendrocyte specific proteins

To investigate the effects of PST overexpression on the concentration of the myelin/oligodendrocyte proteins, Lipid, Western and Northern blot analysis were performed.

CNPase is a protein which is expressed at all stages during the development of oligodendrocytes and represents 4% of the total myelin proteins (Baumann and Pham-Dinh, 2001). To investigate the level of CNPase in PST transgenic mouse brains, myelin of transgenic mice and wild type controls was purified and analyzed by Western blot as the function of age. The level of CNPase was unchanged during myelination and at the adult age in PLP-PST transgenic mice (Fig. 31A).

Fyn is one of nine known members of the Src family of protein tyrosine kinases, which are highly similar in amino acid sequence (Brown and Cooper,

1996). Fyn is expressed in oligodendrocytes and is known to modulate myelination and oligodendrocyte differentiation (Krämer et al., 1999; Osterhout et al., 1999). Therefore, we sought to determine whether the increase of PSA concentration disturbs Fyn expression. Fyn level was unchanged in the myelin of PLP-PST mice, as indicated by Western blot analysis (Fig. 31A). In contrast to Fyn and CNPase, MBP protein level was reduced in the brain homogenate from the line 246 of PLP-PST mice at 2 weeks of age (Fig. 31B). The line 281 shows no reduction of the MBP protein level at all age. To determine whether the reduction of MBP protein occurs at the transcriptional level, northern blot analysis of RNA from brain of 2 and 4 weeks old mice was performed. As expected, MBP mRNA level was also reduced in PLP-PST mice at the same age (Fig. 32A). Quantitatively, reduction of MBP mRNA level was 15 and 30% ($p < 0.05$), respectively in the lines 281 and 246 at 2 weeks of age. At 4 weeks of age, 7% reduction (Fig. 32B) of MBP mRNA was observed in the line 246 and no reduction in the line 281. It seems that 7 % MBP mRNA reduction in the line 246 was not able to drive a visible reduction of MBP protein at 4 weeks of age (Fig. 31B). The same effect was already observed in the line 281 at 2 weeks of age, where MBP mRNA was reduced (Fig. 32B), but not the protein (Fig. 31B).

Previous studies have shown that CST mRNA and activity appears at the embryonic day 11.5 during the mouse brain development (Hirahara et al., 2000, 2004). During oligodendrocyte differentiation, sulfatide first appears at the immature stage of the oligodendrocyte lineage together with GalC (Bansal et al., 1992). Northern blot analysis of the CST gene expression in the PLP-PST mouse brain shows no change in the CST mRNA level compared to wild type control at 2 and 4 weeks of age (Fig. 32A). Consistent with this data, sulfatide and other myelin lipid levels were unchanged in the myelin fraction of PLP-PST mice at 24 weeks of age as shown by TLC analysis (Fig. 31C).
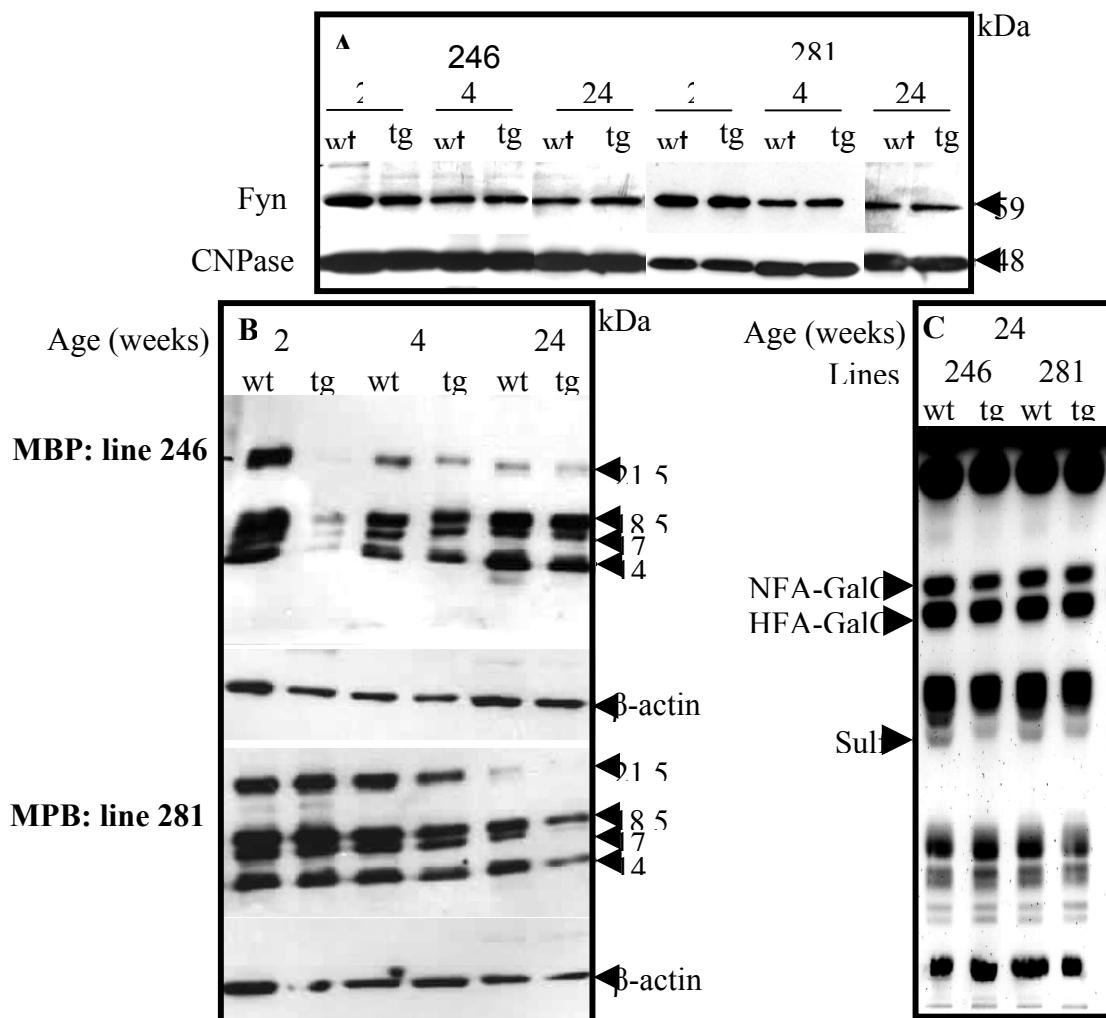
**Fig. 31 Protein and lipid levels in myelin and brains of PLP-PST transgenic mice.** Wild type littermates were used as control mice in all experiments. Myelin and brain protein fractions were SDS-extracted, separated onto 12.5% polyacrylamide gel and blotted onto nitrocellulose membrane using a semidry blotting technique. Bound proteins were detected using anti-MBP, anti-fyn and anti-CNPase antibodies and the appropriate HRP-labeled Ig. In some cases membranes were re-probed with antibody against beta-actin as control of loading. (**A**) Western blot analysis of Fyn and CNPase levels in the myelin samples at 2, 4 and 24 weeks of age. (**B**) Western blot analysis of MBP level in the protein homogenate from transgenic mice and wild-type controls at 2, 4 and 24 weeks of age. For lipid analysis, myelin was purified from transgenic mice and wild type controls at 24 weeks of age according to Norton and Poduslo (1973). Lipids were extracted from myelin using C/M (2:1) and the volume of lipids solution corresponding to 100 µg myelin dry weight was spotted and separated using C/M/W (60:27:4). Lipid Bands were visualized using $CuSO_4/H_3PO_4$ at 170 °C for 2 minutes. (**C**) HPTLC profile of transgenic and wild type littermates.
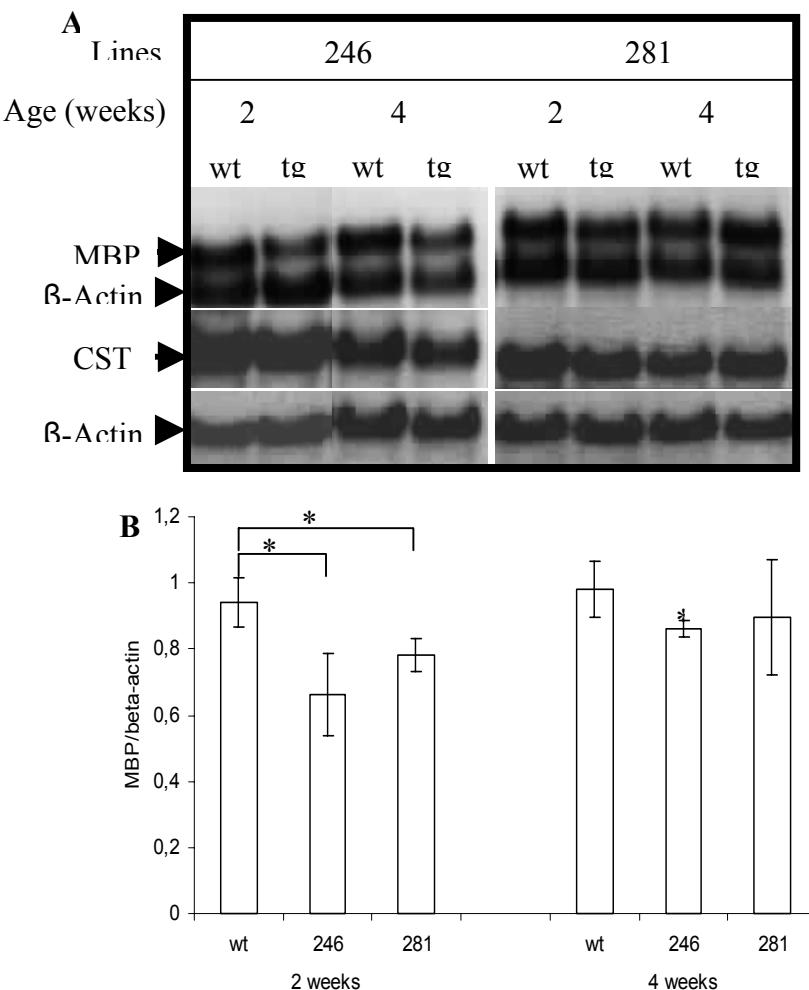
**Fig.32 Myelin specific mRNA expression in PLP-PST transgenic mice**. The expression of CST and MBP mRNA in the brain of transgenic mice (n=3 per line) and wild type controls (n=3) was assessed by Northern blot analysis of total RNA. Total RNA from 2 and 4 weeks old mouse brains was purified by the Trizol reagents and 20 µg were separated in 1% RNAse free agarose gel and transferred onto HybondN[+] membrane. Membrane was finally hybridized with [^{32}P]-labeled 1.3 kb coding regions of MBP or 1.2 kb coding region of the CST cDNA (**A**). Detection was performed by exposing the membrane to pre-flashed Fuji Bioimager screen and subsequently to X-ray film. MBP expression was quantified and the results are given as an average ±SEM (**B**). Asterisks indicate significant differences between transgenic and wild type mice (p<0.05: t-test).

## 9.5 Effects of the elevation of the PSA concentration on the development of oligodendrocytes during myelination

During development, oligodendrocyte precursor cells, generated in the ventricular zone, proliferate and migrate over considerable distances to their destinations (Lee et al. 2000), where they differentiate. Differentiation processes are controlled by the expression of different proteins or lipids at different stages. Differentiated oligodendrocytes are characterized by the change of their morphology and expression of terminal markers such as MBP

and PLP. In contrast, Platelet derived growth factor alpha-receptor (PDGFRα-R) is one of the best-studied and earliest markers for oligodendrocyte progenitors in the CNS. Previous studies have demonstrated that PDGFRα-R positive cells are oligodendrocytes progenitors. Furthermore, purified progenitors from the late embryonic rat spinal cord and brain by immunoselection, differentiate into oligodendrocyte under appropriate culture conditions (Hall et al., 1996; Tekki-Kessaris et al., 2000).
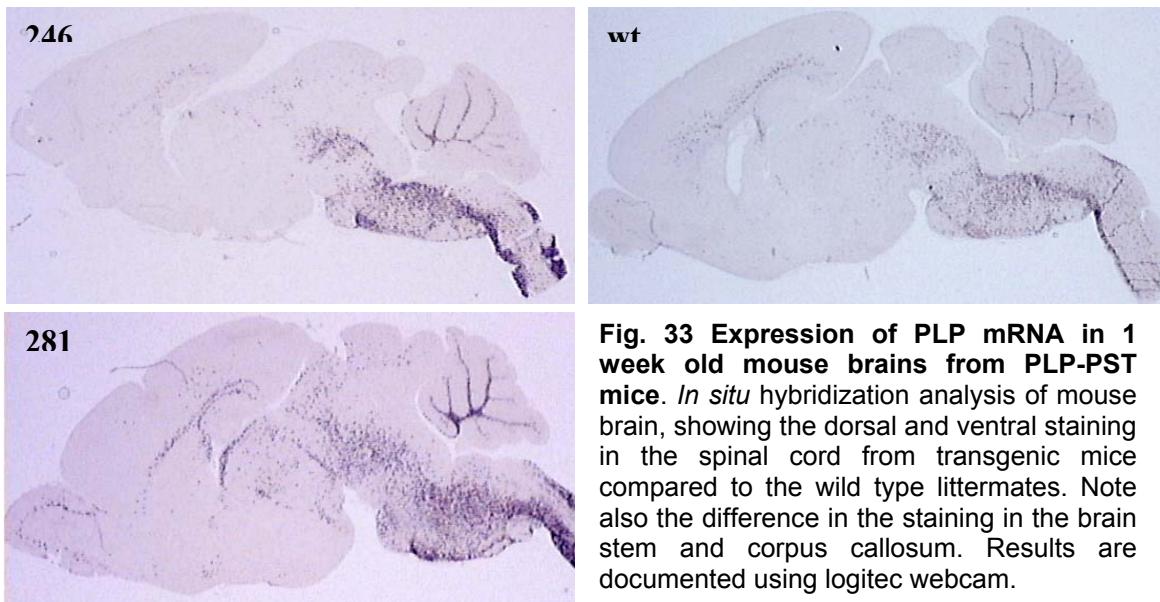


**Fig. 33 Expression of PLP mRNA in 1 week old mouse brains from PLP-PST mice**. *In situ* hybridization analysis of mouse brain, showing the dorsal and ventral staining in the spinal cord from transgenic mice compared to the wild type littermates. Note also the difference in the staining in the brain stem and corpus callosum. Results are documented using logitec webcam.

Because MBP concentration was reduced in the brain of PLP-PST transgenic mice, we sought to determine whether this reduction is caused by the reduction of oligodendrocyte numbers or inhibition of oligodendrocyte differentiation. To investigate these issues, oligodendrocyte numbers were analyzed in selected areas of CNS in PLP-PST transgenic mice and wild type controls during myelination. To facilitate identification and accurate counting of progenitors and differentiated oligodendrocytes, we used both PDGFRα-R and PLP DIG-labeled cRNA.

Hybridization of the brain slices with DIG-labeled PLP cRNA shows that differentiated oligodendrocyte numbers were decreased in the corpus callosum of PLP-PST transgenic mice compared to the wild type controls at one week of age (Fig. 34). Quantitatively, reductions were 36 and 54% (p<0.01) (Fig. 34J), respectively, in the lines 281 and 246. At two (Fig. 35) and four (Fig 36) weeks of age, and in the corpus callosum of PLP-PST mice,

decreases of oligodendrocyte numbers were also found. Decreases were around 25% ($p < 0.05$) in the line 246 (Fig. 37B). In the line 281 and in the corpus callosum, a significant decrease (27%) of oligodendrocyte numbers was observed at two weeks of age (Fig. 37B).

In contrast to the corpus callosum of one week old transgenic mice, a significant increase of differentiated oligodendrocyte number was observed in the brainstem and spinal cord (Fig. 34). Increases were 69 and 92% ($p < 0.01$) in the spinal cord (Fig. 34J) and 41 and 84% ($p < 0.01$) in the brainstem (Fig 37A), respectively, in the lines 246 and 281. In the two lines and at two and four weeks of age, significant increases [at 2 weeks 45% (246) and 36% (281), and at 4 weeks of age 29% (246) and 41% (281)] of oligodendrocyte numbers was observed in the brainstem (Fig. 37A).

At this stage of investigation, it was impossible to draw a conclusion. It was not possible to determine whether the regional increase other decrease of differentiated oligodendrocyte numbers, was due to the changes in the differentiation or proliferation mechanisms in these mice. Therefore, investigation of the number of cells expressing the PDGF alpha-receptor mRNA was important. The expression of the PDGFRα-R in the sagittal sections from transgenic mice and wild type controls was essayed at one and four weeks of age. In contrast to the increase or decrease of differentiated oligodendrocyte (PLP mRNA positive cells) numbers, no change in the number of oligodendrocyte progenitors was observed in the brain of PLP-PST mice compared to the wild-type controls (Fig. 38 and 39, for staining). The number of the PDGFRα-R positive cells counted in three regions (spinal cord, brainstem and corpus callosum) of the brain of transgenic mice was unchanged when compared to the one of the wild-type littermates (Fig. 38J, K & L and 39G & H, for quantity). This result together with the one concerning the expression of the PLP mRNA, allow us to conclude that elevation of the PSA concentration induces the increase of oligodendrocyte differentiation in the spinal cord and brainstem and its decrease in the corpus callosum.
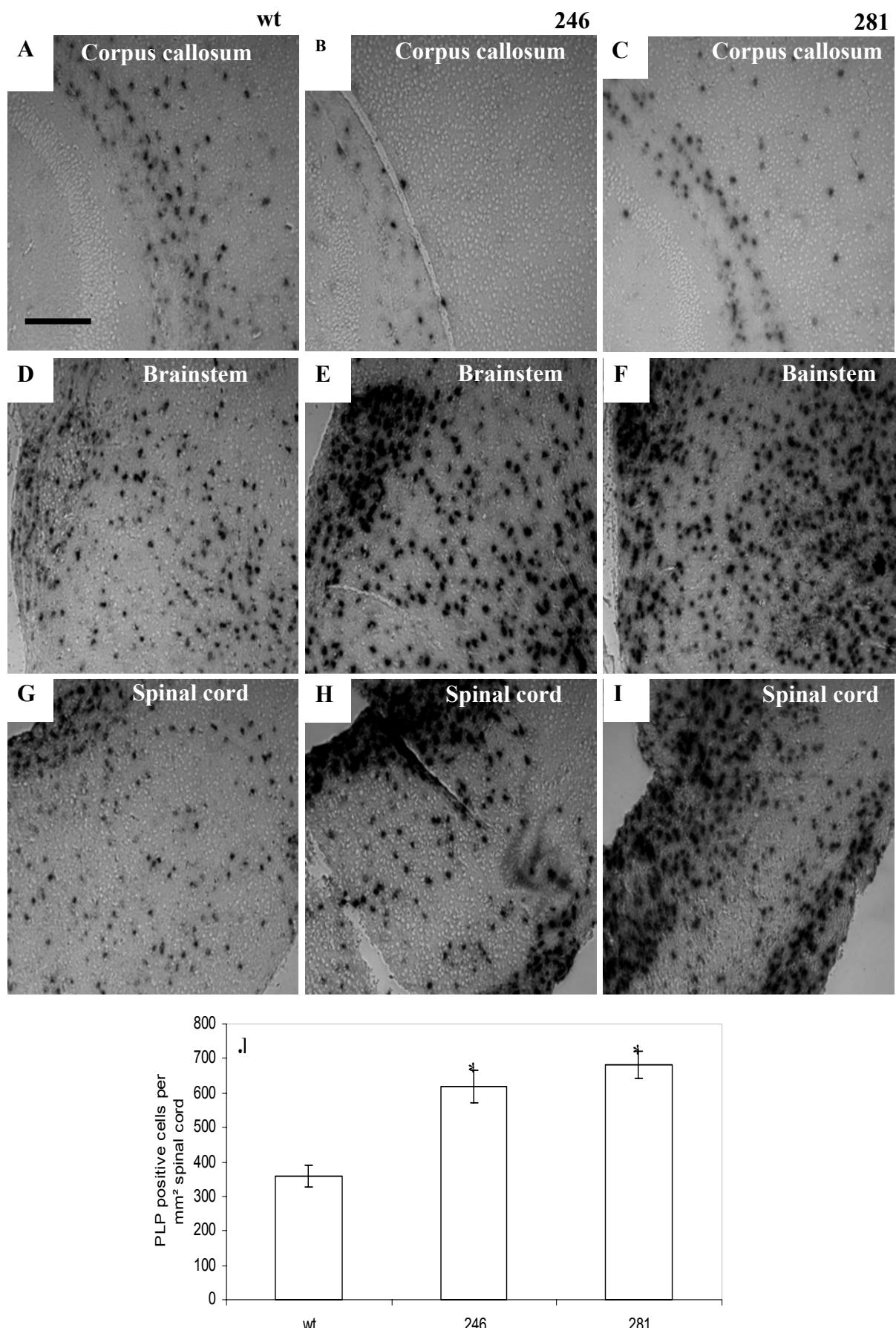
**Fig. 34 PLP mRNA expression in the brain of PLP-PST mice**. Distribution of the PLP mRNA-positive cells in the corpus callosum (**A-C**), brainstem (**D-F**), and spinal cord (**G-I**). Tissue sections (8 µm) from transgenic mice and wild type controls of 1 week of age were hybridized with DIG-labeled

PLP cRNA probe and visualized after 1 hour staining with BCIP/NBT. Quantification of PLP-mRNA positive cells in the spinal cord (**J**) of one weeks old mouse was performed by counting. Three slices were counted per microscopic slide and three mice were analyzed per group (n=3). Counted cells were normalized to the mm² of the spinal cord and the result is given as the mean ± SEM of 9 counts. Asterisks indicate significant differences between transgenic mice and wild type controls. ($p < 0.01$; Anova). Scale bar 100 µm.



**Corpus callosum**          **Bainstem**
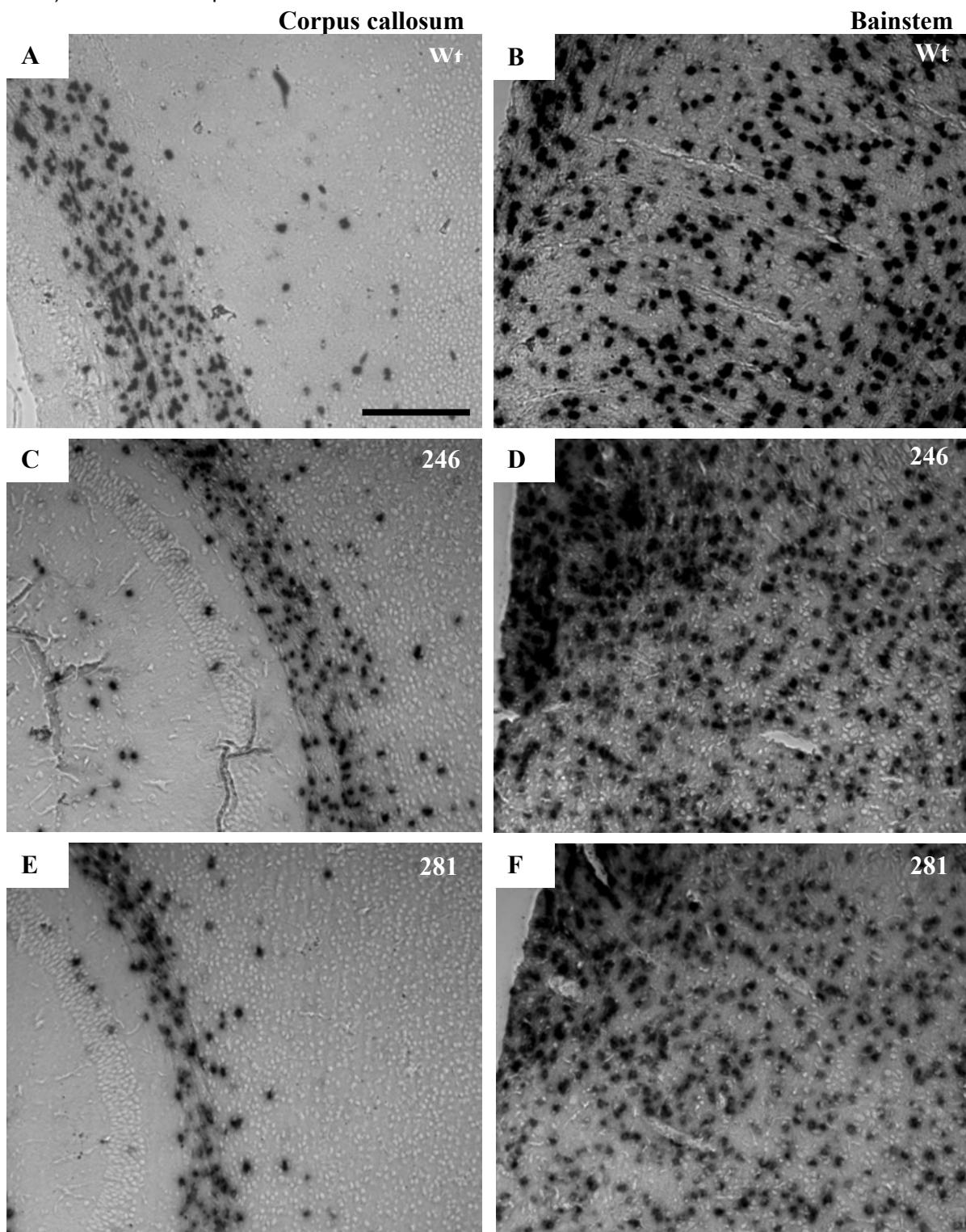
**Fig. 35 PLP mRNA-positive cells in the corpus callosum and brainstem of two weeks old PLP-PST mice**. Distribution of the PLP mRNA-positive cells in the corpus callosum (**A**, **C** & **E**) and brain stem (**B**, **D** & **F**). Tissue sections (8 µm) from transgenic and wild type littermate mice of 2 weeks of age were hybridized with DIG-labeled PLP cRNA probe. Slices were stained for 1 hour using BCIP

and NBT. Positive cells were documented using microscopic analysis on an Axiovert M instrument (Zeiss, Germany). Scale bar 100 µm

**Corpus callosum**                                                    **Brainstem**
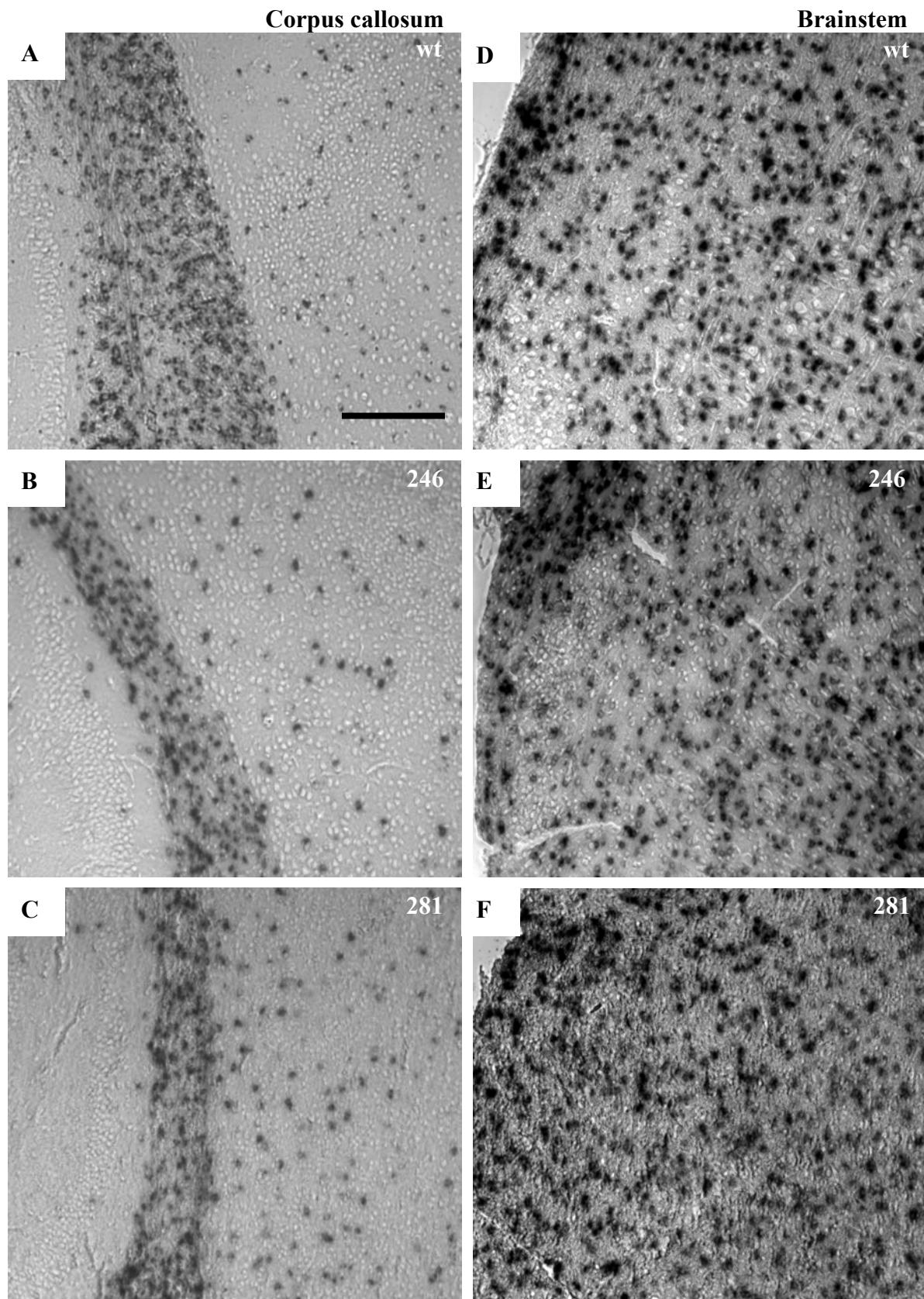


**Fig. 36 Oligodendrocyte differentiation in the corpus callosum and brainstem of weeks old PLP-PST mice**. Distribution of the PLP mRNA-positive cells in the corpus callosum (**A**-**C**) and brain stem (**D**-**E**). Tissue sections (8 µm) from transgenic mice and wild type controls of 4 week of age were

hybridized with DIG-labeled PLP cRNA probe. Positive cells were visualized using BCIP/NBT and documented by electron microscopy (Zeiss, Germany). Scale bar 100 µm
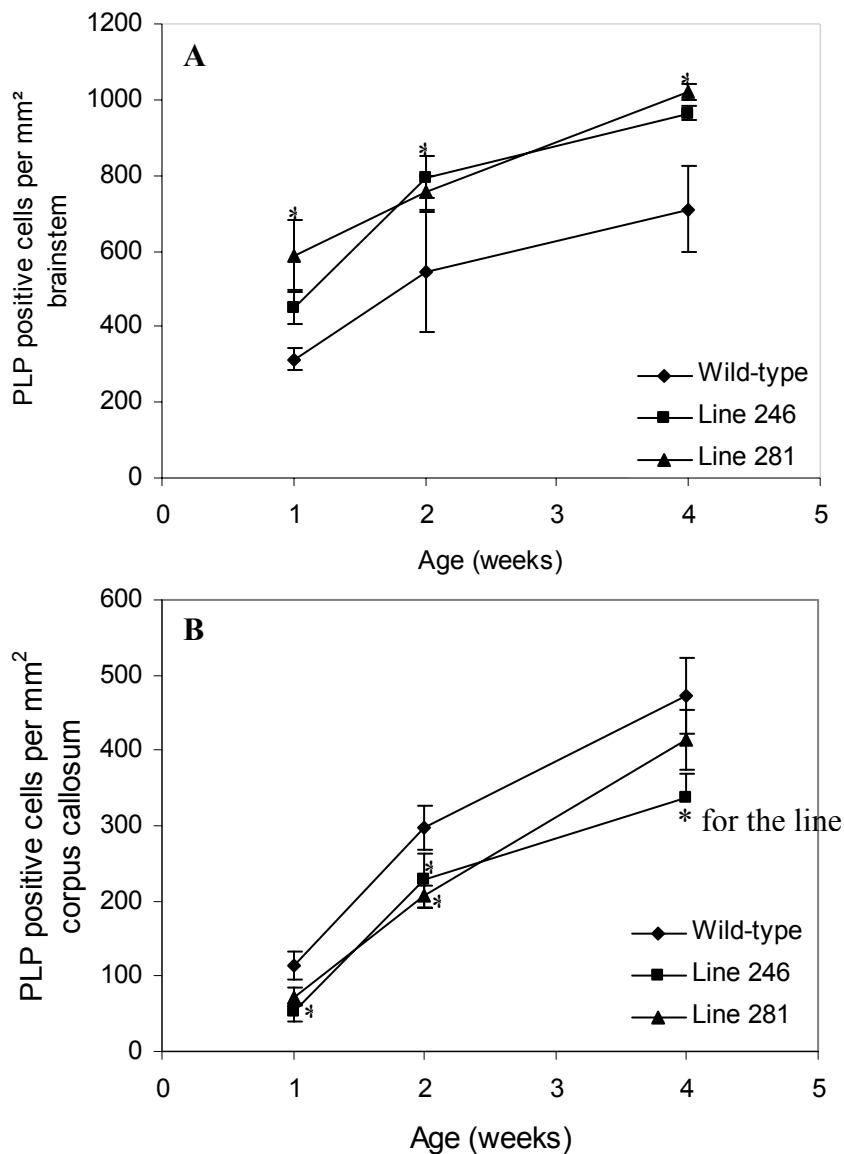


**Fig. 37 Oligodendrocyte levels in the corpus callosum and brainstem PLP-PST transgenic mice**. 8µm brain slices of PLP-PST and wild-type mice were analyzed as a function of time by in situ hybridization. The PLP mRNA expression was assayed as a marker of oligodendrocyte maturation. Tissue sections were hybridized with DIG-labeled PLP cRNA probe and visualized by BCIP/NBT (1 hour) staining. Positive cells were analyzed by electron microscopy and the number of PLP mRNA-positive cells counted. Three brain slices were counted per mouse and per microscopic slide and three mice were analyzed per group (n=3). Counted cells were normalized to the mm² of the counted region and the result is given as the mean ± SEM of 9 counts. (**A**) PLP-mRNA positive cells in the brainstem and (**B**) PLP mRNA-positive cells in the corpus callosum. Asterisks indicate significant differences between transgenic mice and wild type controls. (p<0.01; Anova).
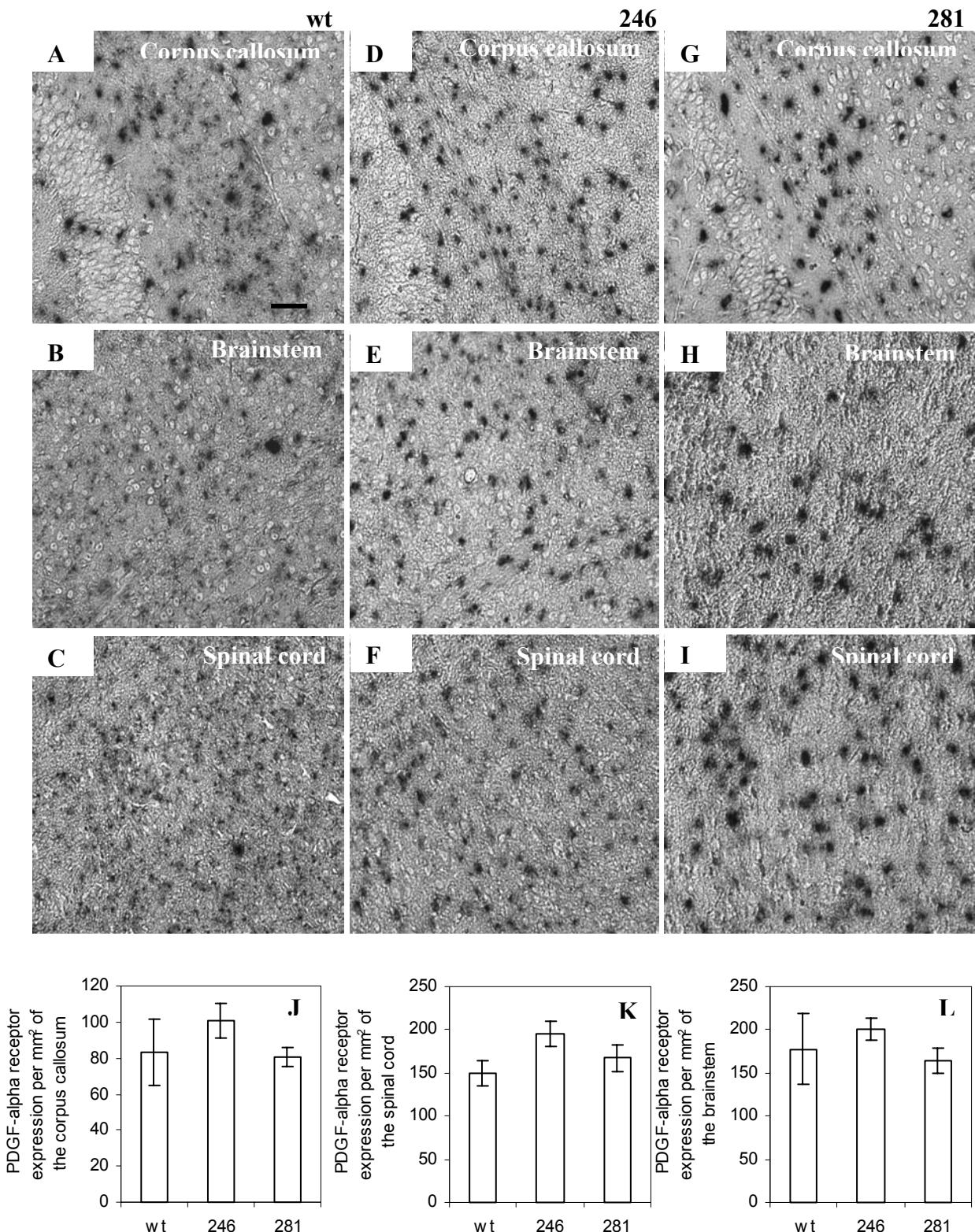
**Fig.38 Expression of PDGF alpha-receptor in PLP-PST transgenic mouse brains**. The expression of the PDGF alpha-receptor in transgenic mice brain was investigated at 2 weeks of age by in situ hybridization using DIG-labeled PDGF α-receptor cRNA. No change is observed in the expression of PDGF α-receptor level in the corpus callosum of (**C & E**) and brainstem (**D & F**) of transgenic mice brain compared to the wild type littermates (**A**) corpus callosum and brainstem (**B**). Quantification [(**J**) corpus callosum, (**K**) spinal cord, (**L**) brainstem] was performed by counting cells in each region. Three brain slices were counted per mouse and per microscopic slide and three mice were analyzed per group (n=3). Counted cells were normalized to the mm² of the counted region and the result is given as the mean ± SEM of 9 counts. Differences are not significant (p>0.05, Anova). Scale bar 50 µm

**Corpus callosum**                                          **Brainstem**
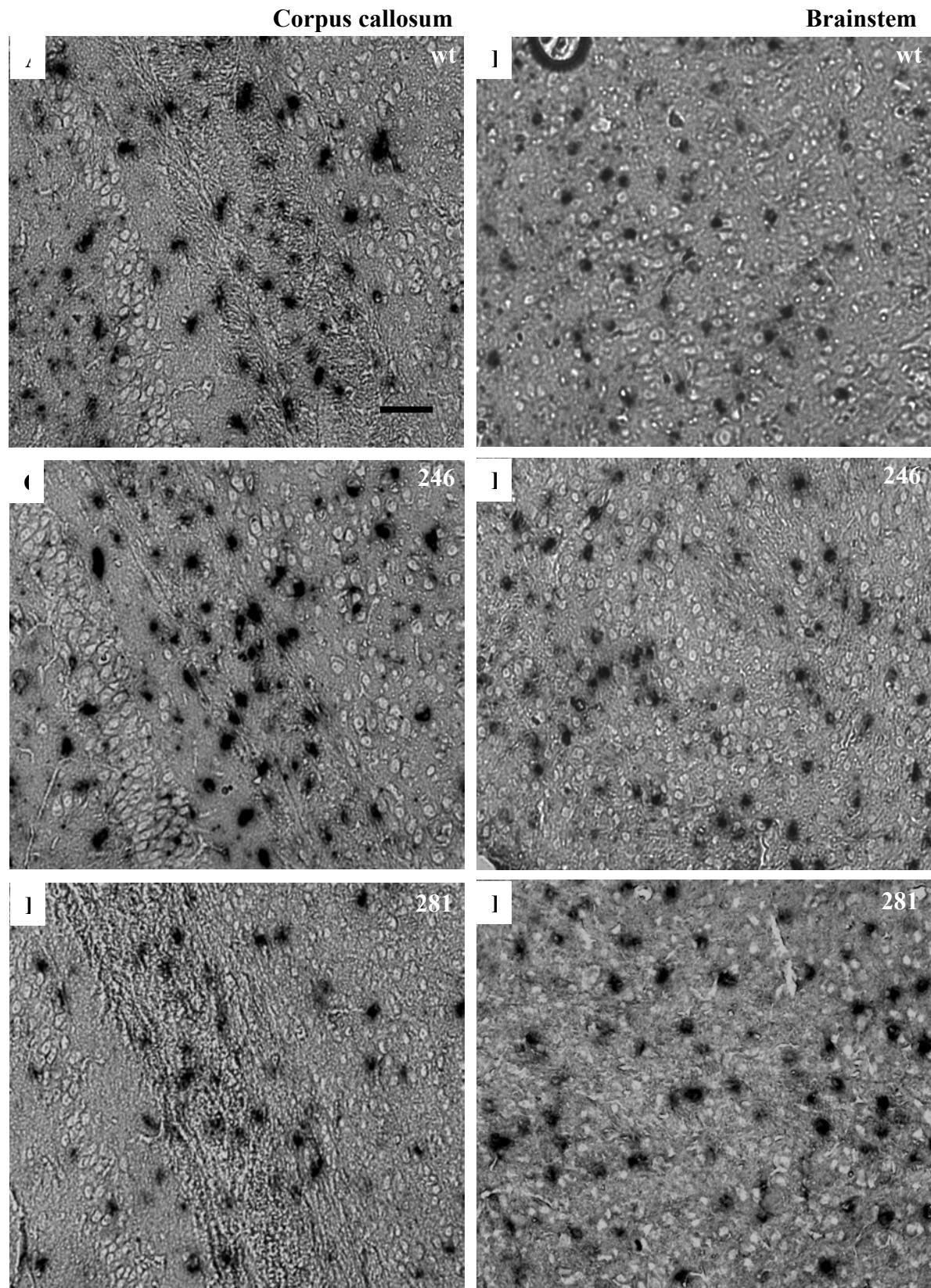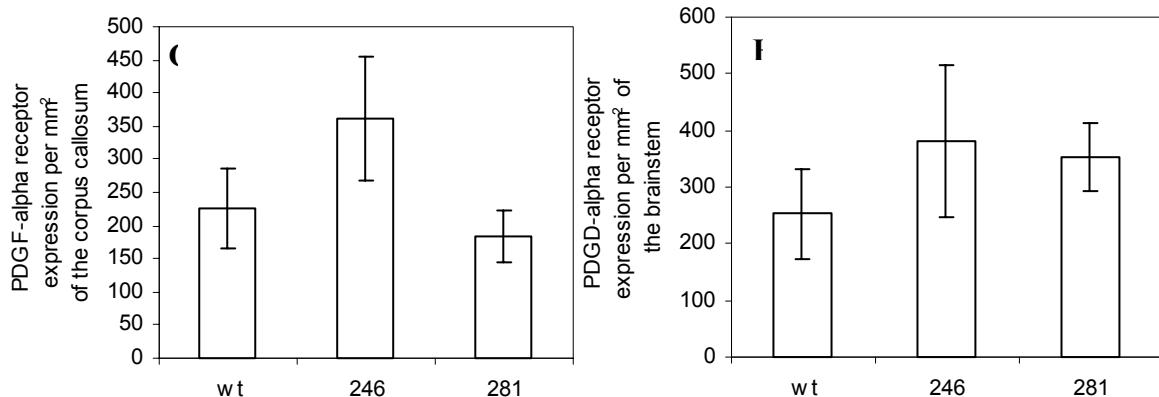
**Fig.39 Expression of PDGFαR in PLP-PST transgenic mice a 4 weeks of age**. The expression of the PDGF α-receptor in transgenic mouse brains was investigated at 4 weeks of age by in situ hybridization using DIG-labeled PDGF α-receptor cRNA. No change is observed in the expression of PDGF α-receptor in the corpus callosum of (**C** & **E**) and brainstem (**D** & **F**) of transgenic mice brain compared to the wild type littermates (**A**) corpus callosum and brainstem (**B**). Quantification [(**G**) corpus callosum, (**H**) brainstem] was performed by counting the cells in each region and three brain slices were counted per mouse and per microscopic slide and three mice were analyzed per group (n=3). Counted cells were normalized to the mm² of the counted region and the result is given as the mean ± SEM of 9 counts. Differences are not significant (P>0.05, Anova). Scale bar 50 μm

## 9.6 Myelin structure in PLP-PST transgenic mice

To determine whether myelin structure is compromised in PLP-PST animals, we analyzed the transgenic mice myelin at 4, 23 and 28 weeks old in two separate areas of the nervous system. PNS axons are correctly ensheathed by compacted peripheral myelin in all PLP-PST transgenic mice lines, with no sign of demyelination or degenerating Schwann cells (Fig. 40A).

In the CNS, to ensure that similar regions were analyzed in each animal, we focused our analysis on discrete location. At four weeks of age, electron microscopy of the optic nerve from transgenic mice show a normal myelination profile with no sign of hypo or demyelination (Fig. 40C) when compared to the optic nerve from wild type mice of 13 weeks old (Fig. 40B). In the same area of the optic nerve, and at the adult age, substantial loss of myelin was observed in transgenic mice (Fig. 40E2 & D3). Furthermore, the myelin sheath appears thinly in the myelinated regions of the optic nerve (Fig. 40D3). Beside the demyelination process observed, redundant myelinated axons were observed, but rarely (Fig. 40D & D4). Another abnormal myelin structure observed in PLP-PST transgenic mice was vacuolated fibers, which arise from the axonal

degeneration due to the reduction of the contact between the myelin sheath and axons (Fig. 40D and E1).
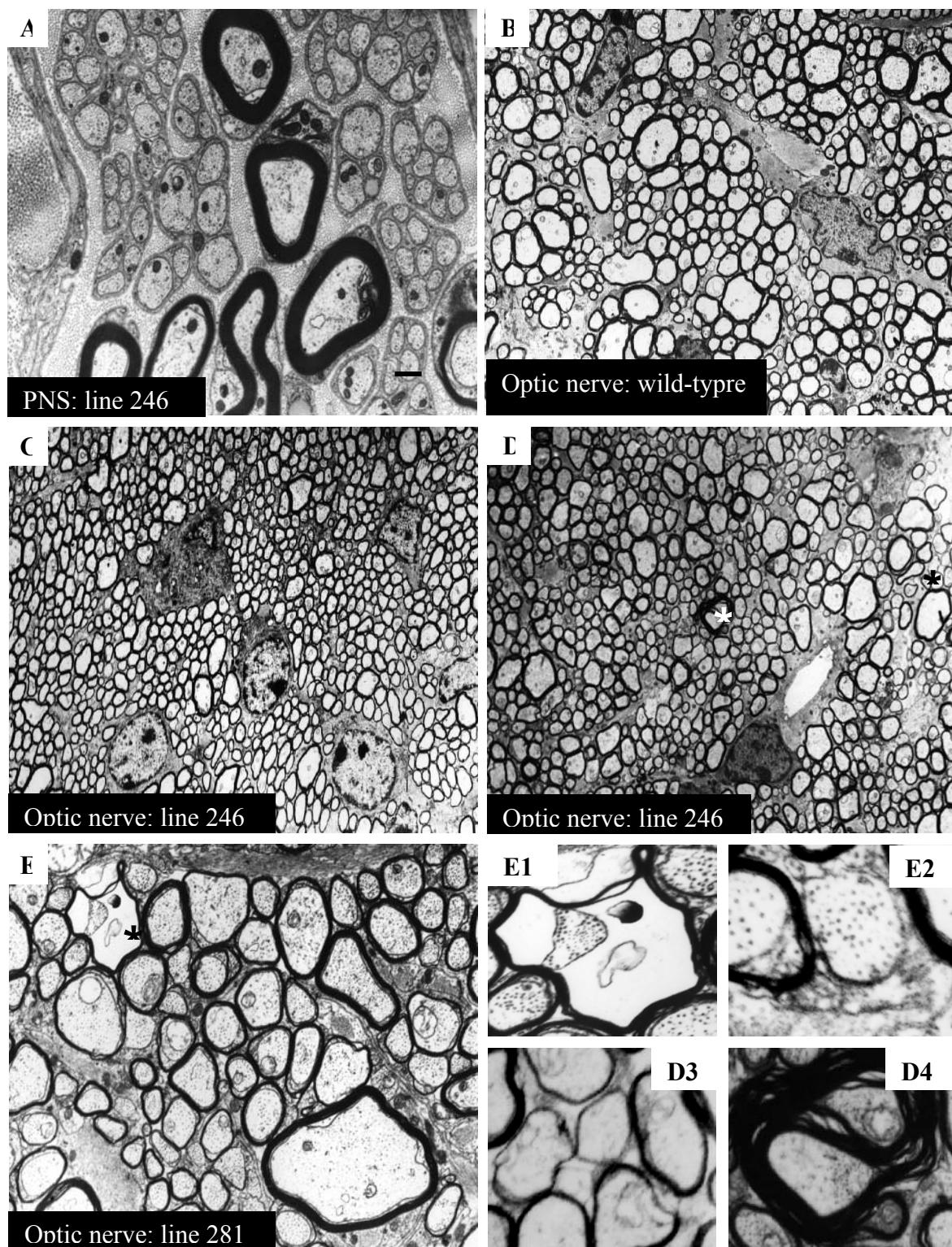


**Fig. 40 Ultrastructure of myelin in the nervous system of PLP-PST transgenic mice**. Semithin cross-sections of the PNS (**A**) from the line 246 (28 weeks) and optic nerve of adult (13 weeks) wild-type (**B**), 4 weeks old (**C**) and adult (28 weeks) from the lines 246 mice (**D**), and 281 (23 weeks) (**E**), was analyzed by electron microscopy. Normal amounts of myelin were present in young animals. Demyelination is detectable in adult mice from the lines 246 and 281. Note the axonal degeneration

(**E1,** asterisk point to area enlarged in E), demyelination (**E2** and **D3,** asterisk points to area enlarged in D and E), and redundant myelination (**D4,** asterisk point to area enlarged in D) observed in PLP-PST transgenic mice. D and F with indices indicate the picture from which the magnification has been done. **A** and **B** (X16,800); **B**, **C** and **D** (X5,600). Scale bar 1 µm

# 10  **DISCUSSION**

Oligodendrocytes development and myelin maintenance are processes controlled by the expression of different cellular markers. At the progenitor stage, oligodendrocytes expresses different molecules such as PSA which help them in their migration to their destinations. Expression of the highly sialylated form of NCAM is developmentally down-regulated, and, in the optic nerve of the mouse, PSA-NCAM progressively disappears from retinal ganglion cell axons during the first two postnatal weeks, with a time course that parallels myelination (Bartsch et al., 1990). In oligodendrocyte, PST (ST8Sia IV) is responsible for the polysialylation of NCAM-120 molecule (Bhat and Silberberg, 1988). Moreover, NCAM-120 carry out functions attributed to oligodendrocyte adhesion molecules and co-localizes together with signal transduction molecules such as F3 and Fyn in rafts (Schachner and Martini, 1995; Krämer et al., 1999). Because PSA level is developmentally down-regulated, transgenic overexpressing PST in oligodendrocyte was generated in order to study the effect of increased concentrations of PSA on oligodendrocyte development and myelin stability.

In the present study, we analyzed oligodendrocytes development, myelination and myelin stability in the presence of an elevated PSA concentration. We demonstrated by in situ hybridization that increased levels of PSA affect the development of oligodendrocyte *in vivo*. A substantial increase of oligodendrocyte numbers in the spinal cord and brainstem of PLP-PST mice were observed during myelination. This elevation of the level of oligodendrocytes could suggest a relation to elevated amount of PSA with the proliferation, since it has been demonstrated *in vitro* and *in vivo* that neuronal cells undergoing division are those which exhibit highest amounts of PSA (Hu et al, 1996; Wang et al., 1996: Hildebrandt al., 1998). Furthermore, another neuroblastoma line, which predominantly expresses PSA during division, fails to divide if pretreated with endoneuraminidase (Hildebrandt al., 1998). In contrast to data supporting a direct role of PSA on the neuroblastoma cells, no

direct evidence supports the relation of the PSA expression and the proliferation of oligodendrocytes. In the case of a possible relation between the proliferation of oligodendrocytes of the spinal cord and brainstem with an increased amount of PSA, it is unclear why the increased amount of PSA causes reduction of differentiated oligodendrocyte numbers in the corpus callosum of PLP-PST mice. Because myelination and oligodendrocytes development are closely related, and because the initiation of myelination occurs in the spinal cord at a much earlier time than in the corpus callosum (Sperber et al., 2001), this difference could be attributed to the regional variability of oligodendrocyte development. Interestingly, mice deficient in Fyn also exhibit a different pattern of regional proliferation: Fyn null mice have reduced oligodendrocyte numbers in the corpus callosum and an unchanged number in the spinal cord (Sperber et al., 2001), the same result obtained in our study.

The other possible explanation for the regional differences in the development of oligodendrocytes is that, oligodendrocytes of the spinal cord and brainstem could require PSA for their development, whereas those of the corpus callosum do not. Consistent with this point of view, it had been proposed that there are distinct subpopulations of oligodendroglial (Del Rio Hortega (1928). Furthermore, forebrain and spinal cord or brainstem oligodendrocytes have distinct morphologies in neuron-free cultures (Bjartmar, 1998). Evidence has also been presented for two independent populations of oligodendrocyte precursors, one characterized by expression of PDGFα-receptors and the other by expression of mRNA for the myelin protein DM20 (Spasky et al., 1998, 2000; Fruttiger et al., 1999). In the case of separate lineages of oligodendrocytes, they may differ in the growth factors and signaling pathways that regulate their development and function.

The second hypothesis could be that the increased amount of PSA in the CNS inhibits the differentiation of oligodendrocytes in the corpus callosum but not in the spinal cord and brainstem. In this case, PSA could be a negative regulator of the differentiation of oligodendrocytes in the corpus callosum and a positive regulator in the spinal cord and brain stem. However, evidence that support

the positive role of PSA on the differentiation of oligodendrocytes has already been presented in vitro. Hence, removal of PSA from NCAM moderately reduced the migration of oligodendrocyte progenitors and induces their differentiation in GD3+, OP and GFAP+ astrocytes (Decker et al., 2000). Moreover, NCAM-120, the carrier of PSA in oligodendrocytes, co-localizes with the GPI-anchored proteins Fyn and F3 in the raft microdomain (Krämer et al., 1999). Consistent with this idea, overexpression of PSA at the adult age, in oligodendrocytes, could disturb the proper organization of the rafts micro domain and disturb the signal transduction processes implicated in the development of oligodendrocytes.

In addition to the regional change of the development of oligodendrocytes in PLP-PST mice, biochemical analysis shows a marked downregulation of MBP at the protein and mRNA levels during myelination and a rescue of MBP level at the adult age. MBP reduction in these mice was more severe in the line with high copy number of transgene insertion (line 246), indicating that MBP reduction correlates with the elevation of PSA concentration, since the line 281 (express low level of PSA) shows also a reduction of MBP mMRNA. It seems like 15% reduction of MBP mRNA in PLP-PST mice was not able to trigger a significant reduction of MBP protein (Fig. 31 and 32). Moreover, a severe MBP reduction was also observed in Fyn-/- mice, (Sperber et al., 2001).

Myelination in the nervous system involves sequential stages of interaction between the myelinating glial cell, the oligodendrocyte, and the neuronal process, the axon. Initial recognition and adhesion, results in wrapping of the glial process around the axon, followed by the laying down of the multilamellar sheath. In the peripheral nervous system of mice overexpressing PST, myelination was normal with no sign of degeneration at the adult age. The myelin thickness was also normal and the axons diameter was unchanged. Despite the elevation of PSA concentration in the CNS, the myelin sheath forms normally, with no sign of dys- or hypomyelination. This result is in contradiction with the one already published (Charles et al., 2000). At the adult age, a significant myelin deficit was observed in the optic nerve of PLP-PST mice. Demyelination in the optic nerve of mice overexpressing PST was

accompanied by axonal degeneration. A possible explanation of this could be the disturbance of the rafts microdomain, which contains molecules such as GPI-anchored proteins Fyn and NCAM-120. However, it is shown that Fyn kinase and F3 are tightly associated with NCAM-120 in rafts (Krämer et al., 1999) and at the adult age, the NCAM-120 does not contain PSA. Although the level of Fyn kinase was unchanged in the myelin fraction of PLP-PST mice, it could be possible that increased amount of PSA on the NCAM-120 at the adult age may disturb the proper organization of the rafts and the signal transduction processes related to the myelin maintenance. Fyn protein and more specific its kinase activity plays crucial role in the myelination and myelin maintenance (Sperber et al., 2001). Does the normal level of Fyn suggest no change of its kinase activity? This question has to be answered. However, Fyn null mice hypomyelinate and show axonal degeneration in the optic nerve at the adult age (Biffiger et al., 2000; Umemori et al., 1999). In addition to the demyelination and axonal degeneration observed in PLP-PST mice, redundant myelinated axons were also observed. This kind of myelin impairment could be explained by the compromised axo-glial recognition and the delay in the mechanism that is required to "inform" glial cells where to lay down myelin, and how much myelin sheath should be laid down. Consistent with this hypothesis, previous research have indicated that MAG modulates glial-axons contact in vivo (Li et al., 1998). Evidence suggests that MAG, NCAM-120 (carrier of PSA in oligodendrocyte), F3 and Fyn may acts as receptors couple to Fyn (Umemori et al., 1994; Krämer et al., 1999).

# 11   <u>CONCLUSION</u>

A decrease in polysialylated NCAM on the surface of oligodendrocytes when matured has been reported previously using immunohistochemical methods (Trotter et al. 1989; Grinspan and Franceschini, 1995). Based on the results presented in the second part of this thesis, it could be concluded that, PSA level is crucial for the normal development of oligodendrocytes during myelination. Furthermore, the molecules that regulate the development of oligodendrocytes together with PSA in the forebrain might be different to those that regulate the same development in the brainstem and spinal cord, since increased level of PSA had different effects on the development of oligodendrocytes of the corpus callosum and those of the brainstem and spinal cord. Moreover, a barely detectable level of PSA at the adult age might be important for an efficient maintenance of the myelin sheath, since increased amount of PSA at the adult age induces demyelination. PSA is a spacer that negatively regulates the adhesion of the myelin sheath to axons. Therefore, it is understandable to conclude that, an elevated concentration of the PSA at the adult age may disturb the signal transduction molecules that regulated an efficient maintenance of the myelin structure, by disturbing the rafts organization. This hypothesis is supported by data that confirm the presence of NCAM-120 in the rafts microdomains (Krämer et al., 1999).

# 12 <u>REFERENCES</u>

***Agrawal HC***. And Hartman BK. (1980) *Proteins of the nervous system*, second ed., Bradshaw, RA. And Schneider DM. Ed., Raven Press, NY, pp. 145-169.

***Allard J., Barron S., Diaz J., Lubetzki C., Zalc B., Schwartz JC., Sokoloff P.*** (1998). A rat G protein-coupled receptor selectively expressed in myelin-forming cells. *Eur J Neurosci*. 3:1045-1053.

***Altman J.*** (1994). Microglia emerges from the fog. *Trends Neuroci*. 17, 47-49.

***Anderson NL., Rembiesa BM., Walla MD., Bielawska A., Bielawski J., Hama H.*** (2004). The human FA2H gene encodes a fatty acid 2-hydroxylase. *J. Biol. Chem*. 279:48562-48568.

***Angevine J. B. and Jr. Sidman R. L***. (1961). Autoradiographic study of cell migration during histogenesis of cerebral cortex in the mouse. *Nature* 192, 766-768.

***Austin J., Suzuki K., Armstrong D., Brady R., Bachhawat BK., Schlenker J., Stumpf D.*** (1970). Studies in globoid (Krabbe) leukodystrophy (GLD). V. Controlled enzymatic studies in ten human cases**.** *Arch. Neurol*. 23:502-512.

***Baader SL, Sanlioglu S, Berrebi AS, Parker-Thornburg J, Oberdick J.*** (1998). Ectopic overexpression of engrailed-2 in cerebellar Purkinje cells causes restricted cell loss and retarded external germinal layer development at lobule junctions. *J Neurosci*. 18:1763-73.

***Bach G. and Neufeld EF***. (1983). Synthesis and maturation of cross-reactive glycoprotein in fibroblasts deficient in arylsulfatase A activity. *Biochem Biophys Res Commun.* 112:198-205.

***Bansal R. and  Pfeiffer SE***. (1989). Reversible inhibition of oligodendrocyte progenitor differentiation by a monoclonal antibody against surface galactolipids. *Proc Natl Acad Sci* U S A. 86:6181-6185.

***Bansal R., Winkler S., Bheddah S***. (1999). Negative regulation of oligodendrocyte differentiation by galactosphingolipids. *J. Neurosci*. 19(18):7913-7924.

Barres. Ben A. (1999). A new role for glia: generation of neuron! *Cell*, Vol. 97, 667-6670.

**Bartsch U., Kirchhoff F., Schachner M. (1990).** Highly sialylated N-CAM is expressed in adult mouse optic nerve and retina. *J Neurocytol*. 19:550-565.

**Baumann N. and Pham-Dinh D**. (2001). Biology of oligodendrocyte and myelin in the mammalian central nervous system. *Physiol Rev*. 81:871-927.

**Biffiger K., Bartsch S., Montag D., Aguzzi A., Schachner M., Bartsch S**. (2000). Severe hypomyelination of the murine CNS in the absence of myelin-associated glycoprotein and Fyn tyrosine kinase. *J. Neurosci*. 20:7430-7437.

**Bhat S. and Silberberg DH**. (1988). Developmental expression of neural cell adhesion molecules of oligodendrocytes in vivo and in culture. *J. Neurochem*. 50:1830-1838.

**Bjartmar C.** (1998). Morphological heterogeneity of cultured spinal and cerebral rat oligodendrocytes. *Neurosci lett*. 247:91-94.

**Blackman RK., Sanicola M., Raftery LA., Gillevet T. and Gelbart WM**. (1991). An extensive 3' cis-regulatory region directs the imaginal disk expression of decapentaplegic, a member of the TGF-beta family in Drosophila. *Development* 111:657-665.

**Blaschuk KL., Frost EE., and ffrench-Constant C.** (2000). The regulation of proliferation and differentiation in oligodendrocyte progenitor cells by alphaV integrins. *Development* 127:1961-1969.

**Bosio A., Binczek E., Stoffel W.** (1996). Functional breakdown of the lipid bilayer of the myelin membrane in central and peripheral nervous system by disrupted galactocerebroside synthesis. *Proc Natl Acad Sci U S A* 93:13280-13285

**Bosio A., Büssow H., Adam J., and Stoffel W.** (1998). Galactosphingolipids and axono-glial interaction in myelin of the central nervous system. *Cell Tissue Res*. 292:199-210.

**Brenner M., Johnson AB., Boespflug-Tangy O., Rodriguez D, Goldman JE. Messing A.** (2001). Mutation in GFAP, encoding glial fibrillary acidic protein, are associated with Alexander disease. *Nature Genet* 27:117-120.

**Brown MT. and Cooper JA**. (1996). Regulation, substrates and functions of src. *Biochim. Biophys. Acta*. 1287:121-149.

**Bruses JL. and Rutishauser U**. (2001). Roles, regulation, and mechanism of polysialic acid function during neural development. *Biochimie* (Paris) 83:635-643

**Büssow H**. (1978). Schwann cell myelin ensheatment CNS axons in the nerve fiber layer of the cat retina. *J. Neurocytol*. 7:207-214.

**Charles P., Hernandez MP., Stankoff B., Aigrot MS., Colin C., Rougon G., Zalc B., Lubetzki C.** (2000). Negative regulation of central nervous system myelination by polysialylated-neural cell adhesion molecule. *PNAS* 97:7585-7590.

**Cheong KH., Zacchetti D., Schneeberger EE., Simons K.** (1999). VIP17/MAL, a lipid raftassociated protein, is involved in apical transport in MDCK cells. *Proc Natl Acad Sci* U S A 96:6241-6248

**Chirgwin JM., Przybyla AE., MacDonald RJ., Rutter WJ**. (1979). Isolation of biologically active ribonucleic acid from sources enriched in ribonuclease. *Biochemistry*. 18: 5294-5301.

**Campagnoni AT. and Macklin WB**. (1988). Cellular and molecular aspects of myelin protein gene expression. *Molecular Neurobiology* 2:41-89.

**Campagnoni AT.,Carey GD. Yu YT**. (1980). In vitro synthesis of the myelin basic proteins: subcellular site of synthesis. *J. Neurochem*. 34:677-686.

**Campagnoni AT., and Skoff RP**. (2001). The pathology of myelin mutants reveal novel biological functions of the MBP and PLP genes. *Brain Pathology* 11:74-91.

**Coetzee T., Suzuki K., Popko B.** (1998) New perspectives on the function of myelin galactolipids. *Trends Neurosci* 21:126-130

**Coetzee T., Xu Li, Fujita N., Marcus J., Suzuki K., Francke U. Popko B.** (1996). Molecular cloning, chromosomal mapping and charaterization of the mouse UDP-galactose:ceramide galactosyltransferase gene. *Genomics* 35:215-222.

**Colas JF. and Schoenwolf GC**. (2001). Towards a cellular and molecular understanding of neurulation. *Dev Dyn*. 221:117-45.

**Costantino-Ceccarini E, Suzuki K**. (1975). Evidence for presence of UDP-galactose:ceramide galactosyltransferase in rat myelin. Brain Res. 8;93(2):358-362.

**Cremer H., Chazal G., Liedo PM., Rougon G., Montaron MF., Mayo W., Le Moal M., Abrous DN**. (2000). PSA-NCAM: an important regulator of hippocampal plasticity. *Int. J. Dev. Neurosci*. 18:213-220.

**Cremer H., Lange R., Christoph A., Plomann M., Vopper G., Roes J., Brown R., Baldwin S., Kraemer P., Scheff S., Barthels D., Rajewsky K., Wille W.** (1994). Inactivation of the N-CAM gene in mice results in size reduction of the olfactory bulb and deficits in spatial learning *Nature* 367:455-459.

**Decker L., Avellana-Adalid V., Nait-Oumesmar B., Evercooren AB-V**. (2000). Oligodendrocyte precursor migration and differentiation: combined effects of PSA residues, growth factors, and substrates. *Mol. Cell Neurosci*. 16:422-439.

**deFerra F., Engh H., Hudson L., Kamhlz J., Puckett C., Molineaux S. Lazzarini RA.** (1985). Alternative splicing account for the four formd of myelin basic protein. *Cell* 43: 721-727.

**del Rio-Hortega P.** (1932). Microglia *in Cytology and Cellular Pathology of the Nervous System*, Vol. 2, (Penfield, W., eds) pp. 481-534, Hocker, New York.

**Deshmukh DS., Inoue T. Pieringer RA**. (1971). The association of galactosyl diglycerides of brain with myelination. *J. Biol. Chem*. 246:5695-5699.

**Doetsch F., and Alvarez-Buylla A**. (1996). Network of tangetial pathways for neuronal migration in adult mammalian brain. *Proc Natl Acad Sci* U S A. 93:14895-14900.

**Doetsch F., Garcia-Verdugo JM. Alvarez-Buylla A**. (1997). Cellular composition and three-dimensional organization of the subventricular germinal zone in the adult mammalian brain. *J. Neurosci*. 17:5046-5061.

**Dong Hong Shin DH, Seonghan K., Wang JL., Kyeong HP., Gye SJ., Kyung HL., Sang HB., Sa SC**. (1999). Spatial and temporal expression of UDP-galactose: ceramide galactosyl transferase mRNA during rat brain development. *Anat. Embryol*. 200:193-201.

**Doyle JP. And Colman DR**. (1993). Glial-neuron interactions and the regulation of myelin formation. *Curr. Opin. Cell Biol*. 5:779-785.

**Drickamer K.** (1993). A conserved disulphide bond in sialyltransferases. *Glycobiology*.3(1):2-3.

**Dupree JL, Girault JA, Popko B**. (1999). Axo-glial interactions regulate the localization of axonal paranodal proteins. *J Cell Biol*. 147:1145-52.

**Dupree JL, Suzuki K, Popko B**. (1998). Galactolipids in the formation and function of the myelin sheath. *Microsc Res Tech*. 41:431-440.

**Durbec P. and Cremer H.** (2001) Revisiting the function of PSA-NCAM in the nervous system. *Mol Neurobiol*. 24:53-54.

**Dyer CA. and Benjamins JA**. (1990) Glycolipids and transmembrane signaling: antibodies to galactocerebroside cause an influx of calcium in oligodendrocytes. *J Cell Biol*. 111:625-33.

**Dyer CA. and Benjamins JA**. (1991). Galactocerebroside and sulfatide independently mediate calcium responses in oligodendrocytes. *J. Neurosci. Res*. 30:699:711.

**Eckhardt M., Bukalo O., Chazal G., Wang L., Goridis C., Schachner M., Gerardy-Schahn R., Cremer H., Dityatev A.** (2000). Mice deficient in the Polysialyltransferase ST8SiaIV/PST-1 allow discrimination of the role of Neural Cell adhesion molecule protein and polysialic acid in neural development and synaptic plasticity. *J. Neurosci*. 20:5234-5244.

**Eckhardt M. and Gerady-Schahn R.** (1998). Genomic organization of the murine polysialyltransferase gene ST8SiaIV (PST). *Glycobiology*. 8:1165-1172.

**Eckhardt M., Muhlenhoff M., Bethe A., Koopman J., Frosch M., Gerardy-Schahn R.** (1995). Molecular characterization of eukaryotic polysialyltransferase-1. *Nature* 373:715-8.

**Eckhardt M., Yaghootfam A., Fewou NS., Zöller I., Gieselmann V**. (2005). A mammalian fatty acid hydroxylase responsible for the formation of alpha-hydroxylated galactosylceramide in myelin. *Biochem. J.* In press.

***Eisenbarth GS, Walsh FS, Nirenberg M***. (1979). Monoclonal antibody to a plasma membrane antigen of neurons. *Proc Natl Acad Sci* U S A. 76:4913-4917.

***Erne B., Sansano S., Frank M., Schaeren-Wiemers N.*** (2002). Rafts in adult peripheral nerve myelin contain major structural myelin proteins and myelin and lymphocyte protein (MAL) and CD59 as specific markers. *J Neurochem* 82:550-562.

***Fanarraga ML., Sommer I., Griffiths IR***. (1995). O-2A progenitors of the mouse optic nerve exhibit a developmental pattern of antigen expression different from the rat. *Glia*. 15:95-104.

***Federoff S***. (1995). Development of microglia. *In Neuroglia*. H. Kettenmann and R. B. Ramson, editors. Oxford University Press, New York. 162-181.

***Figarella-Branger D., Durbec P., Rougon G.*** (1990). Differential spectrum of expression of neural cell adhesion molecule isoforms and L1 adhesion molecules on human neuroectodermal tumors. *Cancer Res*. 50:6364-6370.

***Finne J., Bitter-Suermann D., Goridis C., Finne U***. (1987). An IgG monoclonal antibody to group B meningococci cross-reacts with developmentally regulated polysialic acid units of glycoproteins in neural and extraneural tissues. *J. Immunol*. 138:4402-4407.

***Fok-Seang J. and Miller RH***. (1994). Distribution and differentiation of A2B5+ glial precursors in the developing rat spinal cord. *J Neurosci Res*. 37:219-35.

***Franceschini I., Angata K., Ong E., Hong A., Doherty P., Fukuda M***. (2001). Polysialyltransferase STSia II (STX) polysialylates all of the major isoforms of NCAM and facilitates neurite outgrowth. *Glycobiology* 11:231-239.

***Frank M, Schaeren-Wiemers N, Schneider R, Schwab ME*** (1999) Developmental expression pattern of the myelin proteolipid MAL indicates different functions of MAL for immature Schwann cells and in a late step of CNS myelinogenesis. *J Neurochem* 73:587-597.

***Frank M., van der Haar ME., Schaeren-Wiemers N., Schwab ME***. (1998). rMAL is a glycosphingolipid-associated protein of myelin and apical membranes of epithelial cells in kidney and stomach. *J Neurosci* 18:4901-4913.

**Fruttiger M., Karlsson L., Hall AC., Abramsson A., Calver AR., Bostrom H., Willets K., Bertold CH., Heath JK., Betsholtz C., Richardson WD**. (1999). Deffective oligodendrocyte development and severe hypomyelination in PDGF-A Knockout mice. *Development* 126:457-467.

**Fukuda M.** (1996). Possible roles of tumor-associated carbohydrate antigens. *Cancer Res*. 56:2237-2244.

**Fuss B., Afshari FS., Colello RJ., Macklin WB**. (2001) Normal CNS myelination in transgenic mice overexpressing MHC class I H-2L(d) in oligodendrocytes. *Mol Cell Neurosci* 18:221-234

**Futerman AH., Stieger B., Hubbard AL., Pagano RE**. (1990). Sphingomyelin synthesis in rat liver occurs predominantly at the cis and medial cisternae of the Golgi apparatus. *J. Biol. Chem.* 265:8650-8657.

**Garbay B. and Cassagne C** (1994) Expression of the ceramide galactosyltransferase gene during myelination of the mouse nervous system. Comparison with the genes encoding myelin basic proteins, choline kinase and CTP:phosphocholine cytidylyltransferase. *Dev Brain Res* 83:119-124

**Gardinier MV., Macklin WB., Diniak AJ., Deininger PL**. (1986). Characterization of myelin proteolipid mRNAs in normal and jimpy mice. *Mol Cell Biol* 6:3755-3762

**Gieselmann V., Polten A., Kreysing J., Kappler J., Fluharty A., von Figura K.** (1991). Molecular genetics of metachromatic leukodystrophy. *Dev Neurosci*. 13:(4-5):222-7.

**Graf K., Baltes H., Ahrens H., Helm CA., Husted CA**. (2002). Structure of hydroxylated galactocerebrosides from myelin at the air-water interface. *Biophys J*. 82:896-907

**Grinspan J. and Franceschini B**. (1995). Platelet-derived growth factor is a survival factor for PSA-NCAM+ oligodendrocyte pre-progenitor cells. *J. Neurosci. Res*. 41:540-545.

**Haak D., Gable K., Beeler T., Dunn T.** (1997). Hydroxylation of Saccharomyces cerevisiae ceramides requires Sur2p and Scs7p. *J Biol Chem* 272:29704-29710.

Hakamori S. (1986). Glycosphingolipids. *Sci. Am*. 254(5):44-53.

**Hall A., Giese NA., Richardson WD.** (1996). Spinal cord oligodendrocyte develop from ventrally derived progenitor cells that express PDGF alpha-receptors. *Development*. 122:4085:4094.

**Hanada K., Hara T., Fukawasa M., Yamaji A., Umeda M., Nishijima M**. (1998). Mammalian cell mutants resistant to a sphingomyelin-directed cytolysin. Genetic and biochemichal evidence for complex formation of the LCB1 protein with LCB2 protein for serine palmitoyltransferase. *J. Biol. Chem*.272:33787-33794.

**Hanada K., Nishijima M., Kiso M., Hasegawa A., Fujita S., Ogawa T., Akamatsu Y.** (1992). Sphingolipids are essential for the growth of chinese hamster ovary cells. Restoration of growth of a mutant defective in sphingoid base biosynthesis by exogenous sphingolipids. *J. Biol. Chem*. 267:23527-23533.

**Hardy R. and Reynolds R**. (1991). Proliferation and differentiation potential of rat forebrain oligodendroglial progenitors both in vitro and in vivo. *Development*. 111:1061-1080.

**Hardy R. and Reynolds R**. (1993). Neuron-oligodendroglial interactions during central nervous system development. *J. Neurosci Res.* 36:121-126.

**He X. and Rosenfeld MG**. (1991). Mechanisms of complex transcriptional regulation: implications for brain development. *Neuron* 7: 183-196.

**Hirahara Y, Bansal R, Honke K, Ikenaka K, Wada Y.** (2004). Sulfatide is a negative regulator of oligodendrocyte differentiation: development in sulfatide-null mice. *Glia*. 45(3):269-77.

**Hildebrandt H., Becker C., Gluer S., Rosner H., Gerardy-Schahn R., Rahmann H.** (1998). Polysialic acid on the neural cell adhesion molecule correlates with expression of polysialyltransferases and promotes neuroblastoma cell growth. *Cancer Res*. 59:779-784.

**Hirano A. and Dembitzer HM**. (1967). A structural analysis of the myelin sheath in the central nervous system. *J. Cell Biol.* 34:555-567.

**Holley JA. and Yu RK**. (1987). Localization of glycoconjugate recognized by HNK-1 antibody in mouse and chick embryos during early neural development. *Dev. Neurosci*. 9:105-119.

**Honke K, Hirahara Y, Dupree J, Suzuki K, Popko B, Fukushima K, Fukushima J, Nagasawa T, Yoshida N, Wada Y, Taniguchi N**. (2002). Paranodal junction formation and spermatogenesis require sulfoglycolipids. *Proc Natl Acad Sci* U S A. 99:4227-4232.

**Hu H., Tomasiewicz H., Magnuson T., Rutishauser U**. (1996). The role of polysialic acid in migration of olfactory bulb interneuron precursors in the subventricular zone. *Neuron* 16:735-743

**Hudson LD.** (1992). Amino acid substitutions in proteolipid protein that cause dysmyelination. In: Myelin: Biology and Chemistry (Martenson RE, ed.), pp. 257-276. Boca Raton, Florida, USA: London, England, UK.CCR Press.

**Ida H. and Eto Y**. (1990). Biochemical and morphological studies of dorsal root ganglion and its cultured cells from Twitcher mouse (murine globoid cell leukodystrophy). *Brain Dev*. 12:412-416.

**Igisu H. and Suzuki K**. (1984). Progressive accumulation of toxic metabolite in a genetic leukodystrophy. *Science* 224:753-755

**Inoue T, Dehmukh DS, Pieringer RA** (1971) The association of the galactosyl diglycerides of brain with myelination. I. Changes in the concentration of monogalactosyl diglyceride in the somal and myelin fractions of brain of rats during development. *J. Biol. Chem.* 246:5688-5694.

**Inuzuka T., FujitaN., Sato S., Baba H., Nakamo R., Ishiguro H., Miyatake T.** (1991). Expression of the large myelin-associated glycoprotein isoform during the development in the mouse peripheral nervous system. *Brain Res*. 562:173-175.

**Jeckel D., Karrenbauer A., Birk R., Schmidt RR. Wieland F.** (1990). Sphingomyelin is synthesized in the cis Golgi. *FEBS Lett*. 261:155-157.

**Kamholz J., deFerra F., Puckett C., Lazzarini R**. (1986). Identification of three forms of human myelin basic protein by cDNA cloning. *Proc. Natl. Acad. Sci*. USA. 83:4962-4966.

**Kaya K., Ramesha CS., Thompson GA**. (1984). On the formation of alpha-hydroxy fatty acids. Evidence for a direct hydroxylation of nonhydroxy fatty acid-containing sphingolipids. *J Biol Chem* 259:3548-3553.

***Kibbelaar RE., Mooleanaar CEC., Michalides RJAM., Bitter-Suermann D., Addis BJ., Mooi WJ.*** (1989) Expression of the embryonal neural cell adhesion molecule N-CAM in lung carcinoma. Diagnostic usefulness of monoclonal antibody 735 for the distinction between small cell lung cancer and non-small cell lung cancer. *J. Pathol*. 159:23-28.

***Kihara H., Fluharty AL., O'Brien JS., Fish CH.*** (1982). Metachromatic leukodystrophy caused by a partial cerebroside sulfatase. *Clin Genet*. 21:253-61.

***Kim T., and Pfeiffer SE***. (2002). Subcellular localization and detergent solubility of MVP17/rMAL, a lipid raft-associated protein in oligodendrocytes and myelin. *J Neurosci Res* 69:217-226.

***Kirchner DA. and Blaurock AE***. (1991). Organization, phylogenetic variations and dynamic transitions of myelin. R. E. Martenson (ed.), *Myelin: Biology and Chemistry*. Boca Raton, FL: CRC Press, pp. 413-448.

***Kitazume-Kawaguchi S., Kabata S., Arita M.*** (2001). Differential biosynthesis of polysiac or disialic acid structure by ST8Sia II and ST8Sia IV. *J. Biol. Chem*. 276:15696-15703.

***Kobayashi T., Shinnoh N., Goto I., Kuroiwa Y***. (1995). Hydrolysis of galactosylceramide is catalyzed by two genetically distinct acid β-galactosidases. *J. Biol. Chem*. 260:14982-14989.

***Kolodny EH.; Raghavan S.; Krivit W***. (1991) Late-onset Krabbe disease (globoid cell leukodystrophy): clinical and biochemical features of 15 cases. *Dev. Neurosci*. 13:232-239.

***Komminoth P., Roth J., Lackie PM., Bitter-Suermann D., Heitz PU***. (1991). Polysialic acid of the neural cell adhesion molecule distinguishes small cell lung carcinoma from carcinoids. *Am. J. Pathol*. 139:297-304.

***Koshy KM., Wang J., Boggs JM***. (1999). Divalent cation-mediated interaction between cerebroside sulfate and cerebrosides: an investigation of the effect of structural variations of lipids by electrospray ionization mass spectrometry. *Biophys J*. 77:306-318

***Koul. O., Chou KH., Jungalwala FB.*** (1980). UDP-galactose: ceramide galactosyltransferase in rat brain myelin subfractions during development. *Biochem J*. 186(3):959-69.

***Koul O, Singh I, Jungalwala FB***. (1988) Synthesis and transport of cerebrosides and sulfatides in rat brain during development. *J Neurochem*. 50(2):580-8.

***Kozlov G., Lee J., Gravel M., Ekiel I., Braun PE., Gehring K***. (2002). Assignment of the 1H, 13C and 15N resonances of the catalytic domain of the rat 2',3'-cyclic nucleotide 3'-phosphodiesterase. *J Biomol NMR*. 22(1):99-100.

***Krämer EM., Klein C., Koch T., Boytinck M., Trotter J***. (1999). Compartmentation of Fyn kinase with glycosylphosphatidylinositol-anchored molecules in oligodendrocytes facilitates kinase activation during myelination. *J. Biol. Chem*. 274:29042-29045.

***Kudrycki K., Stein-Izsak C., Behn C., Grillo M., Akeson R., Margolis FL.*** (1993). Olf-1-binding site: characterization of an olfactory neuron-specific promoter motif. *Mol Cell Biol*. 13:3002-3014.

***Kuhn PL., Petroulakis E., Zazanis GA., McKinnon RD***. (1995). Motor function analysis of myelin mutant mice using a rotarod. *Int. J. Dev. Neurosci*. 13:715-722.

***Lai C., Brow MA., Nave KA., Noronha AB., Quarles RH., Bloom FE., Milner RJ., Sutcliffe JG.*** (1987). Two forms of 1B236/myelin-associated glycoprotein, a cell adhesion molecule for postnatal neural development, are produced alternative splicing. *Proc. Natl. Acad. Sci*. USA 84:4337-4341.

***Lee JC., Mayer-Proschel M. Rao MS***. (2000). Gliogenesis in the central nervous system. *Glia* 30:105-121.

Lees MB. (1982). Proteolipids. *Scand. J.Immunol*. 15:147-166.

***Lees MB. And Brown D***. (1984). Proteins in myelin. In: Myelin (Morell P, ed) pp. 197-224) New York: Plenum.

***Lees MB., and Sapirstein VS***. (1983). Myelin-associated enzymes. *Handbook of Neurochemistry*, vol. 4, (2<sup>nd</sup> ed.), Lajtha A., ed., Plenum NY, pp 435-460.

**Levison SW. and Goldman JE**. (1993). Both oligodendrocytes and astrocytes develop from progenitors in the subventricular zone of postnatal rat forebrain. *Neuron* 10:201-212.

**Lewis PD.** (1968). The fate of the subependymal cell in the adult rat brain, with a note on the origin of microglia. *Brain* 91:721-738.

**Li C., Trapp B., Ludwin S., Peterson A., Rode J**. (1998). Myelin associated glycoprotein modulates glia-axon contact in vivo. *J. Neurosci. Res*. 51:210-217.

**Liedtke W., Edelmann W., Bieri PL., Chiu FC. Cowan NJ.** (1996). GFAP is necessary for the integrity of CNS white matter architecture and long-term maintenance of myelination. *Neuron* 17:607-615.

**Ling AE**. (1979). Transformation of monocytes into amoeboid microglia in the corpus callosum of postnatal rats, as shown by labelling monocytes by carbon particles. *J. Anat*. 128:847-858

**Ling EA. and Wong WC**. (1993). The origin and nature of ramified and amoeboid microglia: a historical review and current concepts. *Glia*. 7(1):9-18.

**Livingston BD and Paulson JC**. (1993). Polymerase chain reaction cloning of a developmentally regulated member of the sialyltransferase gene family. *J Biol Chem*. 268:11504-71150.

**Lois C. and Alvarez-Buylla A.** (1993). Proliferating subventricular zone cells in the adult mammalian forebrain can differentiate into neurons and glia. *Proc Natl Acad Sci* U S A. 90:2074-2077.

**Luskin MB., Pearlman AL., Sanes JR**. (1988). Cell lineage in the cerebral cortex of the mouse studied in vivo and in vitro with a recombinant retrovirus. *Neuron* 1:635-647.

**Luzi P., Rafi MA., and Wenger DA**. (1996). Multiple mutations in the GALC gene in patient with adult onset Krabbe disease. *Ann. Neurol*. 40:116-119.

**Macklin WB.** (1992). The myelin proteolipid gene and its expression. In: Myelin: Biology and Chemistry (Martenson RE, ed.), pp. 257-276. Boca Raton, Florida, USA: CCR Press, Inc.

**Martin M., McFarland HF., McFarlin DE**. (1992). Immunological aspects of demyelinating diseases. *Annu. Rev. Immunol*. 10:153-187.

***Martin-Belmonte F., Arvan P., Alonso MA***. (2001) MAL mediates apical transport of secretory proteins in polarized epithelial Madin-Darby canine kidney cells. *J Biol Chem* 276:49337-49342.

***Martin-Belmonte F., Martinez-Menarguez JA., Aranda JF., Ballesta J., de Marco MC., Alonso MA***. (2003) MAL regulates clathrin-mediated endocytosis at the apical surface of Madin-Darby canine kidney cells. *J Cell Biol* 163:155-164.

***Matsuda J., Vanier MT., Saito Y., Tohyama J., Suzuki K***. (2001). A mutation in the Saposin A domain of the sphingolipid activator protein (prosaposin) gene results in a late onset, chonic form of globoid cell leukodystrophy in the mouse. *Hum. Mol. Genet*. 10:1191-1199.

***Matsumoto A., Vanier MT., Oya Y., Kelly D., Popko B., Wenger DA., Suzuki K.*** (1997). Transgenic induction of human galactosylceramidase into twitcher mouse: significant phenotype improvement with a minimal expression. *Develop. Brain Dysfunction* 10:142-154.

***Mckhann GM***. (1982). Multiple sclerosis. *Annu. Rev. Neurosci*. 10:219-239.

***McMahon SS. And McDermott KW***. (2001). Proliferation and migration of glial precursor cells in the developing rat spinal cord. *J. Neurocytology* 30:821-828.

***Morell P., Quarles RH., Norton WT.*** (1994). Myelin formation, structure and biochemistry. G. J. Siegel et al. (ed.). Published by Rven press, Ltd., New York. *Basic Neurochemistry: Molecular, Cellular and Medical Aspects*. Pp. 117-143.

***Mucke L. and Eddleson M.*** (1993). Astrocytes in infectious and immune-mediated diseases of the central nervous system. *FASEB J*. 7:1226-1232.

***Muse ED, Jurevics H, Toews AD, Matsushima GK, Morell P***. (2001) Parameters related to lipid metabolism as markers of myelination in mouse brain. *J Neurochem* 76:77-86

***Mühlenhoff M., Eckhardt M., Bethe A., Frosch M., Gerardy-Schahn R.*** (1996). Polysialylation of NCAM by single enzyme. *Curr. Biol*. 6:1188-1191.

***Mühlenhoff M., Eckhardt M., Gerardy-Schahn R.*** (1998). Polysialic acid: three dimentional-structure, biosynthesis and function. *Curr. Opin. Struct. Biol*. 8:558-564.

***Nakajima K. and Kohsaka S.*** (2001). Microglia: activation and their significance in the central nervous system. *J Biochem* (Tokyo). 130:169-75.

***Nave KA., Lai C., Bloom FE., Milner RJ***. (1987). Splice site selection in the proteolipid protein (PLP) gene transcript and primary structure of the DM20 protein of central nervous system myelin. *Pro. Natl. Acad. Sci*. USA 84:5665-5669.

***Newman SL., Kitamura K., Campagnoni AT***. (1987a). Identification of a cDNA coding for a fifth form of myelin basic protein in mouse. *Proc. Natl. Acad. Sci*. USA 84:886-890.

***Newman SL., Kitamura K., Roth Hj., Kronquist K., Kerlero de Rosbo N., Neuhaus J. Federoff S.*** (1994). Development of microglia in mouse neopallial cell cultures. *Glia*. 11(1):11-7.

***Nonaka G., and Kishimoto Y.*** (1979). Levels of cerebrosides, sulfatides, and galactosyl diglycerides in different regions of rat brain. Change during maturation and distribution in subcellular fractions of gray and white matter of sheep brain*. Biochim Biophys Acta* 572:432-441.

***Norton WT.*** (1977). The myelin sheath. In E. S. Goldensohn and S. H. Appel (eds.). *Scientific Approaches to Clinical Neurology*. Philadelphia: Lea and Febiger, pp. 259-298.

***Norton WT. and Poduslo SE*** (1973).Myelination in rat brain: changes in myelin composition during brain maturation. *J Neurochem*. 21: 759-773.

***Notterpek LM. and Rome LH***. (1994). Functional evidence for the role of axolemma in CNS myelination. *Neuron* 13:473-485.

***Odell GM., Oster G., Alberch P., Burnside B***. (1981). The mechanical basis of morphogenesis. I. Epithelial folding and invagination. *Dev Biol*. 85:446-462.

***Olafson RW., Drummond GI., Lee JF.*** (1969). Studies on 2′,3′-cyclic nucleotide-3′-phosphohydrolase from brain. *Can. J. Biochem*. 47:961-966.

**Omlin FX., Webster HD., Palkovits CG., Cohen SR**. (1982). Immunocytochemical localisation of basic protein in major dense line regions of central and peripheral myelin. *J. Cell Biol*. 95:242-248.

**Ono K., Bansal R., Payne J., Rutishauser U., Miller RH**. (1995). Early development and dispersal of oligodendrocyte precursors in the embryonic chick spinal cord. *Development*. 121:1743-1754.

**O'Rourke NA., Dailey ME., Smith SJ., McConnell SK**. (1992). Diverse migratory pathways in the developing cerebral cortex. *Science*. 258:299-302.

**Osterhout DJ., Wolven A., Wolf RM., Resh MD., Chao MV**. (1999). Morphological differentiation of oligodendrocytes required required activation of Fyn tyrosine kinase. *J. Cell Biol*. 145:1209-1218.

**Pedraza L., Frey AB., Hempstead BL., Colman DR., Salzer JL**. (1991). Differential expression of MAG isoforms during development. *J. Neurosci. Res*. 29:141-148

**Perry VH. and Gordon S**. (1988). Macrophages and microglia in the nervous system. *Trends Neurosci*. 11(6):273-7.

**Pesheva P., Gloor S., Schachner M., Probstmeier R**. (1997). Tenascin-R is an intrinsic autocrine factor for oligodendrocyte differenciation and promotes cell adhesion by a sulfatide-mediated mechanism. *J. Neurosci*. 17(12):4642-4651.

**Powell EM. and Geller HM**. (1999). Dissection of astrocyte-mediated cues in neuronal guidance and process extension. *Glia*, Vol. 26, N°. 1.

**Quarles RH.** (1979). Glycoprotens in myelin and myelin related membranes, *Myelin Chemistry and Biology*, Hashim G., ed., Liss Inc., NY., pp. 55-77.

Quarles RH. (1983). Myelin-associated glycoprotein in development and disease. *Develpoment Neurosci*. 6:285-303.

**Quarles RH., Morell P., McFarlin DE**. (1994). Diseases involving myelin. *Basic Neurochemistry: Cellular, and medical* Aspects. 5th ed., Siegel GJ., ed., Raven Press NY, pp 771-792.

**Raff MC., Mirsky R., Fields KL., Lisak RP., Dorfman SH., Silberberg DH., Gregson NA., Leibowitz S., Kennedy MC**. (1978). Galactocerebroside is a

specific cell-surface antigenic marker for oligodendrocytes in culture. *Nature*. 274:813-816.

***Ramón y Cajal, S***. Reconstitution of my life (E. H. Craigie, trans.). In memoirs of the American Philosophical Society, Vol. 8. Philadelphia, 1937. Reprinted, New York: Garland, 1988. (The most entertaining of all introductions to cellular neurobiology, by the founding father of the subject)

***Rakic P.*** (1974). Mode of cell migration to the superficial layers of fetal monkey neocortex. *J. Comp. Neurol. 145, 61-84*.

***Raine CS.*** (1984). Morphology of myelin and myelination. In P. Morell (ed.), *Myelin*, 2$^{nd}$ ed. New York: Plenum, pp1-41.

***Ranscht B.,Wood PM., Bunge RP.*** (1987). Inhibition of in vitro peripheral myelin formation by monoclonal anti-galactocerebroside. *J Neurosci*. 7: 2936-2947.

***Rasband MN., Tayler J., Kaga Y., Yang Y., Lappe-Siefke C., Nave KA., Bansal R***. (2005). CNP is required for maintenance of axon-glia interactions at nodes of Ranvier in the CNS. *Glia* Short communication. Online published.

***Rettig WJ. and Old LJ***. (1989). Immunogenetics of human cell surface differentiation. *Annu. Rev. Immunol*. 7:481-511.

***Reynolds R. and Wilkin GP***. (1991). Oligodendroglial progenitor cells but not oligodendroglia divide during normal development of the rat. *J. neurocytol*. 20:216-224

***Ridet JL., Malhotra SK., Privat A. Gage FH***. (1997). Reactive astrocytes: cellular and molecular cues to biological function. *Trends in Neurosciences* 20:570-577.

***Roth HJ., Kronquist K., Retorius PJ., Crandall PJ., Crandall BF., Campagnoni AT.*** (1987). Evidence for the expression of four myelin basic protein variants in the developing human spinal cord through cDNA cloning. *J. Neurosci. Res*. 17:321-328.

***Roth J., Taatjes D., Bitter-Suermann D., Finne J.*** (1988). Polysialic acid units are spatially and temporally expressed in developing postnatal rat kidney. *Proc. Natl. Acad. Sci*. U. S. A. 84:1969:1973.

***Rozeik C. and Von Keyserlingk D***. (1987). The sequence of myelination in the brain stem of the rat monitored by myelin basic protein immunohistochemistry. *Dev. Brain res*. 35:183-190.

***Rutishauser U.*** (1996) Polysialic acid and the regulation of cell interactions. *Curr. Opin. Cell.bioll*. 8:679-684.

***Rutishauser U, Acheson A, Hall AK, Mann DM, Sunshine J***. (1988). The neural cell adhesion molecule (NCAM) as a regulator of cell-cell interactions. *Science* 240:53-57.

***Rutishauser U. and Landmesser L.*** (1996). Polysialic acid in the vertebrate nervous system: a promoter of plasticity in cell-cell interactions. *Trends Neurosci*. 19:422-427.

***Saravanan K., Schaeren-Wiemers N., Klein D., Sandhoff R., Schwarz A., Yaghootfam A., Gieselmann V., Franken S***. (2004) Specific downregulation and mistargeting of the lipid raft associated protein MAL in a glycolipid storage disorder. *Neurobiol Dis*, in press.

***Schachner M. and Martini R***. (1995). Glycans and the modulation of neural recognition molecule function. *Trends Neurosci*. 18:183-191.

***Schaeren-Wiemers N., Van der Bijl P. Schwab ME***. (1995a). The UDP-galactose: ceramide galactosyltransferase: Expression pattern in oligodendrocytes and schwann cells during myelination and substrate preference for hydroxyceramide. *J. Neurochem*. 65:2267-2278.

***Schaeren-Wiemers N., Valenzuela DM., Frank M., Schwab ME***. (1995b) Characterization of a rat gene, rMAL, encoding a protein with four hydrophobic domains in central and peripheral myelin. *J Neurosci* 15:5753-5764

***Schelper RL. and Adrian EK.*** (1986). Monocytes become macrophages: they do not become microglia: a light and electron microscopic autoradiographic study using 125-iododeoxyuridine. *J. Neuropathol. Exp. Neurol*. 45:1-19.

***Schmidt-Schultz T. and Althaus HH.*** (1994). Monogalactosysl diglyceride, a marker of myelination, activates oligodendroglial protein kinase C. *Journal of Neurochemistry*. 62:1578-1585.

**Schulte S. and Stoffel W.** (1993). Ceramide UDPgalactosyltransferase from myelinating rat brain: purification, cloning and expression. *Proc. Natl. Acad. Sci*. USA 90:10265-10269.

**Schulte S. and Stoffel W.** (1995): UDP galactose: ceramide galactosyltransferase and glutamate/aspartate transporter. Copurification, separation and characterization of the two glycoproteins. *Eur. J. Biochem*. 233:947-953.

**Schwab ME. and Schnell L**. (1989). Region-specific appearance of myelin constituents in the developing rat spinal cord. *J Neurocytol*. 1989 Apr;18(2):161-9.

**Seki T. and Arai Y.** (1993). Distribution and possible roles of the highly polysialylated neural cell adhesion molecule (NCAM-H) in the developing and adult central nervous system. *Neurosci. Res*. 17:265-290.

**Shah J, Atienza JM, Rawlings AV, Shipley GG** (1995) Physical properties of ceramides: effect of fatty acid hydroxylation. *J Lipid Res* 36:1945-1955.

**Sheikh KA., Sun J., Kawai H., Crawford TO., Proia RL., Griffin JW., and Schnaar RL.** (1999). Mice lacking complex gangliosides develop Wallerian degeneration and myelin defects. *Proc. Natl. Acad. Sci* USA 96:7532-7537.

**Shimomura K, Yahara S, Kishimoto Y, Benjamins JA.** (1984). Metabolism of cerebrosides and sulfatides in subcellular fractions of developing rat brain. *Biochim Biophys Acta*. 795(2):265-70.

**Simons K., and van Meer G**. (1988). Lipid sorting in epithelial cells. *Biochemistry* 27:6197-6202.

**Singh I, Kishimoto Y** (1979) Alpha hydroxylation of lignoceric acid in brain. Subcellular localization of alpha hydroxylation and the requirement for heat-stable and heat-labile factorsnand sphingosine. *J Biol Chem* 254:7698-7704.

**Sommer I. and Schachner M.** (1981). Expression of glial antigens C1 and M1 in developing and adult neurologically mutant mice. *J Supramol Struct Cell Biochem.* 1:53-74.

**Sorg BA., Smith MM., Campagnoni AT**. (1987) Developmental expression of the myelin proteolipid protein and basic protein mRNAs in normal and dysmyelinating mutant mice. *J. Neurochem* 49:1146-1154

**Spassky N., Coujet-Zalc C., Parmantier E., Olivier C., Martinez S., Ivanova A., Ikenaka K., Macklin W., Cerruti I., Zalc B. Thomas J-L.** (1998). Multiple restricted origin of oligodendrocytes. *J. Neurosci*. 18:8331-8343.

**Spassky N., Olivier C., Perez-Villegas E., Goujet-Zalc C., Martinez S., Thomas J-L., Zalc B**. (2000). Single or multiplen oligodendroglial lineages: a controversy. *Glia.* 29:143-148.

**Sperber BR., Boyle-Walsh EA., Engleka MJ., Gadue P., Peterson AC., Stein PL., Scherer SS.,McMorris FA**. (2001). A unique role for Fyn in CNS myelination. *J Neurosci* 21:2039-2047.

**Spörkel O, Uschkureit T., Büssow H., Stoffel W.** (2002). Oligodendrocytes expressing exclusively the DM20 isoform of the proteolipid protein gene: myelination and development. Glia. 37:19-30.

**Sprinkle TJ., Grimes MJ., Eller AG**. (1980a). Isolation of 2′,3′-cyclic nucleotide 3′-phosphodiesterase from human brain. *J. Neurochem*. 34:880-887.

**Sprong H., Kruithof B., Leijendekker R., Slot Jw., Van Meer G., Van der Sluijs P.** (1998). UDP-galactose: ceramide galactosyltransferase is a class I integral menbrane protein of the endoplasmic reticulum. *J. Biol. Chem*. 273:25880-25888.

**Sprong H., van Meer G., van der Sluijs P**. (2000). Analysis of galactolipids and UDP-galactose: ceramide galactosyltransferase. *Methods Enzymol* 311:59-73.

**Stahl N., Jurevics H., Morell P., Suzuki K., Popko B**. (1994). Isolation, characterization, and expression of cDNA clones that encode rat UDP-galactose: ceramide galactosyltransferase. *J. Neurosci. Res*. 38:234-242.

**Stoffel W. and Bosio A.** (1997). Myelin glycolipids and their functions. *Curr Opin Neurobiol*. 7:654-661.

**Streit WJ., Graeber MB., Kreutzberg GW.** (1988). Functional plasticity of microglia: a review. *Glia* 1, 301-307.

**Sugama K., Kim SW., Ida H., Eto Y**. (1990). Psychosine cytotoxicity in rat neural cell culture and protection by phorbol ester and dimetyl sulfoxide. *Pediatr. Res*. 28:473-476.

***Suzuki, K***. (1998). Twenty five years of the "psychosine hypothesis": a personal perspective of its history and present status. *Neurochem. Res.* 23:251-259.

***Suzuki K. and Suzuki Y.*** (1970). Globoid cell leukodystrophy (Krabbe´s disease); deficiency of galactocerebroside-β-galactosidase. *Proc. Natl. Acad. Sci*. USA 66:302-309.

***Suzuki K. Suzuki Y., Suzuki K.*** (1995). Galactosylceramide lipidosis; globoid cell leukodystrophy (Krabbe disease) In The Metabolic and Molecular Bases of Inherited Disease (Scrire CR., Beaudet AL., Sly WS., Valle D., eds) Vol. 2, pp. 2671-2692. McGraw-hill, Inc., New York.

***Suzuki M. and Raisman G.*** (1994). Multifocal pattern of neonatal development of the macroglial framework of the rat fimbria. *Glia* 12:294-308.

***Svennerholm L., Stallberg-Stenhagen S***. (1968). Changes in the fatty acid composition of cerebrosides and sulfatides of human nervous tissue with age. *J Lipid Res* 9:215-225.

***Sweet H***. (1986). Twitcher is on Ch 12. *Mouse Newslett*. 75, 30.

***Taira E. and Baraban JM. (***1997). Identification of a strand-specific Egr response element binding complex enriched in rat brain. *J Neurochem*. 68:2255-2262.

***Takamiya K., Yamamoto A., Furukawa K., Yamashiro S., Shin M., Okada M., Fukumoto S., Haragushi M., Takeda N., Fujimura K., Sakae M., Kishikawa M., Shiku H., Furukawa K., Aizawa S***. (1996). Mice with disrupted GM2/GD2 synhase gene lack complex gangliosides but exhibit only subtle defects in their nervous system. *Proc. Natl. Acad. Sci* USA 93:10662-10667.

***Tamotsu T., Eiko S., Kei-ichi U., Atsushin H., Hiroya H., Minoru T., Tetsuo N., Tsutomu K.*** (2001). Confirmation of minor components of less polar neutral and acid glycolipids in monkey brain tissue. *Journal of lipid research* 42:873-885.

***Tanaka K., Webater H. and De F***. (1993). Effect of psychosine (galactosphingosine) on the survival and the fine structure of cultured Schwann cell. *J. Neuropath. Exp. Neurol*. 29:483-493.

***Taylor CM., Coetzee T., Pfeiffer SE.*** (2002). Detergent-insoluble glycosphingolipid/cholesterol microdomains of the myelin membrane. *J Neurochem* 81:993-1004.

***Taylor CM, Marta CB, Bansal R, Pfeiffer SE.*** (2003). The burgeoning role of lipids in the assembly, structure and function of myelin-forming cells and myelin. In: Lazzarini R., editor. *Myelin and its diseases*. New York: Academic Press p 57-88.

***Tekki-Kessaris N., Woodruff RH., Hall AC., Pringle NP., Kimura S., Stiles D., Rowitch DH., Richardson WD.*** (2000). Sonic hedgehog-dependent oligodendrocyte lineage specification in ventral telencephalon. *Development*, in press.

***Tencomnao T., Yu RK., Kapitonov D*.** (2001). Characterization of the human UDPgalactose:ceramide galactosyltransferase gene promoter. *Biochim. Biophys. Acta* 1517:416-423

***Theele DP. and Steit WJ.*** (1993). A chronicle of microglial ontogeny. *Glia* 7, 5-8.

Trapp BD. (1990). Myelin-associated glycoprotein. Location and potential function. *Ann. NY Acad. Sci*. 605:29-43.

***Trifilieff E., Luu B., Nussbaum JL., Roussel G., Espinosa de los Monteros A., Sabatier JM., Van Rietschoten J.*** (1986). A specific immunological probe for the major myelin proteolipid. Confirmation of a deletion in DM20. *FEBS Lett*. 198:235-239.

***Tropak MB., Johnson PW., Dunn RJ., Roder JC***. (1988). Differential splicing of MAG transcrips durino CNS and PNS development. *Brain Res*. 464:143-155.

***Trotter J., Bitter-Suermann D, Schachner*** M. (1989). Differentiation-regulated loss of polysialylated embryonic form and expression of the different polypeptides of the neural cell adhesion molecule by cultured oligodendrocytes and myelin. *J. Neurosci*. Res. 22:369-383.

***Umemori H., Sato S., Yagi T.,Aizawa S., Yamamoto T***. (1994). Initial of myelination involve fyn tyrosine kinase signaling. *Nature* 367:572-576.

***Umemori H., Kadowaki Y., Hirosawa K., Yoshida Y., Hironaka K., Okano H., Yamamoto T.*** (1999). Stimulation of myelin basis protein gene transcription by Fyn tyrosine kinase for myelination. *The journal of neuroscience*. 19:1393-1397.

***Uschkureit T., Spörkel O., Stracke J., Büssow H. Stoffel W***. (2000). Early onset of axonal degeneration in double (plp-/-mag-/-) and hypomyelinosis in triple (plp-/-mbp-/-mag-/-) mutant mice. *J. Neurosci*. 20:5225-5233.

***van Echten-Deckert G***. (2000) Sphingolipid extraction and analysis by thin-layer chromatography. *Methods Enzymol* 312:64-79.

***Vinken PJ., Bruyn GW., Klawans HL., Koestsier JC***. (1985). *Handbook of Clinical Neurology*, Vol. 47, *Demyelinating Diseases*. Amsterdam: Elsevier.

***Von Figura K., Gieselmann V., Jaeken J.*** (2001). Metachromatic leukodystrophy. In: Scriver, Beaudet, Valle, Sly, editors. The metabolic and molecular basis of inherited disease. New York: Mc Graw Hill, New York, p 3695-3724

***von Figura K, Steckel F, Conary J, Hasilik A, Shaw E***. (1986). Heterogeneity in late-onset metachromatic leukodystrophy. Effect of inhibitors of cysteine proteinases. *Am J Hum Genet*. 39:371-382.

***Vos JP., Lopes-Cardozo M., Gadella MB.*** (1994). Metabolic and functional aspect. *Biochem. Biophys. Acta* 1211:125-140.

***Wang C., Rougon G. Kiss JZ.*** (1994). Requirement of polysialic acid for the migration of theO-2A glail progenitor cell from neurohypophyseal explants. *J. Neurosci*. 14:4446-4457.

***Wang C., Pralong WF., Schulz MF., Rougon G., Aubury JM., Pagluisi S., Robert A., Kiss JZ***. (1996). Functional N-Methyl-D-aspartate receptors on O-2A glial precursor cells: a critical role in regulating polysialic acid-neural cell adhesion molecule expression and migration. *J. Cell Biol*. 135:1565-1581.

***Warf BC., Fok-Seang J. and Miller RH***. (1991). Evidence for the ventral origin of oligodendrocyte precursors in the rat spinal cord. *J. Neurosci*. 11:2477-2488.

***Waxman SG. and Sims TJ.*** (1984). Specificity in the central myelination: evidence for local regulation of myelin thickness. *Brain Res*. 292:179-185.

***Wells GB. and Lester RL.*** (1983). The isolation and characterization of a mutant strain of saccharomyces cerevisiae that requires a long chain base for growth and for synthesis of phosphosphingolipids. *J. Biol. Chem*. 258:10200-10203.

***Wenger DA., Petitpas JW., Pieringer RA..*** (1968). The metabolism of glyceride glycolipids. II. Biosynthesis of monogalactosyl diglyceride from uridine diphosphate galactose and diglyceride in brain. *Biochemistry*. 7:3700-7.

***Wenger DA., Suzuki K., Suzuki Y.*** (2001). Galactosylceramide lipidosis: globoid cell leukodystrophy (Krabbe disease). In: Scriver, Beaudet, Valle, Sly, editors. The metabolic and molecular basis of inherited disease. New York: Mc Graw Hill, New York, p 3669-3692.

***Wilt FH.*** (1987). Determination and morphogenesis in the sea urchin embryo. *Development.* 100:559-76.

***Yamashita T., Wada R., Sasaki T., Geng C., Bierfreund U., Sandhoff K., Proia RL.*** (1999). A vital role for glycosphingolipid synthesis during development and differentiation. *Proc. Natl. Acad. Sci*. USA 96:9142-9147.

***Yao JK, Rastetter GM.*** (1985). Microanalysis of complex tissue lipids by high-performance thin-layer chromatography. *Anal Biochem*. 150:111-6.

***Yonemasu T., Nakahira K., Okumura S., Kagawa T., Espinosa de los Monteros A., de Vellis J, Ikenaka K.*** (1998). Proximal promoter region is sufficient to regulate tissue-specific expression of UDP-galactose: ceramide galactosyltransferase gene. *J Neurosci Res*. 52:757-765.

***Yu WP., Collarini EJ., Pringle NP., Richardson WD*** (1994). Embryonic expression of myelin genes: evidence for a focal source of oligodendrocyte precursors in the ventricular zone of the neural tube. *Neuron* 12:1353-1362.

***Zerlin M., Lewison SW., Goldman JE.*** (1995). Early patterns of migration, morphogenesis and intermediate filament expression of subventricular zone cells in the postnatal rat forbrain. *J. Neurosci*. 15:7238-7249.

# ACKNOWLEDGMENTS

# CURRICULUM VITAE

**NAME:**          **Simon NGAMLI FEWOU**

**E-MAIL:**          sfewou@yahoo.com

## EDUCATION

**University.**

**1991 – 1995:**          Bsc. Biochemistry (Cameroon)

**1995 – 1997:**          Msc. Biochemistry (Cameroon)

**1998 – 2000:**          Doctorate student at the University of Yaounde I (Cameroon). **Thesis have been stopped because of the availability of reagents**

**Oct., 2000:**          Doctorate student at the Faculty of Mathematics and Natural Science at the University of Bonn –Germany

**Secondary school.**

**1983 – 1991:**          GCE A. Level (mathematics & Natural Science)

**Primary school.**

**1975 – 1983:**          First School living certificate.

## Thesis

**PhD. Thesis: "**Functional impacts of transgenic overexpression of UDP-galactose: ceramide galactosyltransferase and Polysialyltransferase on the

development of oligodendrocytes and myelin maintenance." Thesis submitted at the University of Bonn. **May 12, 2005**

**Master thesis**: "Contribution á la fabrication des bioréactifs: Purification du lysozyme á partir du blanc d´oeuf. Department of Biochemistry- University of Yaounde I Cameroon. **May 5, 1997**

## Publications

### 1 Articles

***Simon N. Fewou*, *Heinrich Büssow, Nicole Schaeren-Wiemers, Marie T. Vanier, WendyB. Macklin, Volkmar Gieselmann, and Matthias Eckhardt**. (2005). Reversal of non-hydroxy:alpha-hydroxy galactosylceramide ratio and unstable myelin in transgenic mice overexpressing UDP-galactose: ceramide galactosyltransferase. Submitted at the Journal of Neurochemistry. In Press.

**Matthias Eckhardt, Afshin Yaghootfam, *Simon N Fewou*, Inge Zöller and Volkmar Gieselmann** (2005). A mammalian fatty acid hydroxylase responsible for the formation of alpha-hydroxylated galactosylceramide in myelin. *Biochem J*. In press.

**Diana Klein, Heinrich Büssow, *Simon Ngamli Fewou*, Volkmar. Gieselmann** (2005). Exocytosis of storage material in a lysosomal disorder. *Biochem Biophys Res Commun*. 327:663-667.

**Matthias Eckhardt., *Simon N. Fewou*, Ivonne Ackermann and Volkmar Gieselmann** (2002) N-glycosylation is required for full enzymic activity of the murine galactosylceramide sulphotransferase. *Biochem. J*. 368:317–324

### 2 Abstracts:

***Simon N. Fewou*, H. Büssow, N. Schaeren-Wiemers, V. Gieselmann, M. Eckhardt** (2004). Down-regulation of $\alpha$-hydroxylated galactosylceramide and unstable myelin in transgenic mice overexpressing UDP-galactose: ceramide galactosyltransferase. *Glycoconjugate Journal*. Vol. 21 pp. 393.

**M. Eckhardt, *Simon N. Fewou*, R. Lüllmann-Rauch, V. Gieselmann** (2004) Sulfatide storage in neurons of arylsulfatase A deficient mice overexpressing UDP-galactose: ceramide galactosyltransferase: A mouse model to study the

neuronal phenotype of metachromatic leukodystrophy. *Glycoconjugate Journal*. Vol. 21 pp. 403.

***Simon N. Fewou*, *H. Ramakrishnan, V. Gieselmann, M. Eckhardt*** (2004) Demyelination in transgenic mice overexpressing polysialyltransferase ST8SiaIV in oligodendrocytes. *Glycoconjugate Journal*. Vol. 21 pp.403.


**Symposium attended**

**Nov. 28.30, 2004:**

**International symposium on Glycobiology at Wageningen . The Netherlands**

**Oral communication:** Down-regulation of α-hydroxylated galactosylceramide and unstable myelin in transgenic mice overexpressing UDP-galactose: ceramide galactosyl-transferase.

**Posters:**

**Simon N. Fewou, H. Büssow, N. Schaeren-Wiemers, V. Gieselmann, M. Eckhardt**. Down-regulation of α-hydroxylated galactosylceramide and unstable myelin in transgenic mice overexpressing UDP-galactose:ceramide galactosyltransferase.

**M. Eckhardt**, **Simon N. Fewou, R. Lüllmann-Rauch and V. Gieselmann**. Sulfatide storage in neurons of arylsulfatase A deficient mice overexpressing UDP-galactose: ceramide galactosyltransferase: A mouse model to study the neuronal phenotype of metachromatic leukodystrophy.

**Simon N. Fewou, Hari. Ramakrishnan, Volkmar Gieselmann Matthias. Eckhardt**. Hypomyelination in transgenic mice overexpressing polysialyltransferase ST8SiaIV in oligodendrocytes

**August 19-24, 2001: International symposium on glycoscience. „GLYCO XVI at The Hague- the Netherlands":**

**Poster:**

**Matthias Eckhardt; Simon N. FEWOU and Volkmar Gieselmann**: Expression of soluble cerebroside sulfotransferase in CHO cells.

**April27-28, 2001(Bonn-Germany):** International symposium on Glycoconjugates and contact of the cell surface.

**Dec. 17-19, 1997**: Participation at the Fifth annual conference of the Cameroon Bioscience Committee. Yaounde-Cameroon.

**May. 29-31, 1997**: Participation to the Fourth annual symposium of the Cameroon Biochemical society and Molecular Biology. Buea–Cameroon.

**Dec. 9, 1995**: Participation at the Third annual symposium of the Cameroon Biochemical Society. Yaounde – Cameroon.

**May-June, 1996**: Participation to the workshop on the culture and isolation of the bacteria species. University hospital center in Yaounde–Cameroon.